UNIVERSITÀ DEGLI STUDI DI PALERMO

Dottorato in Scienze Fisiche
Dipartimento di Fisica e Chimica – Emilio Segrè
Settore Scientifico Disciplinare FIS/02

# (Un)conditioned open dynamics in quantum optics

IL DOTTORE
**DARIO CILLUFFO**

IL COORDINATORE
**Prof. GIOACCHINO MASSIMO PALMA**

IL TUTOR
**Prof. FRANCESCO CICCARELLO**

EVENTUALE CO TUTOR

CICLO XXXIII
ANNO CONSEGUIMENTO TITOLO - 2021

*"You are strong because you are imperfect. You are wise because you have doubts."*

Clementine Churchill - Darkest Hour (2017)

# Contents

# List of publications

In this chronological list of peer-reviewed publications, those on which this dissertation is based are asterisked.

1. D. Cilluffo and F. Ciccarello, "Quantum non-Markovian collision models from colored-noise baths", Advances in Open Systems and Fundamental Tests of Quantum Mechanics: Proceedings of the 684. WE Heraeus-Seminar, Bad Honnef, Germany, 2-5 December 2018. Vol. 237. Springer Nature, (2019);

2. D. Cilluffo, S. Lorenzo, G. M. Palma, F. Ciccarello, "Quantum jump statistics with a shifted jump operator in a chiral waveguide", Journal of Statistical Mechanics: Theory and Experiment (10), 104004 (2019);

3. * D. Cilluffo, G. Buonaiuto, S. Lorenzo, G. M. Palma, F. Ciccarello, F. Carollo, I. Lesanovsky, "Witnessing nonclassicality through large deviations in quantum optics" Physical Review Research 2 (2), 023078, (2020) ;

4. * D. Cilluffo, A. Carollo, S. Lorenzo, J. A. Gross, G. M. Palma, F. Ciccarello, "Collisional picture of quantum optics with giant emitters", Physical Review Research 2 (4), 043070, (2020) ;

5. * A. Carollo, D. Cilluffo, F. Ciccarello, "Mechanism of decoherence-free coupling between giant atoms", Physical Review Research 2 (4), 043184 (2020) ;

6. * D. Cilluffo, G. Buonaiuto, I. Lesanovsky, A. Carollo, S. Lorenzo, G. M. Palma, F. Ciccarello, F. Carollo, "Microscopic biasing of discrete-time quantum trajectories", submitted preprint: arXiv 2007.15659 (2020) .

# Abstract

The study of the dynamics of open quantum systems sheds light on dissipative processes in quantum mechanics. Any system under continuous measurement is open and the act of measuring induces abrupt changes of the system's state (collapses). The evolution conditioned to measurement records generates the so-called quantum trajectories. A continuous (unconditioned) evolution of the system is recovered by averaging over a large number of trajectories. Historically this kind of evolution has been the main focus of theoretical investigations. In this dissertation we consider both conditional and unconditional dynamics of quantum optical systems. Unconditioned dynamics is studied through the collision model paradigm. The formalism is described in detail and used for describing generic systems featuring many quantum emitters coupled to a usually one-dimensional field. The negligible-delay regime is widely explored. Collision models are used to unveil the mechanisms underlying the decoherence-free evolution regime typical of these systems, which has received considerable attention in the last years. Then we investigate conditioned dynamics by broadening the study of statistics of quantum trajectories. Specifically, we exploit the information about the emission's full-counting statistics from large deviations to define a nonclassicality witness. Finally we come back to collision models in order to extend the theory of biased quantum trajectories from Lindblad-like dynamics to sequences of arbitrary dynamical maps, providing at once a transparent physical interpretation.

# Introduction

At macroscopic scales the effects of the laws of quantum mechanics are often hidden, so that they look really weird and counterintuitive, but become more and more evident dealing with the microscopic components of matter, if properly isolated from the external environment. Experiments on isolated, or *closed* quantum systems allowed to observe quantum superposition, correlation and entanglement and have been fundamental to test the predictions of quantum mechanics. On the other hand, the study of *open* quantum systems enabled the jump from individual systems to the description of a full quantum world encompassing systems that interact with each other in countless ways and irreversible dynamics. An open quantum system exchanges information with another one, that we call *environment*, and we are generally interested in knowing how it evolves in time.

In general system and environment get entangled, and distinguishing the former from the latter one translates into the partial trace operation over the degrees of freedom of the environment. This process returns an average continuous evolution of the system (described, in the Markovian case by the celebrated *Gorini-Kossakowsky-Sudarshan-Lindblad* (GKSL) master equation [1, 2, 3, 4]) but, on the other hand it deletes every information about exchanges of information between the two.

Notwithstanding, such exchanges are important in themselves and deserve investigation. In fact following the evolution of an open system in the laboratory corresponds typically to follow all the traces it leaves in the surrounding environment, e.g. we can say with absolute certainty that an atom prepared in an excited state has decayed if we detect the excitation (photon) emitted into the environment (electromagnetic field). Note that in general each exchange event corresponds to a sudden, instantaneous modification of the state of the system (e.g. a decaying atom changes from $|e\rangle$ to $|g\rangle$).

The discussion above, even if very simplified, encompasses two important features of the dynamics of open quantum systems, which echo the well-known existing dichotomy within continuous evolution and collapses in closed system theory. Indeed closed systems' states evolve according to the Schrödinger equation, but a measurement causes the wavefunction collapse, breaking the continuous evolution.

However, measuring is nothing but coupling the system to another one (the detector) that gathers information from it [5, 4]. An average over such information (i.e. maximizing our ignorance about the result of a measurement) returns a continuous evolution without any traces of collapses, in other words an evolution that is

*not conditioned* by past outcomes. Instead, keeping trace of the results, the evolution is said to be *conditioned*: the detector outcome is in general a signal featuring phases of continuous evolution interspersed with abrupt jumps which we call *trajectory*. Trajectories correspond to fluctuating signals obtained by monitoring single quantum systems in the laboratory [6].

In this dissertation we consider both kinds of open evolution within the context of quantum optics.

This Introduction has the purpose of guiding the reader in a simple way through these two central topics and formulating the main questions we will address in the main text. For what concerns the unconditioned evolution of open quantum systems, our main question will be how a new but well-established method for studying it, known as collision model [7, 8], extends to generic one-dimensional optical setups of great interest.

Then we focus on conditioned evolution, dealing with the information from the statistics of time records of quantum jumps occurring along the evolution of optical systems. Here also the study of the asymptotic features of quantum trajectories, although based on basic principles of thermodynamics [9], are becoming increasingly popular within the field of statistical mechanics applied to open quantum systems In this regard, the main purpose of the present study is investigating if these methods can go beyond the pure theoretical speculation and find applications in quantum optics. The answer to this question, as we will see, is yes, and not only that: we will discover that, through the lenses of thermodynamics of quantum trajectories [10], collision models theory yields us remarkable insights and also possible experimental implementations.

The study of the interaction of quantum emitters, such as multi-level systems or resonators, with a field modeled as a continuum of bosonic modes, is one of the main topics in quantum optics. For this purpose we introduce the paradigm of quantum collision models, with special attention to the extension to one-dimensional optical systems with many emitters [11, 12, 13, 14, 15, 16, 17, 18, 19, 20, 21, 22, 23, 24]. Collision models are being routinely used in various areas such as weak continuous measurements [17, 25, 26], non-Markovian quantum dynamics [8, 27, 28, 29, 30, 31, 32, 33, 34, 35, 36], quantum thermodynamics [37, 38, 39, 40, 41, 42] and even quantum gravity [43, 44]. The basic idea is decomposing the field into discrete time bins (each with an associated bosonic mode) travelling at constant speed and colliding one at a time with the emitter. The trace over the time bin's degrees of freedom yields the unconditioned evolution of the system. In layman's terms, we introduce a simplified environment simulator [4] which captures the main features of the overall environment. This responds to the idea that, in general, only few environmental degrees of freedom are decisive in driving the evolution of the system. Within the framework of waveguide QED [45, 46, 47, 48, 49, 50], time bin of one-dimensional field takes the form of discrete slices traveling in line along the waveguide. For this reason some refers to collision models in one-dimensional quantum optics as to Space Discretized

Waveguide models [51].

So far only collision models for pointlike quantum emitters were fully developed (only one coupling point). While systems with emitters featuring two coupling points were considered in the regime of long time delays [11, 12, 14], a comprehensive formulation of the negligible-delay regime (occurring in most experiments) has been lacking until now.

Recently the interest about negligible-delay regime has grown [52, 53, 54, 55, 56] because setups with multilocal (or giant) emitters coupled to a waveguide provide a platorm in which decoherence-free dynamics [57], i.e. , particular dynamics which is less sensitive to decoherence due to the form of their coupling to the dissipative environment, naturally arises. The collison model picture is not only a tool useful to derive the time evolution of open systems, but it also allows to answer to fundamental questions about the origin of such remarkable effects in waveguide QED systems.

A quantum trajectory can be defined as the evolution of a system conditioned on the results of measurements made on that system [58]. Since in general system and environment get entangled during evolution, an ideal measurement on the bath has the effect to disentangle them and, in particular, project them into a pure state.

This means that it is possible, in principle, to monitor the system by only projecting the state of the environment over an appropriate orthonormal basis. Note that this implies that we have a freedom in choosing this basis, and moreover that the same dynamics can produce infinite ensembles of quantum trajectories [26, 59, 58]. As specified before, we will focus on quantum optical systems under photon counting measurements, which corresponds to projecting the state of the environment over the Fock basis.

It is worth noting that in many situations of interest in quantum optics, such as cavity fields and atoms interacting with vacuum-state environment [4, 60], a quantum jump corresponds to the loss or the gain of a photon exchanged with the environment, hence the statistics of quantum jumps corresponds exactly to the photon counting statistics (assuming perfect detection).

Driven by this correspondence, the question arises whether the information gained through the statistical-physics approach to quantum trajectories, in particular the so-called *thermodynamics of quantum trajectories* [61] based on *large deviation theory* [62, 63, 64, 65], might prove useful for applications. This is one of the main aims of this dissertation. This approach is based on considering each trajectory as a realization of a stochastic process, and the set of all the possible realizations as a statistical ensemble. The full-counting statistics (FCS) of photon counting distribution is a very important source of knowledge about the system [66, 67, 68, 69] and offers in general a powerful theoretical method to study fluctuations in nonequilibrium quantum systems.

Within the large deviation formalism it is possible to derive the full-counting

statistics and, by consequence, characterize the trajectories ensemble through functions analogous to thermodynamic potentials.

The aforementioned correspondence between quantum jumps and measurements suggest that it could be possible to use the info from large deviation approach to make predictions about the statistical features of the emitted radiation. This, in a way, reverses the usual point of view of theory of open quantum systems, by looking at the system as to a source of radiation to be characterized. We will put forward a methodology to witness nonclassicality of the output field from a generic quantum optical setup via the statistics of time-integrated photocurrents. Specifically we will express a known nonclassicality witness (Vogel's criterion [70, 71, 72]) for bosonic fields fully in terms of the source master equation, thus bypassing the explicit calculation of the output light state.

Furthermore, large deviation theory provides powerful tools both for studying rare events or emission patterns and, more interestingly, for tuning the open system dynamics by acting on master equations, in order to enhance the occurrence of such rare events [73]. The formalism used so far did not allow to go far beyond numerical applications due to the complexity of the operations involved even for small systems nor to provide a transparent physical interpretation to them. Thus, our last question will be whether it is possible to describe such tuning simply in terms of changes performed on a microscopic model underpinning the open dynamics. We will see that it is possible just invoking collision models.

Next we provide an outline of this dissertation. The first three chapter of this dissertation consist of essentially known material. In Chapter 1 we review the basics of open quantum systems theory. In the discussion we focus on simple but paradigmatic examples to emphasize the physical motivations behind the Introduction of the well known tools, which commonly apply within the literature. We will then focus on memoryless dynamics and derive the general master equation (Lindblad master equation) governing the system's time evolution. In Chapter 2 we review the general theory of collision models. We will show how, under minimal assumptions, they are powerful in describing a wide variety of dynamics. In Chapter 3 we will focus on quantum trajectories by introducing the main tools of large deviation theory. Based on this background, in the last two chapters we present our original results. In Chapter 4 we apply collision models to derive the Lindblad master equation of a set of multi-local (giant) emitters coupled to a one-dimensional field in an arbitrary white-noise Gaussian state, which condenses into a single equation and extends a variety of quantum optics and, in particular, waveguide QED. Furthermore we will see how the collision model framework can capture the microscopic mechanism behind the emergence of nontrivial decoherence-free subspaces in these systems. In Chapter 5 we show two applications of the quantum trajectory formalism. Statistical properties of photon-counting trajectories carry remarkable information about quantum correlations of the emitters. We will express a known nonclassicality witness for bosonic fields fully in terms of the source master equation. In the last part

we present a microscopic theory for biasing the quantum trajectories is formulated, based on collision model. In this case too, collision models provide both a simplification and clear physical interpretation of the theory of biased quantum trajectories generated by the action of arbitrary dynamical maps.

Chapters on applications end with a small summary of the main results. Details about calculations and insights will be presented inside boxes, in order to avoid the use of appendices and make the text easier to read.

# Chapter 1

# Open quantum systems

> Ἄκουσον τοίνυν, υἱέ, ἅ μοι δοκεῖ δεῖν σε μή ἀγνοεῖν , καὶ νοήμων γενοῦ, ἵνα κτήσῃ κυβέρνησιν.
>
> "Hear now, my son, those things of which I think you should not be ignorant"
>
> *Constantine VII Flavius*
> *De Administrando imperio, 1*

In this chapter we introduce the basic formalism of quantum mechanics and open quantum system theory. Our goal will be the formulation of the Lindblad master equation which governs the evolution of the open quantum systems in the Markovian regime. Basic references on this subject are provided by seminal works by Kossakowsky and Lindblad [1, 2] and Refs. [4, 3, 74]. Here we will try a different approach: we highlight the limits of the usual unitary quantum theory when considering the interaction with the environment, using as example the dynamics of a decaying two-level atom.

## 1.1 Closed memoryless dynamics

The behaviour of closed quantum systems, i.e. quantum systems which do not exchange energy and matter with another one [74], is efficiently predicted according to Schrödinger equation

$$i\hbar \frac{\partial}{\partial t} |\Psi(t)\rangle = \hat{H} |\Psi(t)\rangle \tag{1.1}$$

where $\hat{H}$ is a self-adjoint operator. The formal solution of (1.1) is

$$|\Psi(t)\rangle = \hat{U}(t,t_0) |\Psi(t)\rangle \ , \ \ \hat{U}(t,t_0) = \mathcal{T} \exp\left\{ -\frac{i}{\hbar} \int_{t_0}^{t} \mathrm{d}t' \hat{H}(t'-t_0) \right\} , \tag{1.2}$$

where we introduced the unitary propagator $\hat{U}(t, t_0)$ from time $t_0$ to $t$ and the time-ordering operator $\mathcal{T}$. Unitarity of evolution operator [$\hat{U}(t, t_0)^\dagger = \hat{U}(t, t_0)^{-1}$] guarantees probability (norm) conservation and, more in general, the time invariance of scalar product between any quantum state of the system's Hilbert space $\mathcal{H}$:

$$\langle \Psi | \hat{U}^\dagger \hat{U} | \Phi \rangle = \langle \Psi | \Phi \rangle \quad \forall | \Psi \rangle, | \Phi \rangle \in \mathcal{H}. \tag{1.3}$$

The main consequence of Eq. (1.3) is that unitary time evolution is a bijection on the Hilbert space $\mathcal{H}$, implying that it is *reversible*. Note that the set of propagators has the structure of a group under matrix product operation, and in particular they satisfy *semigroup composition* (semigroup property)

$$\hat{U}(t_2, t_1) \cdot \hat{U}(t_1, t_0) = \hat{U}(t_2, t_0) \quad \text{for} \quad t_0 < t_1 < t_2. \tag{1.4}$$

Thus the time evolution of the state $|\Psi(t_0)\rangle$ from $t_0$ to $t_2$ and that of $|\Psi(t_1)\rangle$ from $t_1$ to $t_2$ will return the same state $|\Psi(t_2)\rangle$. This means that the system follows a deterministic trajectory in the state space regardless of the past history. This property is usually referred as to *lack of memory* or *Markovianity*. Remarkably, it is easy to note that Eq. (1.4) for unitary propagators implies Eq. (1.1): according to Eq. (1.4) the time evolution of a state from time $t$ to $t + \mathrm{d}t$ reads

$$|\Psi(t + dt)\rangle = \hat{U}(t + \mathrm{d}t, t_0) |\Psi(t_0)\rangle = \hat{U}(t + \mathrm{d}t, t) |\Psi(t)\rangle \,, \tag{1.5}$$

with the infinitesimal propagator given by

$$\hat{U}(t + \mathrm{d}t, t) = \mathbb{1} + \hat{G}(t)\mathrm{d}t + \mathcal{O}(\mathrm{d}t^2) \,, \quad \hat{U}(t + \mathrm{d}t, t)^\dagger \hat{U}(t + \mathrm{d}t, t) = \mathbb{1} + \mathcal{O}(\mathrm{d}t^2) \,. \tag{1.6}$$

Thus, up to the first order in $\mathrm{d}t$, it must be $\hat{G}(t) = -\hat{G}(t)^\dagger$, which implies that the generator is given by $\hat{G} = -i\hat{H}$ with $\hat{H}$ Hermitian, thus recovering Eq. (1.1). Note that the demonstration works only if non-identity terms in infinitesimal generator are proportional to the first power of $t$.

## 1.2 Non-unitary dynamics and density matrix

What we have seen in the previous paragraph changes radically when dealing with an open quantum system, i.e. a system which interacts with another one (usually referred as to external *environment* or *bath*). In this section we introduce the paradigmatic example of the decay process of a two-level atom. This example will accompany us throughout this chapter and beyond. Here we will use it to convince ourselves that:

- time evolution of open quantum systems is not unitary;
- kets are not appropriate for the description of open quantum systems.

The system under consideration is the atom, while the environment is the electromagnetic field, which we assume for simplicity to be initially the vacuum state $|0\rangle$. If the atom is initially in the excited state $|e\rangle$, after some time it will release the excitation to the environment (i.e. it emits a photon), collapsing in the ground state $|g\rangle$. If however the initial state is $|g\rangle$, the atom will remain in the ground state. This well-known transformation preserves the norm of quantum states but violates the bijectivity.

More in detail assume we can represent the environment as an ancillary two-level system (probe) coupled to the atom, and that the system-environment coupling Hamiltonian is of the form

$$\hat{H} = J(\hat{\sigma}_+^A \hat{\sigma}_-^E + \hat{\sigma}_-^A \hat{\sigma}_+^E)\,, \tag{1.7}$$

where superscripts A and E indicate the atom and the probe, respectively, and $J$ is the coupling strength. Thus we are dealing with a new closed system composed of the atom and the probe. If the state at time $t_0$ is $|\Psi(t_0)\rangle = |e\rangle_A \otimes |g\rangle_E \equiv |e\,g\rangle$, after evolution under $\hat{U}(t, t_0) = \exp\left\{-\frac{i}{\hbar}\hat{H}(t - t_0)\right\}$, we find

$$|\Psi(t)\rangle = \hat{U}(t, t_0)\,|\Psi(t_0)\rangle = \alpha\,|g\,e\rangle + \beta\,|e\,g\rangle\ , \tag{1.8}$$

where $\alpha$ and $\beta$ are complex amplitudes depending on $t$ and $J$, and $|\alpha|^2 + |\beta|^2 = 1$.

What is the state of the atom at time $t$? It's easy to convince ourselves that this state cannot be represented by a ket.

Here we assume using ordinary projective measurement (measurement theory will be reviewed in the next section). A projective measurement on the system checking whether it is in its ground or excited state is defined through the projection operators

$$\hat{P}_g = |g\rangle\langle g| \otimes \mathbb{1}\,, \tag{1.9}$$
$$\hat{P}_e = |e\rangle\langle e| \otimes \mathbb{1}\,, \tag{1.10}$$

thus we have probability $p_g = \langle\Psi(t)|\,\hat{P}_g\,|\Psi(t)\rangle = |\alpha|^2$ and $p_e = \langle\Psi(t)|\,\hat{P}_e\,|\Psi(t)\rangle = |\beta|^2$ to measure the atom in ground and excited state respectively. The state of the atom after evolution therefore can be represented as a classical average

$$\rho_A = |\alpha|^2\,|g\rangle\langle g| + |\beta|^2\,|e\rangle\langle e| = \mathrm{Tr}_E\{|\Psi(t)\rangle\langle\Psi(t)|\} = \mathrm{Tr}_E\{\rho_{AE}(t)\}\,, \tag{1.11}$$

where $\rho_A$ and $\rho_{AE} = |\Psi(t)\rangle\langle\Psi(t)|$ are matrices and $\mathrm{Tr}_E$ encodes the operation of *partial trace* over the probe's degrees of freedom. Notice that the state of the atom is no more described by a ket but through a matrix, $\rho_A$, called *density operator* of the atom. The partial trace in the last term takes the meaning of an *average* over all the possible states of the probe. Given a quantum state lying in a bipartite Hilbert space $\mathcal{H}_A \otimes \mathcal{H}_B$, partial trace over $B$ returns a state of the Hilbert space $\mathcal{H}_B$. For this reason, since the projector $\rho_{AE}(t) = |\Psi(t)\rangle\langle\Psi(t)|$ in Eq. (1.11) encodes all the

information about the joint atom-probe state, the state $\rho_A$ obtained by partial trace over probe's space is called *reduced state*.

A density operator represents an ensemble of possible quantum states of the system that occur according to a classical probability distribution, i.e. a classical (incoherent) superposition of quantum states. Density operators are Hermitian, positive and have unit trace. Like for all Hermitian operators, there are infinitely many decompositions, in particular they can be decomposed in terms of an orthonormal basis $\{|e_i\rangle\}$ of Hilbert space of the system ($\dim\{\mathcal{H}\} = d$)

$$\rho = \sum_i^d \lambda_i |e_i\rangle\langle e_i| \,. \tag{1.12}$$

A quantum state which is known without (classical) uncertainty is said to be a *pure state*. Otherwise it is *mixed*, like the state in Eq. (1.11). A pure state is what can be exactly described through a ket. States entering the average in definition Eq. (1.12) are pure. Classical probabilities $\lambda_i$ encode our uncertainty on the state under consideration. However, given a mixed state $\rho_A = \sum_i p_i(|i\rangle\langle i|)_A$, it is always possible to define a pure state $|\Psi_{AB}\rangle$ in an enlarged Hilbert space $\mathcal{H}_A \otimes \mathcal{H}_B$ such that the reduced density matrix in $\mathcal{H}_A$ corresponds to $\rho_A$

$$|\Psi_{AB}\rangle = \sum_i \sqrt{p_i}\, |i\rangle_A |i\rangle_B \,. \tag{1.13}$$

The new state is said to be a *purification* for $\rho_A$ [75]. In general for a pure state $\mathrm{Tr}\{\rho^2\} = 1$, while in general $\mathrm{Tr}\{\rho^2\} \leq 1$.

Here we introduced density matrices as the correct solution of the problem of describing open systems' states that are in general mixed (as shown in the example), but they are the most general way of defining any quantum state: a pure state's density matrix is a single projector, like the state $\rho_{AE}$ of atom-probe joint system shown in Eq. (1.11).

We conclude this section with general considerations about the time evolution of density operators. Closed systems' states evolve according to Eq. (1.1), hence, assuming unchanged statistical weights, i.e. convexity-preserving evolution

$$\rho(t) = \sum_i \lambda_i |e_i(t)\rangle\langle e_i(t)| = \sum_i \lambda_i \hat{U}(t,t_0) |e_i(0)\rangle\langle e_i(0)| \hat{U}^\dagger(t,t_0) = \hat{U}(t,t_0)\rho(t_0)\hat{U}^\dagger(t,t_0) \,. \tag{1.14}$$

Plugging Eq. (1.6) into the above equation we have

$$\rho(t + \mathrm{d}t) = \rho(t) - \frac{i}{\hbar}[\hat{H}, \rho(t)]\mathrm{d}t \,, \tag{1.15}$$

thus the infinitesimal variation of density operator (Liouville-Von Neumann equation) reads

$$\dot{\rho} = -\frac{i}{\hbar}[\hat{H}, \rho]\,, \tag{1.16}$$

which carries the same information in Eq. (1.1).

If the system is open things get complicated. Basically we start from the state $\rho_{SE}$ describing the closed system composed of the system $S$ and the environment $E$ and, from Eq. (1.14), we have

$$\rho_S(t + \mathrm{d}t) = \mathrm{Tr}_E\{\hat{U}(t + \mathrm{d}t, t)\, \rho_{SE}(t)\, \hat{U}^\dagger(t + \mathrm{d}t, t)\}\,. \tag{1.17}$$

Deriving a general analogue of Eq. (1.16) for the reduced density matrix $\rho_S$ is currently an open problem, which can be solved only in special cases.

In the following we will deepen the study of a particular class of open dynamics governed by the celebrated GKSL or *Lindblad* master equation (ME). First, however, we will focus on the structure of dynamical maps borrowing the language of measurement theory.

Actually a quantum system being measured is the most familiar example of open quantum system, as we need it to interact with a detector, which plays the role of the environment. System and detector get correlated and measurement outcomes unveil properties of the system, as we can see also in our basic example (see Eq. (1.8)). Viceversa, any Markovian open quantum dynamics can be seen as the time evolution of a system under continuous monitoring performed by a "watching environment" [4].

## 1.3 Quantum measurement theory: projection and POVMs

We briefly review the measurement theory starting from the first ones which are usually introduced: projective (orthogonal) measurements. Given an observable $\hat{A}$, i.e. an Hermitian operator on Hilbert space of the system $\mathcal{H}$, it can be decomposed as

$$\hat{A} = \sum_i a_i\, |a_i\rangle\langle a_i| = \sum_i a_i \hat{P}_i\,, \tag{1.18}$$

with $\hat{P}_i = |a_i\rangle\langle a_i|$ orthogonal projector ($\hat{P}_i\hat{P}_j = \delta_{ij}\hat{P}_j$, $\sum_i \hat{P}_i = \mathbb{1}$) onto the eigenspace with eigenvalue $a_i$. Each eigenvalue corresponds to one possible outcome of a measurement. Assuming the system in state $\rho$, the expectation value of the measurement of observable $\hat{A}$ reads

$$\mathrm{Tr}\{\rho\, \hat{A}\} = \sum_i a_i\, \mathrm{Tr}\{\rho\, \hat{P}_i\}\,, \tag{1.19}$$

which means that we can obtain the outcome $a_i$ with probability $p_i = \mathrm{Tr}\{\rho\,\hat{P}_i\}$. Given the outcome $a_i$, the normalized state of the system is

$$\rho_i = \frac{\hat{P}_i\,\rho\,\hat{P}_i}{p_i}\,. \tag{1.20}$$

Despite they are the usual paradigm of measurement in many introductory textbooks, projective measurements often do not correspond to what happens in a laboratory [75]. As an example, consider photodetection performed on the state $|\psi\rangle_S = \alpha_0\,|0\rangle + \alpha_1\,|1\rangle$ of the electromagnetic field through a unit-efficiency detector. Standard photodetectors convert radiation into electric pulses and incoming photons are usually destroyed. Thus, whatever the measurement outcome is, the final state of the electromagnetic field will be $|0\rangle$. This process cannot be described through a projective measurements scheme. Notwithstanding, as we did for the decaying atom example, we can enlarge the system by coupling it to a probe $D$ simulating the detector behaviour, with initial state $|\chi\rangle_E = |0\rangle$. The interaction, $\hat{U}_{\mathrm{SE}}$, *swaps* system and environment according to

$$\hat{U}_{\mathrm{SE}}\,|\psi\rangle_S\,|0\rangle_E = |0\rangle_S\,|\psi\rangle_E\,, \qquad \hat{U}_{\mathrm{SE}} = \begin{bmatrix} 1 & 0 & 0 & 0 \\ 0 & 0 & 1 & 0 \\ 0 & 1 & 0 & 0 \\ 0 & 0 & 0 & 1 \end{bmatrix}. \tag{1.21}$$

Then a standard projective measurement performed on $D$ ($\hat{P}_i = |i\rangle\langle i|$, $i = 0, 1$) does the job and the final state of the field is the vacuum. Since we are actually interested in the system, it is more useful to describe the process above in terms on operators acting only on the system. This can be done by projecting the evolved state in Eq. (1.21) on the state of $D$

$$\langle 0|_E\,\hat{U}_{\mathrm{SE}}\,|\psi\rangle_S\,|0\rangle_E = \hat{M}_0\,|\psi\rangle_S\,, \tag{1.22}$$

$$\langle 1|_E\,\hat{U}_{\mathrm{SE}}\,|\psi\rangle_S\,|0\rangle_E = \hat{M}_1\,|\psi\rangle_S\,, \tag{1.23}$$

where operators $\hat{M}_0 = |0\rangle\langle 0|$ and $\hat{M}_1 = |0\rangle\langle 1|$ act on the system's space and correspond to zero and one detected photon respectively, with $p_j = \langle\psi|_S\,\hat{M}_j^\dagger\hat{M}_j\,|\psi\rangle_S = |\alpha_j|^2$, $(j = 0, 1)$ associated probabilities. Note that, since $\sum_j p_j = 1$, then

$$\sum_j \hat{M}_j^\dagger\hat{M}_j = \mathbb{1}\,. \tag{1.24}$$

This scheme can be used to describe any measurement process on quantum systems. Assume the joint system-probe initial state be a product state

$$\rho(t_0) = \rho_S \otimes |0\rangle_E\langle 0|\,. \tag{1.25}$$

Then it evolves according to Eq. (1.14) and measurements on probe are introduced through the projectors $\hat{P}_k = |k\rangle_E\langle k|$

$$\hat{P}_k\,\hat{U}_{SE}\,\rho_S\otimes(|0\rangle\langle 0|)_E\,\hat{U}_{SE}^\dagger\,\hat{P}_k = \hat{M}_k\,\rho_S\,\hat{M}_k^\dagger\otimes(|k\rangle\langle k|)_E\,. \tag{1.26}$$

The probability associated to each outcome is $p_k = \mathrm{Tr}_S\{\rho_S\hat{M}_k^\dagger\hat{M}_k\}$, and normalization of probability ensures that Eq. (1.24) holds.

Since operators $\hat{M}_k$ are positive, each $\hat{M}_k$ is said to be the POVM (Positive Operator-Valued Measure) element associated to the outcome $k$ of our measurement and the set $\hat{M}_k$ is the POVM. Given an outcome $k$, the state of the system reads

$$\rho_S^{(k)} = \frac{\hat{M}_k\,\rho_S\,\hat{M}_k^\dagger}{p_k}\,, \tag{1.27}$$

which is the equivalent of Eq. (1.20) for POVMs. A projective measurement is a particular case of a POVM with Hermitian rank-1 elements [17, 75].

## 1.4 Quantum operations

We can use the same formalism to describe a generic open quantum dynamics since, as in the first example, the environment can be seen as a (in general complex) quantum system which correlates with system $S$ collecting information about its state, i.e. performing a continuous monitoring on the system [4]. Again, a projective measurement on the closed system's state $\rho_{SE}$ returns, for the reduced state $\rho_S$, the combination of all the possible outcome-conditioned states of the system with probabilities associated to each result as weights

$$\rho_S(t+\Delta t) = \sum_k p_k\,\rho_S^{(k)}(t) = \sum_k \hat{M}_k\,\rho_S(t)\,\hat{M}_k^\dagger = \mathrm{Tr}_E\{\hat{\mathcal{U}}\,\rho_S(t)\otimes(|0\rangle\langle 0|)_E\hat{\mathcal{U}}^\dagger\}\,, \tag{1.28}$$

where $\Delta t$ the duration of interaction between system and environment and the last identity comes from Eq. (1.26). Given a POVM, it is always possible to recover a unitary matrix $\hat{\mathcal{U}}$ acting on system and environment, so that the last identity holds: this important result is known as *Stinespring dilation theorem*. Note that we are assuming the environment in pure state $|0\rangle_E$, but this does not affect the generality of Eq. (1.28) since we can always take a purification of the environment.

Although measurements and evolution of systems interacting with environment can be thought as very distant concepts, the mathematical tools we use in describing them are just the same. This unified framework is known as *quantum operation formalism* [75]. In general whenever we transform a quantum state we are performing a *quantum operation*

$$\rho' = \mathcal{E}(\rho)\,, \tag{1.29}$$

where $\mathcal{E}$ is the operation or *map*, i.e. a superoperator acting on the state space associated with the system. An operation is a well-defined physical map if the following three requirements are fulfilled:

1. $\mathcal{E}$ is *trace preserving*, i.e. $\mathrm{Tr}\{\mathcal{E}(\rho)\} = 1$;
2. $\mathcal{E}$ is *convex-linear*, i.e. $\mathcal{E}(\sum_i p_i \rho_i) = \sum_i p_i \mathcal{E}(\rho_i)$
3. $\mathcal{E}$ is completely positive, i.e. for any extension of system's Hilbert space $\mathcal{H} = \mathcal{H}_S \otimes \mathcal{H}_E$, the map $\mathcal{E} \otimes \mathbb{1}_E$ is positive.

The map must transform a density matrix into a new one, so the first assumption implies the conservation of probability. We already assumed the second one in Eq. (1.14): the components of statistical mixture evolve independently of each other. Finally, the third requirement corresponds to the statement that if the system is coupled to another one which does not evolve, any density matrix describing the two systems must evolve into another well defined density matrix [76].

These three requirements are equivalent to the following definition of quantum map

$$\mathcal{E}(\rho) = \sum_k \hat{K}_k \rho \hat{K}_k^\dagger , \qquad \sum_k \hat{K}_k^\dagger \hat{K}_k = \mathbb{1} , \tag{1.30}$$

which is known as *Kraus representation* of map $\mathcal{E}$, where the $\hat{K}_k$ are linear operators acting on the system's Hilbert space. Note that this expression matches with Eq. (1.28). Here POVM elements are replaced by *Kraus operators* $\{\hat{K}_k\}$

$$\hat{K}_k = {}_E\langle k| \hat{\mathcal{U}} |0\rangle_E \tag{1.31}$$

where $\hat{\mathcal{U}}$ is the unitary operator describing the interaction between system and environment. If only one Kraus operator is sufficient for describing the action of a map, for completeness relation in Eq. (1.30), it turns out that this operator must be unitary. Thus the quantum operation framework encompasses both open and closed system dynamics.

## 1.5 Memoryless quantum map: GKSL master equation

Armed with tools of quantum operation formalism, we finally come back to the problem of finding a closed form of master equation for open quantum systems. We assume system and environment in product state at initial time $t_0$ (Eq. (1.25)) and the evolution of reduced density matrix of the system $\rho$ (from here the label $S$ will be dropped when not necessary) reads

$$\rho(t) = \Phi(t, t_0)\rho(t_0) . \tag{1.32}$$

The evolution of a closed system is unitary and memoryless in terms of Eq. (1.4). We now relax the unitary constraint but we keep the Markov property, which in the quantum map formalism takes the form

$$\Phi(t, t_0) = \Phi(t, t_1)\, \Phi(t_1, t_0) \ , \quad t_0 < t_1 < t. \tag{1.33}$$

Thus, under these hypotheses, we have

$$\rho(t + \mathrm{d}t) = \Phi(t + \mathrm{d}t, t)\, \rho(t) = \sum_k \hat{K}_k\, \rho(t)\, \hat{K}_k^\dagger \,, \tag{1.34}$$

where dependences of Kraus operators on time are omitted. We also require that the analogous of Eq. (1.6) for maps holds

$$\Phi(t + \mathrm{d}t, t) = \mathcal{I} + \mathcal{G}\mathrm{d}t \,, \tag{1.35}$$

where $\mathcal{I}$ is the identity map and $\mathcal{G}$ is a quantum map that in general depends on time. We take the following expansion of Kraus operators in time

$$\hat{K}_k = \hat{K}_k^{(0)} + \hat{K}_k^{(1)} \mathrm{d}t + \mathcal{O}(\mathrm{d}t^2) \,. \tag{1.36}$$

According to Eq. (1.35), for $\mathrm{d}t = 0$ the map reduces to the identity map $\mathcal{I}(\rho) = \mathbb{1}\,\rho\,\mathbb{1}$, thus only one of the Kraus operators must have the identity as zero-th order component (we choose $\hat{K}_0^{(0)}$), and $\hat{K}_k^{(0)} = 0$ if $k \neq 0$. This condition unveils that expansion in Eq. (1.36) is not correct for describing open systems, since contributions of $\hat{K}_{k\neq 0}$ are $\propto \mathrm{d}t^2$ and the map reduces to only one Kraus operator, $\hat{K}_0\,\rho\,\hat{K}_0^\dagger$ ($\hat{K}_0^\dagger\,\hat{K}_0 = \mathbb{1}$) up to the first-order in $\mathrm{d}t$, i.e. the evolution must be unitary. Since the map depends quadratically on Kraus operators, we take the $\sqrt{\mathrm{d}t}$-expansion

$$\hat{K}_k = \hat{K}_k^{(0)} + \hat{K}_k^{(1)}\, \sqrt{\mathrm{d}t} + \hat{K}_k^{(2)}\, \mathrm{d}t + \mathcal{O}(\mathrm{d}t^2) \,. \tag{1.37}$$

Constraint on $\hat{K}_0^{(0)}$ still holds and, in addition, we have $\hat{K}_0^{(1)} = 0$ because at lower order there should be no terms $\propto \sqrt{\mathrm{d}t}$ (cf. Eq. (1.35)). Plugging Eq. (1.36) in Eq. (1.34) (we omit the time dependence of $\rho$) we get

$$\sum_k \hat{K}_k\,\rho\,\hat{K}_k^\dagger = \rho + \hat{K}_0^{(2)}\rho\,\mathrm{d}t + \rho\hat{K}_0^{(2)\,\dagger}\,\mathrm{d}t + \sum_{k\neq 0} \hat{K}_k^{(1)}\,\rho\,\hat{K}_k^{(1)\,\dagger}\,\mathrm{d}t \,, \tag{1.38}$$

which leads to the finite-difference equation

$$\frac{\mathrm{d}\rho}{\mathrm{d}t} = \hat{A}\,\rho + \rho\,\hat{A}^\dagger + \sum_k \hat{L}_k\,\rho\,\hat{L}_k^\dagger \,, \tag{1.39}$$

where for the sake of clarity we replaced $\hat{K}_0^{(2)}$ by $\hat{A}$ and $\hat{K}_k^{(1)}$ by $\hat{L}_k$. In terms of the hermitian and anti-hermitian parts of $\hat{A}$, $\hat{K} = \frac{1}{2}(\hat{A} + \hat{A}^\dagger)$ and $-i\,\hat{H} = \frac{1}{2}(\hat{A} - \hat{A}^\dagger)$

respectively, we get

$$\frac{\mathrm{d}\rho}{\mathrm{d}t} = -i[\hat{H},\rho] + \{\hat{K},\rho\} + \sum_k \hat{L}_k\,\rho\,\hat{L}_k^\dagger\,. \tag{1.40}$$

Due to the completeness relation Eq. (1.30)

$$\sum_k \hat{K}_k^\dagger\,\hat{K}_k = \mathbb{1} + \sum_k \hat{L}_k^\dagger\,\hat{L}_k\,\mathrm{d}t + 2\hat{K}\,\mathrm{d}t \quad\Rightarrow\quad \hat{K} = -\frac{1}{2}\hat{L}_k^\dagger\,\hat{L}_k\,, \tag{1.41}$$

we finally end up with the GKSL or *Lindlad master equation*

$$\dot{\rho} = -i[\hat{H},\rho] + \sum_k \left(\hat{L}_k\,\rho\,\hat{L}_k^\dagger - \frac{1}{2}\{\hat{L}_k^\dagger\,\hat{L}_k,\rho\}\right)\,. \tag{1.42}$$

The Lindblad master equation is the most general way to describe the evolution of a density matrix under the Markov hypothesis.

# Chapter 2

# Memoryless Collision models and stochastic evolution

Si può fare con il collisionale.

"It can be done using collision models."

*Francesco Ciccarello*

Quantum Collision Models for open quantum systems were first introduced in [77] and have been a recurrent subject in the past 50 years, within the context of weak measurements theory [26], non-Markovian quantum dynamics [78] and, with a wide variety of applications, in quantum thermodynamics [41]. The basic idea is to describe the interaction between a quantum system and its environment as resulting from repeated interactions with ancillary systems (probes) which jointly embody the environment. So far collision models have been mainly intended as toy models enabling to tackle conceptual problems in open quantum systems theory, which would be most probably intractable with standard microscopic models. Notwithstanding, even in the case of Markovian dynamics, the collision model description often turns out to be a powerful and advantageous tool to work out MEs in a simpler way compared to traditional methods [3]. On the other hand, the repeated interaction pattern allows a deeper understanding of interesting phenomena occurring in optical systems. In the first part of this chapter we will review the formalism of memoryless collision models considering an abstract model in which system and environment are unspecified. The goal will be the full derivation of the Lindblad ME (cf. Eq. (1.42)) under minimal hypotheses. The model described in the first part provides theoretical foundation of applications in Chapter 4. The second part will be devoted to the study of *conditioned evolution* of quantum states and formulation of stochastic Schrödinger equation for photon counting within the collision model formalism. This result will allow us to introduce and discuss the thermodynamic formalism of quantum trajectories and applications in the next chapters.

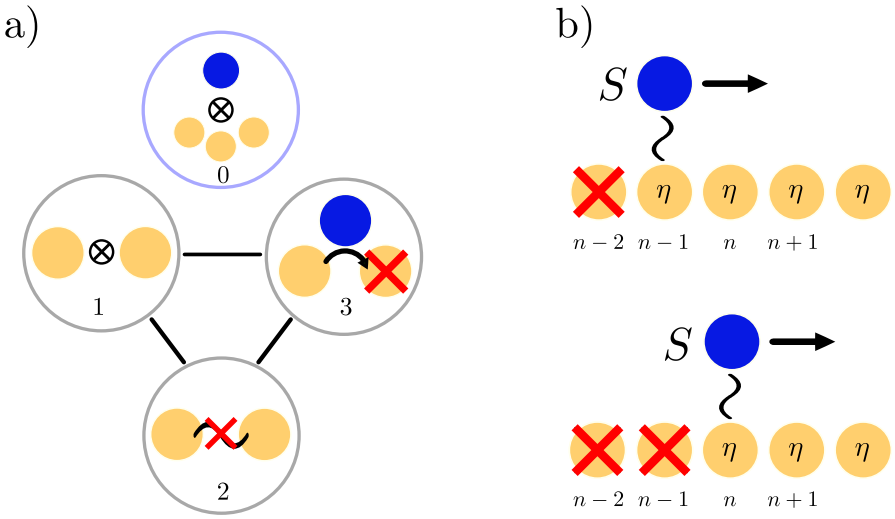


FIGURE 2.1: Basic memoryless collision model. The system (blue ball) interacts with the environment composed of a collection of ancillae (yellow balls) sharing a common state. (a): Conditions 2.1: ancillae are uncorrelated (1) and non-interacting (2); each ancilla interacts with the system only once, then it is discarded (3). Additionally, system and bath are initially uncorrelated (0). (b): Sketch of a memoryless collision model. Top: the $n-1$-th collision between $S$ and ancilla. After interacting (bottom) they are disentangled and ancilla is discarded. Then the system interacts with the next ancilla and cycle repeats.

## 2.1 Review of Collision Models

The main idea underpinning collision models can be summarized in few lines: a quantum system $S$ interacts with an environment (or bath) $E$ composed of a large collection of identical probes (ancillae) in a common initial state $\eta$. The system evolves through a sequence of pairwise interactions with each probe, we call *collisions*. Although the model looks quite simple, it can describe a wide variety of complex dynamics depending on the assumptions we make about the form of the interaction and the dynamics of the probes.

We will consider the following three minimal assumptions (see Fig. 2.1):

1. probes are uncorrelated, i.e. the initial state of the bath is $(\eta \otimes \eta \otimes ...)$;
2. probes do not interact with each other;
3. each probe is discarded after the interaction with the system and is replaced with a fresh one before the next collision.

As *zeroth assumption* we also have Eq. (1.25), which in this context reads

$$\sigma_0 = \rho_0 \otimes (\eta \otimes \eta \otimes ...)\,, \tag{2.1}$$

where subscript 0 indicates the initial time, $\sigma$ the joint system-environment state and $\rho_0$ is the state of $S$.

We now demonstrate that these assumptions imply the system undergoes a Markovian dynamics, thus we can derive a ME in Lindblad form in order to describe the dynamics of the system.

Each collision is a unitary transform $\hat{U}_n$ involving system and probe for a time $\Delta t$, generated by the global Hamiltonian

$$\hat{H}_n = \hat{H}_S + \hat{V}_{S\,n}\,, \tag{2.2}$$

where $\hat{H}_S = \omega_0\,\hat{h}_S$ is the free Hamiltonian of the system at the characteristic frequency $\omega_0$ while $\hat{V}_{S\,n} = g\,\hat{v}_{S\,n}$ couples the system and the $n$-th ancilla at the characteristic frequency $g$. After $n$ collisions, according to assumptions 2.1, the state of the system will read

$$\rho_n = \mathrm{Tr}_B\{\hat{U}_n ... \hat{U}_1\,\sigma_0\,\hat{U}_1^\dagger ... \hat{U}_n^\dagger\} = \mathrm{Tr}_{B_n}\{\hat{U}_n\,\rho_{n-1}\,\eta\,\hat{U}_n^\dagger\}\,, \tag{2.3}$$

which, in terms of the completely positive map

$$\mathcal{E}[\rho] = \mathrm{Tr}_{B_n}\{\hat{U}_n\,\rho\,\eta\,\hat{U}_n^\dagger\} \tag{2.4}$$

can be expressed as

$$\rho_n = \mathcal{E}[\rho_{n-1}] = \mathcal{E}^n[\rho_0]\,. \tag{2.5}$$

Note that the last identity is a discrete version of the semigroup property in Eq. (1.4). Thus a collision model under hypotheses 2.1 returns a Markovian dynamics. We expect this dynamics to be governed by a Lindblad ME in the continuous time limit.

For small $\Delta t$ and assuming $\omega_0 \ll g$ we expand the collision unitary as (from now on we take $\hbar = 1$)

$$\hat{U}_n = e^{-i\hat{H}_n\Delta t} = \mathbb{1} - i(\hat{H}_S + \hat{V}_{S\,n})\,\Delta t - \frac{\hat{V}_{S\,n}^2}{2}\,\Delta t^2 + \mathcal{O}(\Delta t^3)\,, \tag{2.6}$$

and the variation of the state per unit step reads

$$\Delta\rho_n = -i[\hat{H}_S, \rho_n]\Delta t - i\,\mathrm{Tr}_{B_n}\{[\hat{V}_{S\,n}, \rho\,\eta]\}\Delta t + i\,\mathrm{Tr}_{B_n}\left\{\hat{V}_{S\,n}\,\rho\eta\,\hat{V}_{S\,n} - \frac{1}{2}[\hat{V}_{S\,n}^2, \rho\,\eta]_+\right\}\Delta t^2\,, \tag{2.7}$$

where $[\ ,\ ]_+$ denotes the anti-commutator parenthesis. Plugging now the definition of corrected system Hamiltonian

$$\hat{H}_S' = \hat{H}_S + g\mathrm{Tr}_{B_n}\{\hat{v}_{S\,n}\eta\}\,, \tag{2.8}$$

and dissipator

$$\mathcal{D}[\rho] = \Gamma \sum_{ij} \left( \hat{L}_{ij}\, \rho\, \hat{L}_{ij}^{\dagger} - \frac{1}{2} [\hat{L}_{ij}^{\dagger}\, \hat{L}_{ij}, \rho]_{+} \right) , \tag{2.9}$$

with $\hat{L}_{ij} = \sqrt{p_j} \langle i|\hat{v}_{S\,n}|j\rangle$, being $p_j$ the classical probabilities defining the state of probes ($\eta = \sum_k p_k |k\rangle\langle k|$), and $\Gamma = g^2 \Delta t$, we have the finite differences master equation

$$\frac{\Delta \rho_n}{\Delta t} = -i\, [\hat{H}'_S, \rho_n] + \mathcal{D}[\rho_n]\, . \tag{2.10}$$

In the limit $\Delta t \to 0$ and $g \to \infty$ (keeping $\Gamma$ positive and finite) we achieve the continuous-time limit

$$\frac{\mathrm{d}\rho}{\mathrm{d}t} = -i\, [\hat{H}_S + \hat{H}'_S\, , \rho] + \mathcal{D}[\rho]\, , \tag{2.11}$$

which corresponds to the Lindblad ME (1.42). In general $\hat{H}'_S$ can diverge as $g \to \infty$, but, as we will see later on, in many typical situations it is finite or zero. By the way it represents an energy shift we can get around by renormalizing the free Hamiltonian of the system [7]. Remarkably, note that at this point we did not make any assumption on the specific system and ancilla we are considering, but the intrinsic memorylessness of the collision model leads to a Lindblad ME. Therefore, conversely, any Markovian dynamics can in principle be described through an appropriate collision model.

The abstract model above is useful to describe how collision models work, but in general a collisional description of open dynamics requires appropriate processing of the system-environment coupling Hamiltonian, returning the discretized coupling Hamiltonian $\hat{V}_{S\,n}$ from a system-bath microscopic model. In chapter 4 the collision model description will be decisive in understanding the microscopic physical mechanisms underlying a wide variety of phenomena of practical interest in quantum optics.

## 2.2 Quantum trajectories

In Chapter 1 we have shown how any open dynamics can be described as the evolution of a system under continuous measurement performed by another one we call environment. The key step from Eq. (1.27) and (1.28) consists in averaging over all the possible outcomes $k$ of the POVM, yielding an unconditioned evolution for the open system's state. Here we step back to conditioned states $\rho^{(k)}$. Conditioned states are curious object whose dynamics exhibits the *double face* of quantum theory: a continuous evolution ruled by Shrödinger's equation (Eq. (1.1)) punctuated by sudden jumps corresponding to instantaneous, discontinuous change of state whenever the system is observed, i.e. a measurement is performed. Within collision model

framework, we will formulate here the equation governing the evolution of conditioned states, which, predictably, will feature an explicit measurement-depending term. Thus we expect to find a *stochastic* master equation (SME). Differently with respect to what we have seen in the previous section, we will now *read* the state of each ancilla through a projective measurement before throwing it away. Without loss of generality we will assume the system in a pure initial state. This entitles us to use kets instead of density operators in the following. SMEs solutions are patterns in space-state of the system usually named *quantum trajectories* [4, 26]. On the other hand, there is a one-to-one correspondence between each jump occurring in system evolution and outcomes of projective measurement on ancillae, therefore in some literature the complementar point of view is preferred, and quantum trajectory takes the meaning of *quantum jump trajectory* (see Fig. 2.2), i.e. the time record of such outcomes (see e.g. [79] for photodetection trajectories). In this work we will refer mainly to this latter definition of trajectories if not otherwise specified.

### 2.2.1 Stochastic Schrödinger equation for photon counting

Consider the abstract collision model presented in Sec. 2.1, and the unitary-collision expansion in Eq. (2.6) which we report here for convenience

$$\hat{U}_n = \mathbb{1} - i\,(\omega_0\,\hat{h}_S + g\,\hat{v}_{Sn})\,\Delta t - \frac{g^2}{2}\hat{v}_{Sn}^2\,\Delta t^2 + \mathcal{O}(\Delta t^3)\,. \tag{2.12}$$

Since $g = \sqrt{\dfrac{\Gamma}{\Delta t}}$ we have

$$\hat{U}_n = \mathbb{1} - i\,\omega_0\,\hat{h}_S\Delta t + \sqrt{\Gamma\,\Delta t}\,\hat{v}_{Sn} - \frac{\Gamma}{2}\hat{v}_{Sn}^2\,\Delta t + \mathcal{O}(\Delta t^3)\,. \tag{2.13}$$

At time $t$, before the collision, system and environment are in product state $|\psi\rangle_t = |\psi_S\rangle \otimes |0_E\rangle$ (cf. Eq. (1.25)), thus after the collision the joint state reads

$$|\psi\rangle_{t+\Delta t} = (\mathbb{1} - i\,\omega_0\,\hat{h}_S\Delta t)\,|\psi_S\rangle\;|0_E\rangle + \sqrt{\Gamma\,\Delta t}\hat{v}_{Sn}\,|\psi_S\rangle\;|0_E\rangle - \frac{\Gamma}{2}\hat{v}_{Sn}^2\,\Delta t\,|\psi_S\rangle\;|0_E\rangle\;. \tag{2.14}$$

We are now at the point in which we must choose what kind of measurement we want to describe, i.e. onto which basis ancilla's state is going to be projected after collision. We call this operation *defining an unraveling* [17, 26, 80]. In particular, for the purpose of this work, we aim to describe photoncounting measurements, thus we will project the state of the ancilla onto the $z$ basis $\{|0\rangle, |1\rangle\}_E$. The jump operators is then defined as $\hat{L} = \langle 1|\hat{v}_{Sn}|0\rangle$ (we assume, for simplicity $\langle j|\hat{v}_{Sn}|j\rangle = 0$ [26]), and we recast Eq. (2.14) as

$$|\psi\rangle_{t+\Delta t} - |\psi\rangle_t = \sqrt{\Gamma\Delta t}\,\hat{L}\,|\psi_S\rangle\,|1_E\rangle - i\,\Delta t\,\hat{H}_{\text{eff}}\,|\psi_S\rangle\,|0_E\rangle\;, \tag{2.15}$$

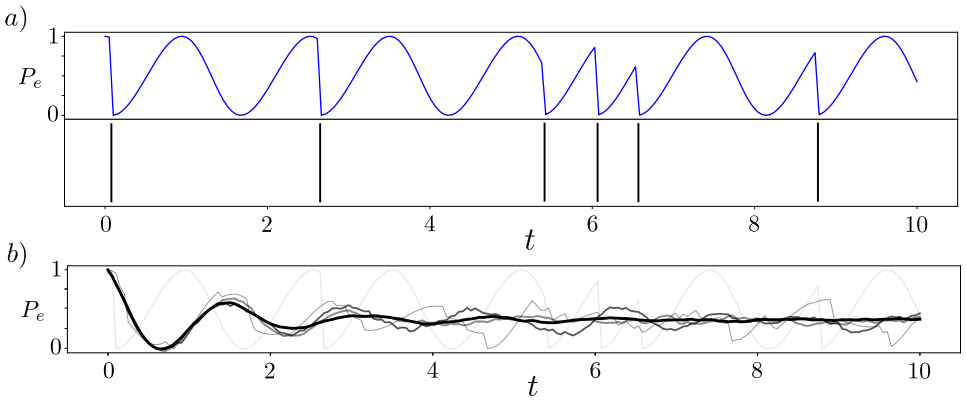


FIGURE 2.2: Population $P_e$ of the excited state of a coherently driven two-level system with damping. (a) Stochastic evolution of population. The clearly visible Rabi oscillations are broken by abrupt changes (jumps) in populations. On the bottom the correspondent quantum jump trajectory. (b) Averaged continuous evolution. The continuous evolution (black curve) is recovered by averaging over a large number of trajectories. Grayscale curves correspond to averages over an increasing number of trajectories.

where we defined the non-Hermitian effective Hamiltonian $\hat{H}_{\text{eff}} = \omega_0 \hat{h}_S - \frac{i\Gamma}{2}\hat{L}^\dagger\hat{L}$. In the equation above are clearly identifiable the two kinds of evolution the system undergoes: note that the first term, which describes changes in ancilla's state, i.e. emission, is $\propto \sqrt{\Delta t}$. The latter ($\propto \Delta t$) keeps the anicilla's state unchanged, resulting in no emission and free evolution of the system. If the measurement outcome is 0, then the state of the system will read

$$|\psi_S\rangle^{(0)}_{t+\Delta t} = \frac{\left(\mathbb{1} - i\hat{H}_{\text{eff}}\Delta t\right)|\psi_S\rangle_t}{\sqrt{\langle\psi_S|\,\mathbb{1} + i\left(\hat{H}^\dagger_{\text{eff}} - \hat{H}_{\text{eff}}\right)\Delta t\,|\psi_S\rangle}} \simeq \left(\mathbb{1} - i\hat{H}_{\text{eff}}\Delta t + \frac{\Gamma}{2}\langle\hat{L}^\dagger\hat{L}\rangle\Delta t\right)|\psi_S\rangle_t \tag{2.16}$$

where the last approximation holds in the limit of small collision times. The result is a small perturbative change of the state of the system (continuous evolution). Conversely, if the measurement returns 1 we have an abrupt change

$$|\psi_S\rangle^{(1)}_{t+\Delta t} = \frac{\hat{L}\,|\psi_S\rangle_t}{\sqrt{\langle\hat{L}^\dagger\hat{L}\rangle}}\,. \tag{2.17}$$

Combining the last two results, the *Stochastic Schrödinger equation* (SSE) is finally achieved

$$|\psi_S\rangle_{t+\Delta t} - |\psi_S\rangle_t = \left(-i\hat{H}_{\text{eff}} + \frac{\Gamma}{2}\langle\hat{L}^\dagger\hat{L}\rangle\right)|\psi_S\rangle_t\,\Delta t + \left(\frac{\hat{L}}{\sqrt{\langle\hat{L}^\dagger\hat{L}\rangle}} - \mathbb{1}\right)|\psi_S\rangle_t\,\delta N \tag{2.18}$$

where $\delta N$ is a stochastic variable (noise) giving the result of measurement on the ancilla. In the case of photon counting we deal with Poissonian noise, i.e. $(\delta N)^2 =$

$\delta N$ and $\langle \delta N \rangle = \langle \hat{L}^\dagger \hat{L} \rangle \Gamma \Delta t$. A quantum jump trajectory is then the time record of the values the stochastic variable $\delta N$ takes during the evolution, and represents in all respect a signature of the interaction between system and environment probes. Averaging over the stochastic process corresponds to tracing over the environment and lead us to the deterministic evolution Eq. (1.42) [59] (see Fig. 2.2-b). This is the working principle of quantum jump MonteCarlo method for solving the dynamics of open quantum systems [4].

# Chapter 3

# Thermodynamics of quantum trajectories

> "Why do we deal with the subject now at all? Why not wait a half a year, or a year, until we know the mathematics of probability better, and we learn a little quantum mechanics, and then we can do it in a more fundamental way? The answer is that it is a difficult subject, and the best way to learn is to do it slowly!"
>
> *Richard Feynman, Lectures on Physics 1, 39-1*

According to classical thermodynamics, the observed macroscopical state of a system is the result of the coexistence of microscopic configurations (*microstates*) which determine the value of measurable quantities (observables). In terms of generalized coordinates, each state is represented by a point $\sigma$ in the phase space $\Sigma$ and the outcome of a measurement of a generic observable $f$ is the well-known ensemble average [81]

$$\langle f \rangle = \int_{\Sigma} d\,\sigma\, f(\sigma)\Delta(\sigma)\,, \tag{3.1}$$

where $\Delta(\sigma)$ is a normalized density function in phase space. The values of observable quantities shared by the *overwhelming majority* of available microstates result in the *typical* state of system [9], whereas *atypical* configurations determine fluctuations. Even in the simplest scenario, typical and often trivial microstates can coexist together with configurations having features dramatically far from typicality. From Eq. (3.1) one can straightforwardly note that a change of system capable of turning rare events typical requires changes in $\Delta(\sigma)$ which definitly depend on extensive parameters of the system. Note that in principle this may involve deep changes in the dynamics of microscopic components of the system (note that the expression of $\Delta(\sigma)$ determines the statistical ensemble consistent with the observed behaviour of the systems [81]). In recent works [82] it has been shown that quantum jump trajectories define a statistical ensemble for the emission dynamics just like microstates do for classical thermodynamics. Statistics of trajectories and modifications of the

dynamics enhancing atypical events, i.e. changing the density in phase space, have been studied in the context of Large Deviation theory [10, 83]. In this chapter we present the fundamentals of large deviation theory with the aim to introduce the tools that we will employ to study photon counting in Chapter 5. An comprehensive discussion of large deviation theory is out of the scope of this dissertation. Here we provide a self-consistent "practical" picture. Further details about large deviation theory can be found in Refs. [62, 63, 64].

## 3.1 Elements of Large Deviation theory

Consider a stochastic discrete variable $X$ and the empirical mean over a sample of size $N$

$$\langle X \rangle_N = \frac{1}{N} \sum_{n=0}^{N} X_n \,. \tag{3.2}$$

In the limit of large $N$ the behaviour of the empirical mean is described by the Law of Large Numbers. The Central Limit Theorem rules small fluctuations around the asymptotic value. The Large Deviation Theory instead describes large fluctuations and rare events and can be seen as a generalization of the Central Limit Theorem. In general, let us consider the stochastic variable

$$A_N = \frac{1}{N} \sum_{n=0}^{N} f(X_n) \,, \tag{3.3}$$

with $f$ a function of the random variable. Let $P(A_N \in B)$ be the probability that the variable $A_N$ takes a value in the set $B$. The probability $P$ is said to satisfy a large deviation principle with rate $\varphi_B$ if the following limit

$$\lim_{N\to\infty} -\frac{1}{N} \log P(A_N \in B) = \varphi_B \tag{3.4}$$

exists or, in other words, if

$$P(A_N \in B) \xrightarrow[N\to\infty]{} e^{-N\varphi_B} \,. \tag{3.5}$$

For continuous stochastic variables one just needs to consider probability densities $p(A_N = b)db = P(A_N \in [b, b+db])$, and in the large $N$ limit

$$\lim_{N\to\infty} -\frac{1}{N} \log P(A_N \in [b, b+db]) = -\lim_{N\to\infty} \left( \frac{1}{N} \log p(A_N = b) + \log(db) \right) = \varphi(b) \,, \tag{3.6}$$

where we assumed $db \neq 0$.

Rate functions (also called *Cramér functions*) encode all the information about the behaviour of the stochastic process $A_N$ at large $N$. In particular for values of $b$ such

that $\varphi(b) \neq 0$ the probabilities decrease exponentially as $N$ grows, whereas they survive as $\varphi$ approaches zero, corresponding to a certain value $\tilde{b}$. We call the latter *typical* values, and *untypical* or *rare* the former. Thus large deviation theory can be defined, in practice, as a set of efficient tools to establish if a large deviation principle holds for a given stochastic process and to evaluate the corresponding rate function.

Deriving rate functions through direct calculation of limit in Eq. (3.6) in general may be non-trivial. We next introduce a fundamental result due to Gärtner and Ellis that will be useful in practical situations and allow to circumvent the problem.

**Theorem 1** *(Gärtner-Ellis)*

*Let $A_N$ be a random variable indexed by positive integers $N$ and let us define the scaled cumulant generating function of $A_N$ as*

$$\theta(s) = \lim_{N\to\infty} \frac{1}{N} \log\langle e^{NsA_N}\rangle \,, \tag{3.7}$$

*with $s \in \mathbb{R}$ and*

$$\langle e^{NsA_N}\rangle = \int_{\mathbb{R}} da\, e^{Nsa} p(A_N = a) \,, \tag{3.8}$$

*the moment generating function of the variable $A_N$. If $\theta(s)$ exists and is differentiable $\forall s \in \mathbb{R}$, then it is possible to formulate a large deviation principle for $p(A_N)$ as*

$$p(A_N) \simeq e^{-N\varphi(a)} \tag{3.9}$$

*with the rate function given by the Legendre-Fenchel transform*

$$\varphi(a) = \sup_{s\in\mathbb{R}} \{sa - \theta(s)\} \,. \tag{3.10}$$

The Gärtner-Ellis Theorem includes two fundamental results: it characterizes the asymptotic behaviour of scaled cumulant generating function through the function $\theta(s)$. On the other hand, it provides a way to calculate the rate $\varphi(a)$. Another remarkable consequence is that, since rate functions are Legendre-Fenchel transforms, they are convex functions and, by inversion, $\theta(s) = \sup_a \{sa - \varphi(a)\}$. This implies that rate functions are always non-negative since $\theta(s = 0) = 0$ by definition. On the other hand, this was expected since a negative value of $\varphi$ leads to a diverging probability.

In the case that the rate function has a global minimum $a_0$, i.e. $\varphi(a_0) = 0$, the expansion around $a_0$ up to the 2nd order in $a$ reads

$$\varphi(a) \simeq \frac{1}{2} \partial_a^2 \varphi\Big|_{a_0} (a - a_0)^2 \,, \tag{3.11}$$

hence the probability density can be approximated as

$$p(A_N = a) \simeq e^{-\frac{1}{2}\partial_a^2\varphi|_{a_0}(a-a_0)^2} \,, \tag{3.12}$$

which is a form of the Central Limit theorem. This Gaussian approximation works in a small range around the typical value, whereas adding terms to the expansion in Eq. (3.11) allows to encompass more details about the behaviour of the distribution $p(a)$ far from $a_0$, up to the tails (hence the name *large deviation*).

## 3.2 Large deviation theory of Markov processes

In this section we show the application of large deviation theory to homogeneous Markov processes (see Box 1).This example is paradigmatic since it marks the starting point for applying large deviations to quantum trajectories in quantum Markovian dynamics.

### Box 1: Markov processes: definitions and notation

A generic stochastic process $\{X_i\}$ (with $X_i$ belonging to a finite set) is called *stationary* if

$$p(X_1 = x_1, X_2 = x_2, ..., X_n = x_n) = p(X_{1+m} = x_1, X_{2+m} = x_2, ..., X_{n+m} = x_n) \quad \forall n, m\,, \tag{3.13}$$

i.e. the joint probability is invariant under arbitrary index shifts. $X_i$ takes the name of *state* of the process at *time* n. The process is a *Markov process* if, for $n \in \mathbb{N}$,

$$p(X_{n+1} = x_{n+1}|X_n = x_n, X_{n-1} = x_{n-1}, ..., X_1 = x_1) = p(X_{n+1} = x_{n+1}|X_n = x_n)\,, \tag{3.14}$$

thus the joint probability distribution reads

$$p(x_1, x_2, ..., x_n) = p(x_1)p(x_2|x_1)...p(x_n|x_{n-1})\,, \tag{3.15}$$

which is the analogous of property (1.4) for probabilities. A Markov process in which $p(x_{n+1}|x_n)$ does not depend on $n$ is called *homogeneous* and is characterized only by the initial state and a *probability transition matrix* $P = P_{ij}$, with $P_{ij} = p(X_{n+1} = i|X_n = j)$. A Markov process is said to be *irreducible* if, starting from a state $X_i$, it is possible to reach any other state in a finite number of steps. If $P_{ii} \neq 0 \forall i$, i.e. the minimum path from $X_i$ to itself has only one step, the Markov process is called *aperiodic*. Finally it can be proved that a Markov process which is irreducible and aperiodic (*ergodic*) features a unique stationary distribution

$$p(x_{n+1}) = \sum_{x_n} p(x_n) P_{x_n x_{n+1}}\,. \tag{3.16}$$

We denote with $\{X_i\}$ the Markov process and consider the sample mean in Eq. (3.3) with each $X_i$ belonging to a set denoted with $\Lambda$, and $f : \Lambda \to \mathbb{R}^d$, $d \geq 1$. Hence the joint probability distribution (cf. Eq. (3.15) in Box 1) reads

$$p(X_1, X_2, ..., X_N) = p(X_1) \prod_{i=2}^{n} p(X_i|X_{i-1})\,. \tag{3.17}$$

Our goal is deriving the large deviation principle for this probability distribution. The associated moment generating function is

$$\langle e^{NsA_N} \rangle = \sum_{\{X_i\}} p(X_1) e^{s \cdot f(X_1)} p(X_2|X_1) e^{s \cdot f(X_2)} ... p(X_N|X_{N-1}) e^{s \cdot f(X_N)} \,. \tag{3.18}$$

Defining the *biased* probabilities

$$p_s(X_1) := p_s(X_1) e^{s \cdot f(X_1)} \tag{3.19}$$

$$p_s(X_i|X_{i-1}) := p(X_i|X_{i-1}) e^{s \cdot f(X_i)} \,, \tag{3.20}$$

and plugging them into Eq. (3.18) we have

$$\langle e^{NsA_N} \rangle = \sum_{\{X_i\}} p_s(X_1) p_s(X_2|X_1) ... p_s(X_N|X_{N-1}) \,. \tag{3.21}$$

This expression can be further simplified as follows. Consider the simple case of a single step in a Markov process with only two distinct states, i.e. $\Lambda = \{a, b\}$. Thus in this case the moment generating function reads

$$\begin{aligned} \sum_{X_1, X_2 = a,b} p_s(X_1) p_s(X_2|X_1) &= p_s(a) p_s(a|a) + p_s(a) p_s(b|a) + p_s(b) p_s(a|b) + p_s(b) p_s(b|b) \\ &= \sum_{j \in \Lambda} (\mathbf{P}_s \cdot \mathbf{p}_s)_j \,. \end{aligned} \tag{3.22}$$

Where $(\mathbf{P}_s)_{ji} = p_s(j|i)$ are the elements of the transition matrix and we defined the probability vector $(\mathbf{p}_s)_i = p_s(X_1 = i)$. The extension to $N$ steps yields

$$\langle e^{NsA_N} \rangle = \sum_{j \in \Lambda} (\mathbf{P}_s^{N-1} \cdot \mathbf{p}_s)_j \,. \tag{3.23}$$

The asymptotic behaviour of moment generating function depends on the behaviour of transition matrix $\mathbb{P}_s^N$ as $N \to \infty$. If the Markov process is ergodic, then there is a unique stationary probability distribution and the transition matrix, according to Perron-Frobenius theorem [84], has a unique *dominant* eigenvalue $\Theta(P_s)$. For large $N$ the contribution of $\Theta(P_N)$ will be the most relevant, i.e. $\langle e^{NsA_N} \rangle \simeq \Theta(P_s)^N$ and the smaller eigenvalues, together with the related components of $\mathbf{p}_s$, will be neglected. Thus, according to Eq. (3.7)

$$\theta(s) = \log \Theta(P_s) \,, \tag{3.24}$$

hence the rate function reads (cf. Eq. (3.10))

$$\varphi(k) = \sup_s \{k \cdot s - \log \Theta(P_s)\} \,. \tag{3.25}$$

The above provides a general recipe to work out rate functions for ergodic Markov processes. For completeness we conclude this section by commenting also the cases

in which the process is not ergodic. If the Markov process is not irreducible we have more than one stationary distribution and a rate function exists but strictly depends on the initial state. In terms of transition matrix elements, there are several competing eigenvalues. Finally, if the process is periodic there are no stationary distributions and the large deviation principle in the form above does not hold [63].

## 3.3 Large deviations in open quantum systems

The formalism in the previous sections can be employed *mutatis mutandis* for describing quantum Markovian dynamics. We will assume that the considered Markov processes are ergodic or at least aperiodic. The main goal of this section is to provide a non-comprehensive but essential explanation of the way in which large deviation theory tools can be used to infer long-time properties of the unconditional dynamics $\rho(t)$ and the respective quantum jump trajectories.

Quantum jump operators $\hat{L}_j$ in Eqs. (1.42) and (2.18) describe non-unitary relaxation processes. Here we call *event* the action of a specific jump operator on the system. In these terms a quantum trajectory is a collection of time-ordered events. In practical problems we will often focus on events due to a single jump operator, but in general we have the freedom of choosing which subset of the jump operators generates an event and which do not. Let $K$ be the number of such events after time $t$ and $\rho^{(K)}(t)$ the reduced density matrix of the system obtained by projecting the full density operator $\rho_S$ onto the subspace with $K$ recorded events [60], i.e.

$$\rho_S(t) = \sum_K \rho^{(K)}(t)\,. \tag{3.26}$$

Thus the probability to observe $K$ events after time $t$ reads

$$P_t(K) = \mathrm{Tr}\{\rho^{(K)}(t)\}\,. \tag{3.27}$$

Our aim is to derive a large deviation principle for this probability distribution. At long times the moment generating function reads (cf. Eq. (3.7))

$$Z_t(s) = \sum_{K=0}^{\infty} P_t(K) e^{-sK} \simeq e^{t\theta(s)}\,. \tag{3.28}$$

We will refer to the real variable $s$ as the *conjugate field* of $K$. Thus the Gärtner-Ellis theorem implies that

$$P_t(K) \simeq e^{t\varphi(K/t)} \tag{3.29}$$

with the large deviation function given by $\varphi(k) = \sup_s\{ks - \theta(s)\}$. So far, this is quiet similar to the procedure shown in the previous section. What remains to do is finding the $\theta(s)$. Here, a problem arises since we are dealing with the evolution of the conditioned density operator $\rho^{(K)}$, which obeys the hierarchical master equation

(time dependences are omitted)

$$\dot{\rho}^{(K)} = \mathcal{L}_0 \rho^{(K)} + \mathcal{L}_{+1} \rho^{(K-1)} + \mathcal{L}_{-1} \rho^{(K+1)} , \tag{3.30}$$

where we decomposed the full generator $\mathcal{L}$ into three different contributions, the first one responsible for the continuous evolution ($\mathcal{L}_0$), and the other two for the jump evolution, resulting in the addition ($\mathcal{L}_{+1}$) and the subtraction ($\mathcal{L}_{-1}$) of an event to the total number $K$. The Laplace transform

$$\rho_s = \sum_K \rho^{(K)} e^{-sK} \tag{3.31}$$

yields

$$\dot{\rho}_s = \left(\mathcal{L}_0 + e^{-s}\mathcal{L}_{+1} + e^{s}\mathcal{L}_{-1}\right) \rho_s = \mathcal{L}_s \rho_s . \tag{3.32}$$

We call $\rho_s$ the *tilted density matrix* and $\mathcal{L}_s$ the *tilted Lindblad (or Liouvillian) superoperator*. In the reminder of this dissertation, we will not consider incoherent driving processes, thus $\mathcal{L}_{+1}$ will be always zero. Thus, for example, if we have $N_J$ jump operators in our dynamics and we count only jumps due to operator $\hat{L}_1$, the resulting ME will take the form

$$\mathcal{L}_s \rho = -i[\hat{H}, s] + \sum_{\mu=1}^{N_J} \left( \hat{L}_\mu \rho \hat{L}_\mu^\dagger - \frac{1}{2}\{\hat{L}_\mu^\dagger \hat{L}_\mu, \rho\} \right) + (e^{-s} - 1)\hat{L}_1 \rho \hat{L}_1^\dagger . \tag{3.33}$$

This is very similar to the standard one (cf. Eq. (1.42)), except for the last term. When $s \neq 0$ Eq. (3.32) indeed does not correspond to a well-defined physical dynamics since $\mathcal{L}_s$ is not trace preserving. However, as will be clear shortly, it provides the solution to our problem. We indeed note that Eq. (3.28) can be rearranged as

$$Z_t(s) = \mathrm{Tr}\left\{ \sum_{K=0}^{\infty} \rho^{(K)}(t) e^{-sK} \right\} = \mathrm{Tr}\left\{\rho_s(t)\right\} = \mathrm{Tr}\left\{ e^{t\mathcal{L}_s} \rho_s(0) \right\} . \tag{3.34}$$

The last identity is the equivalent of Eq. (3.23), therefore $\theta(s)$ is the largest eigenvalue of $\mathcal{L}_s$. Once $\theta(s)$ is known, we have direct access to the full counting statistics, i.e. all the *scaled* cumulants and, consequently, the moments of the distribution [85]. In particular the events' occurrence rate, also called *average activity* [10], reads

$$\partial_s \theta(s) = \frac{1}{t} \frac{1}{Z_t(s)} \sum_K (-K) P_t(K) e^{-sK} = -\frac{\langle K \rangle_s}{t} . \tag{3.35}$$

Analogously, the 2nd order derivative of $\theta(s)$ corresponds to the scaled variance

$$\partial_s^2 \theta(s) = \frac{1}{t} \frac{\left(\sum_K K^2 P_t(K) e^{-sK}\right) Z_t(s) - \left(\sum_K K P_t(K) e^{-sK}\right)^2}{Z_t^2(s)} = \frac{1}{t}\left(\langle K^2 \rangle_s - \langle K \rangle_s^2\right) . \tag{3.36}$$

Higher-order cumulants are obtained likewise.

## 3.4 From rare to typical: the Quantum Doob transform

In the previous section we introduced large deviation functions $\varphi$ and $\theta$ and the way in which they characterize the behaviour of average quantities defined on a quantum trajectories ensemble. In fact we formulated a proper thermodynamics of counting process [82] in which the counting variable $K$ is a macroscopic observable while single trajectories the microstates. The moment generating function takes the role of a partition function while $\varphi$ and $\theta$ embody entropy and free energy, respectively [10]. As promised in the Introduction, we next consider the problem of enhancing the probabilities of rare events. We will refer to this task as *biasing the trajectories*. Here we summarize the main theoretical results that will be used in Chapter 5. A comprehensive study can be found in [73].

Setting $s = 0$, Eq. (3.28) is a simple sum of probabilities. For $s \neq 0$ the exponential bias breaks the normalization and each term of the sum $P_t(K)e^{-sK}$ can no longer be considered as a proper probability. Notwithstanding, we can fix this issue by defing

$$P_t^s(K) = \frac{e^{-sK}P_t(K)}{Z_t(s)}\,. \tag{3.37}$$

Now each $P_t^s(K)$ is a well defined probability. We call them *biased probabilities*. For $s > 0$ these probabilities enhance the occurrence of trajectories featuring smaller-than-typical values of $K$, while for $s < 0$, instead, larger values of $K$ are favored [61, 86].

A question naturally arises: what kind of dynamics can produce an ensemble of trajectories such that the counting statistics is that described by the biased distribution $P_t(K)$? Also, is there a way to reproduce this dynamics from the information we have?

The answer to the last question is yes and the solution is the *quantum Doob transform*, which turns the original dynamics into a new one making rare trajectories typical. Basically, for a given value of $s$, just like dividing by $Z_t(s)$ "adjusts" the biased probabilities so quantum Doob transform fixes the tilted Liouvillian superoperator defined in Eq. (3.32), which returns a well-defined ME. The price to pay is a dramatic change of the original Hamiltonian and jump operators.

Assume now that we are interested in the statistics described by the distribution $P_t^{s=z}(K)$ and that we are counting events due to the jump operators belonging to the subset $\mathcal{J}$ ($\dim \mathcal{J} \leq N_J$). Then the Doob transformed Lindblad ME reads [73]

$$\tilde{\mathcal{L}}^{(z)}\rho = -i[\tilde{H}^{(z)},\rho] + \sum_{\mu=1}^{N_J}\left(\tilde{L}_\mu^{(z)}\rho\tilde{L}_\mu^{(z)\dagger} - \frac{1}{2}\{\tilde{L}_\mu^{(z)\dagger}\tilde{L}_\mu^{(z)},\rho\}\right), \tag{3.38}$$

with

$$\tilde{L}_\mu^{(z)} = e^{\frac{1}{2}f_\mu(z)} \ell_z^{1/2} \hat{L}_\mu \ell_z^{-1/2} \tag{3.39}$$

$$\tilde{H}_z = \frac{1}{2}\ell_z^{1/2} \left( H - \frac{i}{2} \sum_{\mu=1}^{N_J} \hat{L}_\mu^\dagger \hat{L}_\mu \right) \ell_z^{-1/2} + H.c. \,, \tag{3.40}$$

the new jump and Hamiltonian operator. Here, $f_\mu(z) = -z$ if $\hat{L}_\mu \in \mathcal{J}$ and zero otherwise while $\ell_z$ is the *left eigenmatrix* of $\mathcal{L}_{s=z}$, i.e. the solution of the eigenvalue equation

$$\mathcal{L}_z^*[\ell_z] = \theta(z)\ell_z \,, \tag{3.41}$$

where $\mathcal{L}^*$ is the dual of $\mathcal{L}$. The dynamics described by $\tilde{\mathcal{L}}_{0,z}$ is completely positive and trace preserving whose trajectory statistics is fully described by the moments given by the derivatives of $\theta(s)$ for $s = z$.

Quantum Doob transform is the formal solution to our problem. Nevertheless a clear microscopic interpretation of the changes affecting the original system evolution under this operation is still difficult. Indeed, even for small systems analytical expressions of $\theta(s)$ and $\ell_s$ may be demanding to work out. In Chapter 5, by exploiting quantum collision models, we will extend the theory of biased quantum trajectories from Lindblad-like dynamics to sequences of arbitrary dynamical maps, providing at once a transparent physical interpretation. In particular we will show how, from a microscopic viewpoint and for short collision times, the quantum Doob transform corresponds to adding extra collisions which enforce the system to follow a desired rare trajectory.

# Chapter 4

# Collisional picture of quantum optics with multi-local couplings

In this chapter we will apply the collision model framework on particular quantum optical systems of many emitters (atoms or resonators), each generally interacting with an electromagnetic field at many coupling points ("giant" emitters, see Box 2). We will derive a Lindblad master equation (ME) of a set of giant atoms coupled to a (generally chiral) waveguide field in an arbitrary white-noise Gaussian state, which condenses into a single equation and extends a variety of quantum optics and waveguide-QED MEs. In Sec. 4.9 we will study in detail the mechanisms underpinning the rise of DF subspaces in such systems, showing the predictive power of collision models in a problem of practical interest. More details are available in our recent publications [87, 88].

## 4.1 Introduction

We present a general theory of the collision model-based description of quantum optics in the case of many emitters. We allow each of these to generally couple to the field at many coupling points so as to encompass systems such as the so called "giant" atoms , or bosonic oscillators/atomic ensembles coupled to 1D fields in looped geometries [89, 90] as explicitly discussed in Ref. [91]. The framework is first formulated by considering a unidirectional field (just like in standard input-output formalism [92]) and then extended to a bidirectional field. While both the regimes of

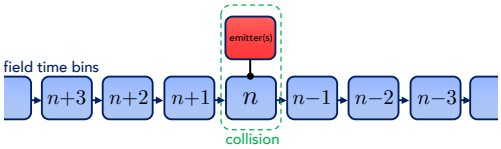


FIGURE 4.1: Basic collision-model description of the emitter-field dynamics. The field is decomposed into non-interacting time bins traveling at constant speed. One at a time, these undergo a short two-body interaction with the emitter (collision). In the regime of negligible time delays, a similar conveyor-belt picture holds for many emitters each of which can be giant (i.e., interacting with the field at many coupling points).

negligible and long time delays are discussed, our main focus is the former. In the latter case, it will be proven that each collision can be effectively represented as a collective coupling of all the emitters with one field time bin (playing the role of the ancilla in the abstract collision model) plus an internal coherent dipole-dipole interaction between the emitters.The latter is described by a Hamiltonian originating from the intrinsic system's chirality (in the conveyor-belt picture of Fig. 1 time bins travel from left to right).

**Box 2: Giant atoms [49, 54]**

Natural atoms are considered pointlike when they interact with optical frequencies. Indeed according to the dipole approximation

$$r \ll \lambda$$

where $r$ represents the size of the atom and lambda the wavelength of the field (see figure on the right). Recently in circuit [56] and waveguide QED experiments [94, 46], multilevel systems (in this context called "artificial atoms") were coupled to guided fields at multiple points with spacing $\Delta x \simeq \lambda$.

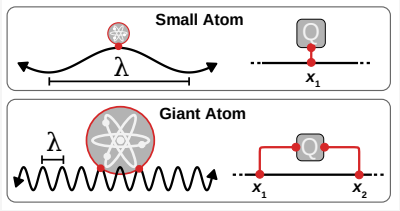


Giant atom
(from Kannan et al. Nature 583,775-779(2020)) [93]

Although these systems, which in this context are referred as "giant atoms", have a size of the order of the field wavelength (far from dipole approximation range), they can be treated as dipole at each coupling point. Multiple coupling points give origin to interesting nontrivial interference effects that can result in unexpected time evolution in system with many giant atoms.

As will be illustrated in detail, the results in this section extend to a variety of master equations used in waveguide QED [95, 48, 47, 49]. Moreover, we show that the recently discovered possibility to realize decoherence-free Hamiltonians with giant emitters [53, 91] is naturally predicted in the collisional picture, without the need to resort to a master equation formulation.

## 4.2 Microscopic model

The general emitters-field microscopic model we consider is essentially the same as that underpinning the standard input-output formalism of quantum optics [92] and related theories such as SLH [96].

Let $S$ be a system made out of $N_e$ quantum "emitters" of frequency $\omega_0$ and associated ladder operators $\hat{A}_j$, $\hat{A}_j^\dagger$ for $j = 1, ..., N_e$. The nature of these operators is left unspecified, hence in particular each emitter could be a harmonic oscillator or a pseudo-spin. The emitters are weakly coupled to a unidirectional bosonic field with normal-mode ladder operators $\hat{b}_\omega$, $\hat{b}_\omega^\dagger$ such that $[\hat{b}_\omega, \hat{b}_{\omega'}] = [\hat{b}_\omega^\dagger, \hat{b}_{\omega'}^\dagger] = 0$ and $[\hat{b}_\omega, \hat{b}_{\omega'}^\dagger] = \delta(\omega - \omega')$. The $j$th emitter interacts with the field at $\mathcal{N}_j$ distinct coupling points. For $\mathcal{N}_j = 1$ we retrieve the standard local coupling and the emitter is called "normal" [see Fig. 4.2(a)]. Instead, if $\mathcal{N}_j \geq 2$, the coupling is multi-local and the

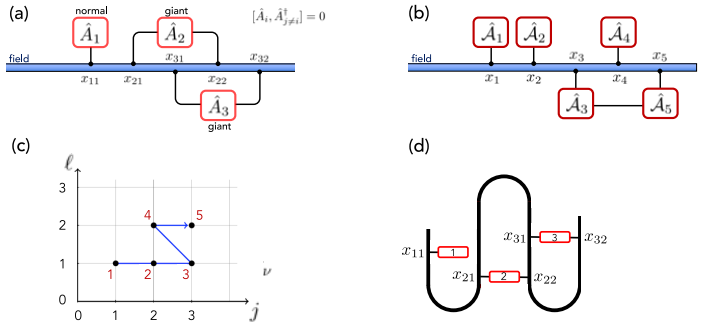


FIGURE 4.2: A set of (generally giant) emitters coupled to a unidirectional field. (a): A normal emitter (such as 1) interacts with the field at a single coupling point ($x_{11}$ in the figure), while a giant emitter has two or more coupling points (like emitters 2 and 3 here). (b): Instead of a double index as in (a), we can use a single index $\nu$ to label coupling points from left to right, defining for each a ladder operator $\hat{\mathcal{A}}_\nu$. By doing so, we can incorporate the coordinate-dependent phase factor (e.g., $\hat{\mathcal{A}}_4 = e^{-ik_0 x_{22}}\hat{A}_2$). Thus, formally, the system is equivalent to a set of normal but *not* independent emitters, i.e., $[\hat{\mathcal{A}}_\nu, \hat{\mathcal{A}}^\dagger_{\nu'}]$ for $\nu \neq \nu'$ is generally non-zero (e.g., $[\hat{\mathcal{A}}_1, \hat{\mathcal{A}}^\dagger_2] = e^{ik_0(x_{21}-x_{11})}[\hat{A}_1, \hat{A}^\dagger_2] = 0$ but $[\hat{\mathcal{A}}_2, \hat{\mathcal{A}}^\dagger_4] = e^{ik_0(x_{22}-x_{21})}[\hat{A}_2, \hat{A}^\dagger_2] \neq 0$). (c): Mapping from indexing (b) to (a) is described by the pair of index functions $j = \mathcal{J}_\nu$ and $\ell = \mathcal{L}_\nu$. These and the inverse mapping can be represented through the plotted diagram, where values of $\nu$ (in red) label the black dots. The Cartesian coordinates of each dot indicate the corresponding pair $(j, \ell)$. The diagram thus encodes the coupling points topology. (d): Implementation of the setup in (a) via a looped unidirectional waveguide.

emitter is dubbed "giant" [see Figs. 4.2(a) and (d)]. The spatial coordinate of the $\ell$th coupling point of the $j$th emitter is $x_{j\ell}$ (the field is along the $x$-axis). Under the usual rotating-wave approximation (RWA) and assuming white coupling, the total Hamiltonian reads (we set $\hbar = 1$)

$$\hat{H} = \hat{H}_S + \hat{H}_f + \hat{V} \tag{4.1}$$

$$\hat{H}_S = \sum_{j=1}^{N_e} \omega_0 \, \hat{A}^\dagger_j \hat{A}_j \,, \quad \hat{H}_f = \int d\omega \, (\omega_0 + \omega) \, \hat{b}^\dagger_\omega \hat{b}_\omega \,, \tag{4.2}$$

$$\hat{V} = \sum_{j=1}^{N_e} \sum_{\ell=1}^{\mathcal{N}_j} \sqrt{\frac{\gamma}{2\pi}} \, e^{i\omega_0 \tau_{j\ell}} \int d\omega \, e^{i\omega \tau_{j\ell}} \, \hat{A}^\dagger_j \hat{b}_\omega + \text{H.c.} \,, \tag{4.3}$$

where all integrals run over the entire real axis compatibly with the RWA.

Here, $\tau_{j\ell} = x_{j\ell}/v$ is the coordinate in the time domain of each coupling point (the field dispersion law is $\omega = vk$). Note that here $\omega$ are frequencies measured from the emitters' energy $\omega_0$ (i.e., detunings in fact). We also point out that each coupling point has an associated position-dependent phase factor $e^{i\omega_0 \tau_{j\ell}}$, which can be equally written in the space domain as $e^{ik_0 x_{j\ell}}$ with $k_0 = \omega_0/v$.

Instead of $\omega$-dependent normal modes, the field can be equivalently represented in terms of time modes with ladder operators

$$\hat{b}_t = \tfrac{1}{\sqrt{2\pi}} \int d\omega\, \hat{b}_\omega e^{-i\omega t}\,, \tag{4.4}$$

fulfilling bosonic commutation rules

$$[\hat{b}_t, \hat{b}^\dagger_{t'}] = \delta(t-t'),\ [\hat{b}_t, \hat{b}_{t'}] = [\hat{b}^\dagger_t, \hat{b}^\dagger_{t'}] = 0\ . \tag{4.5}$$

In the interaction picture with respect to $\hat{H}_0 = \hat{H}_S + \hat{H}_f$ the ladder operators transform as $\hat{A}_j \to \hat{A}_j e^{-i\omega_0 t}$ and $\hat{b}_\omega \to \hat{b}_\omega e^{-i(\omega_0+\omega)t}$, respectively, so that the joint emitter-field state $\sigma$ now evolves according to $\dot{\sigma} = -i\,[\hat{V}_t, \sigma]$, where

$$\hat{V}_t = \sqrt{\gamma} \sum_{j,\ell} \hat{A}^\dagger_j e^{i\omega_0 \tau_{j\ell}}\, \hat{b}_{t-\tau_{j\ell}} + \text{H.c.} \tag{4.6}$$

Now, following Ref. [91], it is convenient to introduce an index $\nu = 1, ..., \mathcal{N}$ labeling all the coupling points from left to right, i.e., $x_1 < x_2 < ... < x_{\mathcal{N}}$ [see Fig. 4.2(b)] or equivalently in the time domain $\tau_1 < \tau_2 < ... < \tau_{\mathcal{N}}$ (here $\mathcal{N} = \sum_{j=1}^{N_e} \mathcal{N}_j$ is the total number of coupling points). For each coupling point $\nu$, we define a corresponding ladder operator as

$$\hat{\mathcal{A}}_\nu = \hat{A}_j\, e^{-ik_0 x_{j\ell}}\,, \tag{4.7}$$

with $\hat{A}_j$ the ladder operator of the corresponding atom and $e^{-ik_0 x_{j\ell}}$ the corresponding phase shift. For instance, in the case of Fig. 4.2(a): $\mathcal{A}_5 = \hat{A}_3 e^{-ik_0 x_{32}} = \hat{A}_3 e^{-i\omega_0 \tau_{32}}$. Formally, the mapping between $(j,\, \ell)$ and $\nu$ is a expressed by a pair of discrete functions $j = \mathcal{J}_\nu$ and $\ell = \mathcal{L}_\nu$, a diagrammatic representation of which is shown in Fig. 4.2(c). Note that ladder operators $\{\hat{\mathcal{A}}_\nu\}$ with different indexes do not necessarily commute, that is $[\hat{\mathcal{A}}_\nu, \hat{\mathcal{A}}^\dagger_{\nu'\neq\nu}]$ is generally non-zero [e.g., in Fig. 4.2(b), $[\mathcal{A}_1, \mathcal{A}^\dagger_3] = 0$ but $[\mathcal{A}_3, \mathcal{A}^\dagger_5] \neq 0$]. In this way the system could be thought as a set of $\mathcal{N}$ normal emitters (as many as the coupling points), which yet are *not* independent. Their dynamics is governed by the Hamiltonian [cf. Eq. (4.6)]

$$\hat{V}_t = \sqrt{\gamma} \sum_{\nu=1}^{\mathcal{N}} \hat{\mathcal{A}}^\dagger_\nu\, \hat{b}_{t-\tau_\nu} + \text{H.c.} \tag{4.8}$$

For a bidirectional field, each normal frequency $\omega$ now has associated right-going and left-going modes with ladder operators $\hat{b}_\omega$ and $\hat{b'}_\omega$, respectively ($\hat{b'}_\omega$ fulfill commutation rules analogous to $\hat{b}_\omega$). In the total Hamiltonian (4.1), the field and

coupling Hamitonians are replaced by

$$\hat{H}_f = \int d\omega\, (\omega_0 + \omega)\, (\hat{b}^\dagger_\omega \hat{b}_\omega + \hat{b'}^\dagger_\omega \hat{b'}_\omega)\,, \tag{4.9}$$

$$\hat{V} = \sqrt{\tfrac{\gamma}{2\pi}} \sum_{j,\ell} e^{i\omega_0 \tau_{j\ell}} \int d\omega\, e^{i\omega\tau_{j\ell}}\, \hat{A}^\dagger_j\, \hat{b}_\omega + \sqrt{\tfrac{\gamma'}{2\pi}} \sum_{j,\ell} e^{-i\omega_0 \tau_{j\ell}} \int d\omega\, e^{i\omega\tau_{j\ell}}\, \hat{A}^\dagger_j\, \hat{b'}_\omega + \text{H.c.}\,, \tag{4.10}$$

where we allowed generally different coupling strengths to right- and left-going modes so as to encompass chiral dynamics [97] (the previous unidirectional case is retrieved for $\gamma' = 0$).

Note the different phase factors in right-going terms compared to left-going ones. A detailed derivation of the microscopic Hamiltonian is reviewed in Box 3.

## Box 3: Derivation of the microscopic Hamiltonian

Consider a one-dimensional bosonic field with normal-mode ladder operators $\hat{a}_k$ and $\hat{a}_k^\dagger$ ($k \in \mathbb{R}$ continuous wavevector), weakly and non-locally coupled to $N_e$ quantum emitters. Let $\omega_k$ with $\omega_k = \omega_{-k}$ be the dispersion law.
By defining $\hat{b}_k = \hat{a}_{k\geq 0}$ and $\hat{b'}_k = \hat{a}_{k<0}$, the free field and coupling Hamiltonian read

$$\hat{H}_f = \int_{-\infty}^{0} dk\ \omega_k\, \hat{b'}_k^\dagger \hat{b'}_k + \int_0^\infty dk\ \omega_k\, \hat{b}_k^\dagger \hat{b}_k\,, \qquad \hat{V} = \sum_{j=1}^{N_e} \sum_{\ell=1}^{\mathcal{N}_j} \hat{V}_{j\ell}\,. \tag{4.11}$$

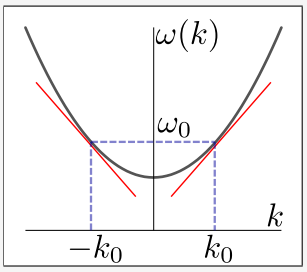

Dispersion law linearization

with

$$\hat{V}_{j\ell} = \hat{A}_j^\dagger \int_0^\infty dk\, \tfrac{g_k}{\sqrt{2\pi}}\, e^{ikx_{j\ell}} \hat{b}_k + \hat{A}_j^\dagger \int_{-\infty}^{0} dk\, \tfrac{g_k}{\sqrt{2\pi}}\, e^{ikx_{j\ell}} \hat{b'}_k + \text{H.c.} \tag{4.12}$$

where $g_k$ is the coupling rate with mode $k$ and $x_{j\ell}$ the coordinate of the $\ell$th coupling point of the $j$th emitter. Since the coupling is weak, the emitters significantly interact only with a narrow field's bandwidth centered at the emitter frequency $\omega_0 = \omega_{k_0} = \omega_{-k_0}$. Accordingly (see insert figure), the dispersion law and coupling rates are approximated as [50]

$$\omega_{k\geq 0} \simeq \omega_0 + v(k-k_0)\,,\ \ \omega_{k<0} \simeq \omega_0 - v(k+k_0)\,, \tag{4.13}$$

$$g_{k\geq 0} \simeq g_{k_0} = g\,,\ g_{k<0} \simeq g_{-k_0} = g'\,, \tag{4.14}$$

with $v = \partial_k \omega_k$ the field's group velocity. At the same time, the limits of integration in each integral in Eqs. (4.11) and (4.12) can be extended to the entire real axis. Next, by making the variable change $k - k_0 \to k$ in integrals featuring $\hat{b}_k$'s and $-(k+k_0) \to k$ in integrals featuring $\hat{b'}_k$'s, (4.11) and (4.12) are turned into

$$\hat{H}_f = \omega_0 \int_{-\infty}^{\infty} dk\, (\hat{b}_k^\dagger \hat{b}_k + \hat{b'}_k^\dagger \hat{b'}_k) + \int_{-\infty}^{\infty} dk\, vk\, \hat{b}_k^\dagger \hat{b}_k + \int_{-\infty}^{\infty} dk\, vk\, \hat{b'}_k^\dagger \hat{b'}_k\,, \tag{4.15}$$

$$\hat{V}_{j\ell} = \hat{A}_j^\dagger\, e^{ik_0 x_{j\ell}} \int_{-\infty}^{\infty} dk\, \tfrac{g}{\sqrt{2\pi}}\, e^{ikx_{j\ell}} \hat{b}_k + \hat{A}_j^\dagger\, e^{-ik_0 x_{j\ell}} \int_{-\infty}^{\infty} dk\, \tfrac{g'}{\sqrt{2\pi}}\, e^{-ikx_{j\ell}} \hat{b'}_k + \text{H.c.}\,, \tag{4.16}$$

Note the appearance of phase factors $e^{\pm ik_0 x_{j\ell}}$. Finally, changing to the frequency domain $\omega$ we end up with

$$\hat{H}_f = \int_{-\infty}^{\infty} d\omega\, \omega\, \hat{b}_\omega^\dagger \hat{b}_\omega + \int_{-\infty}^{\infty} d\omega\, \omega\, \hat{b'}_\omega^\dagger \hat{b'}_\omega\,, \tag{4.17}$$

$$\hat{V}_{j\ell} = \hat{A}_j^\dagger\, e^{i\omega_0 \tau_{j\ell}} \int_{-\infty}^{\infty} d\omega\, \sqrt{\tfrac{\gamma}{2\pi}}\, e^{i\omega\tau_{j\ell}} \hat{b}_\omega + \hat{A}_j^\dagger\, e^{-i\omega_0 \tau_{j\ell}} \int_{-\infty}^{\infty} d\omega\, \sqrt{\tfrac{\gamma'}{2\pi}}\, e^{-i\omega\tau_{j\ell}} \hat{b'}_\omega + \text{H.c.}\,, \tag{4.18}$$

where $\tau_{j\ell} = x_{j\ell}/v$, $\hat{b}_\omega = \hat{b}_k/\sqrt{v}$, $\hat{b'}_\omega = \hat{b'}_k/\sqrt{v}$, $\gamma = g^2/v$ and $\gamma' = g'^2/v$.

Left-going time modes are defined analogously to (4.4) as

$$\hat{b'}_t = \tfrac{1}{\sqrt{2\pi}} \int d\omega\, \hat{b'}_\omega\, e^{-i\omega t}\,, \tag{4.19}$$

fulfilling commutation rules analogous to (4.5).

Proceeding similarly to the unidirectional case leads to the interaction-picture coupling Hamiltonian [cf. Eq. (4.8)]

$$\hat{V}_t = \sqrt{\gamma} \sum_{\nu=1}^{\mathcal{N}} \hat{\mathcal{A}}_\nu^\dagger \hat{b}_{t-\tau_\nu} + \sqrt{\gamma'} \sum_{\nu=1}^{\mathcal{N}} \hat{\mathcal{A}'}_\nu^\dagger \hat{b}'_{t+\tau_\nu} + \text{H.c.} \tag{4.20}$$

with $\hat{\mathcal{A}}_\nu$ defined as in (4.7) and $\hat{\mathcal{A}'}_\nu$

$$\hat{\mathcal{A}'}_\nu = \hat{A}_j \, e^{ik_0 x_{j\ell}} \,, \tag{4.21}$$

where $j = \mathcal{J}_\nu$ and $\ell = \mathcal{L}_\nu$ (note however the change of phase compared to $\hat{\mathcal{A}}_\nu$).

## 4.3 Collision model derivation

Here we address the derivation of the collision model for a unidirectional field (the generalization to the bidirectional case is presented in Section 4.8 ).

Two regimes stand out:

1. Negligible time delays: $\tau_{\mathcal{N}} - \tau_1 \ll \gamma^{-1}$ (hence $\tau_{\mathcal{N}} - \tau_1$ can be replaced with $\tau_\nu - \tau_{\nu-1}$ for all $\nu$'s);
2. Non-negligible time delays: significant value of $\gamma(\tau_\nu - \tau_{\nu-1})$ for any $\nu$ (say of the order of $\sim 0.1$ or larger).

Most of the present section concerns the regime of *negligible time delays* (1) (our main focus), which still occurs in the vast majority of experimental setups (see e.g. Ref. [45] for a discussion on circuit-QED systems). Nevertheless, we begin with some general considerations and properties common to both regimes.

Consider a time mesh defined by $t_n = n\Delta t$ with $n = 0, 1, ...$ integer and $\Delta t$ the time step (later on this will be interpreted as the collision time). In the interaction picture the propagator $\hat{\mathcal{U}}_t$ can be decomposed as [98]

$$\hat{\mathcal{U}}_t = \hat{\mathcal{T}} \, e^{-i \int_{t_0}^{t} ds \, \hat{V}(s)} = \prod_{n=1}^{[t/\Delta t]} \hat{\mathcal{U}}_n \,, \tag{4.22}$$

with $\hat{V}(s)$ given in Eq. (4.6) and $\hat{\mathcal{T}}$ the usual time-ordering operator, and where each unitary $\hat{\mathcal{U}}_n$ describes the evolution in the time interval $t \in [t_{n-1}, t_n]$

$$\hat{\mathcal{U}}_n = \hat{\mathcal{T}} \, e^{-i \int_{t_{n-1}}^{t_n} ds \, \hat{V}_s} \,. \tag{4.23}$$

This discretization of the joint dynamics underpins the collision-model description (in any regime). Throughout, we will consider a time step much shorter than the characteristic interaction time, i.e., $\Delta t \ll \gamma^{-1}$. Accordingly, we apply Magnus expansion [99] and approximate (4.23) up to second order in $\Delta t$ as

$$\hat{\mathcal{U}}_n \simeq \mathbb{1} - i \, (\hat{\mathcal{H}}_n^{(0)} + \hat{\mathcal{H}}_n^{(1)})\Delta t - \tfrac{1}{2}(\hat{\mathcal{H}}_n^{(0)})^2 \Delta t^2 \tag{4.24}$$

with $\mathbb{1}$ the identity operator and

$$\hat{\mathcal{H}}_n^{(0)} = \tfrac{1}{\Delta t}\int_{t_{n-1}}^{t_n} ds\, \hat{V}_s\,, \tag{4.25}$$

$$\hat{\mathcal{H}}_n^{(1)} = \tfrac{i}{2\Delta t}\int_{t_{n-1}}^{t_n} ds \int_{t_{n-1}}^{s} ds'\, [\hat{V}_{s'}, \hat{V}_s] \tag{4.26}$$

(note that $\hat{\mathcal{H}}_n^{(0)}$ and $\hat{\mathcal{H}}_n^{(1)}$ are Hermitian).

Using (4.8), $\hat{\mathcal{H}}_n^{(0)}$ more explicitly reads

$$\hat{\mathcal{H}}_n^{(0)} = \frac{1}{\Delta t}\int_{t_{n-1}}^{t_n} ds \sqrt{\gamma} \sum_\nu \hat{\mathcal{A}}_\nu\, \hat{b}^\dagger_{s-\tau_\nu} + \text{H.c.} = \sqrt{\tfrac{\gamma}{\Delta t}} \sum_\nu \hat{\mathcal{A}}_\nu \left( \tfrac{1}{\sqrt{\Delta t}} \int_{t_{n-1}-\tau_\nu}^{t_n-\tau_\nu} ds\; \hat{b}^\dagger_s \right) + \text{H.c.}\,, \tag{4.27}$$

while $\hat{\mathcal{H}}_n^{(1)}$ is the sum of three terms

$$\hat{\mathcal{H}}_n^{(1)} = \hat{\mathcal{H}}_{\text{vac}}^{(1)} + \hat{\mathcal{H}}_{\text{th}}^{(1)} + \hat{\mathcal{H}}_{\text{sq}}^{(1)} \tag{4.28}$$

with [100]

$$\hat{\mathcal{H}}_{\text{vac}}^{(1)} = i\tfrac{\gamma}{2\Delta t} \sum_{\nu\nu'} \hat{\mathcal{A}}^\dagger_{\nu'} \hat{\mathcal{A}}_\nu \int_{t_{n-1}}^{t_n} ds \int_{t_{n-1}}^{s} ds'\, [\hat{b}_{s'-\tau_{\nu'}}, \hat{b}^\dagger_{s-\tau_\nu}] + \text{H.c.}\,, \tag{4.29}$$

$$\hat{\mathcal{H}}_{\text{th}}^{(1)} = i\tfrac{\gamma}{2\Delta t} \sum_{\nu\nu'} [\hat{\mathcal{A}}^\dagger_{\nu'}, \hat{\mathcal{A}}_\nu] \int_{t_{n-1}}^{t_n} ds \int_{t_{n-1}}^{s} ds'\; \hat{b}^\dagger_{s-\tau_\nu} \hat{b}_{s'-\tau_{\nu'}} + \text{H.c.}\,, \tag{4.30}$$

$$\hat{\mathcal{H}}_{\text{sq}}^{(1)} = i\tfrac{\gamma}{2\Delta t} \sum_{\nu\nu'} [\hat{\mathcal{A}}_{\nu'}, \hat{\mathcal{A}}_\nu] \int_{t_{n-1}}^{t_n} ds \int_{t_{n-1}}^{s} ds'\; \hat{b}^\dagger_{s-\tau_\nu} \hat{b}^\dagger_{s'-\tau_{\nu'}} + \text{H.c.}\,. \tag{4.31}$$

## 4.4 Negligible time delays

When time delays are negligible we can coarse grain the dynamics over a time scale defined by $\Delta t$ such that

$$\tau_{\mathcal{N}} - \tau_1 \ll \Delta t \ll \gamma^{-1}\,, \tag{4.32}$$

meaning that the overall length of the coupling points array (hence the distance between any pair $\tau_\nu - \tau_{\nu'}$) is negligible compared to the time step defining the time scale [see Fig. 4.3(a)].

We can take advantage of (4.32) and obtain approximated expressions of $\hat{\mathcal{H}}_n^{(0)}$ and $\hat{\mathcal{H}}_n^{(1)}$. As for $\hat{\mathcal{H}}_n^{(0)}$, the lower and upper limits of integration of each integral appearing in (4.27) can be approximated as $t_{n-1} - \tau_\nu \simeq t_{n-1}$ and $t_n - \tau_\nu \simeq t_n$ so that (we set $\tau_1 = 0$ throughout)

$$\int_{t_{n-1}-\tau_\nu}^{t_n-\tau_\nu} ds\; \hat{b}_s \simeq \int_{t_{n-1}}^{t_n} ds\; \hat{b}_s = \sqrt{\Delta t}\, \hat{b}_n\,, \tag{4.33}$$

where we defined the $\hat{b}_n$'s as

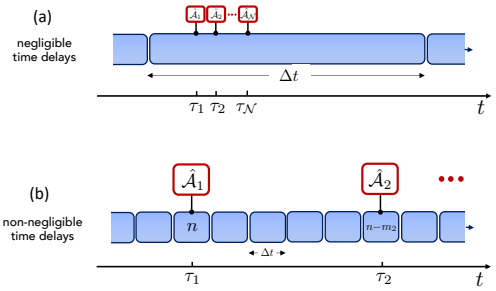


FIGURE 4.3: Effective collision model for a unidirectional field in the regimes of negligible (a) and non-negligible (b) time delays. (a): Negligible time delays, $\tau_\nu - \tau_{\nu-1} \ll \Delta t \ll \gamma^{-1}$ for any $\nu$. The time bin is much larger than the distance (in the time domain) between coupling points. Note, though, that so long as time delays are finite (no matter how short) the behavior is different from the ideal case of colocated coupling points: the fact that each time bin collides first with $\nu = 1$, then $\nu = 2$ etc. produces the effective Hamiltonian (4.40). (b): Non-negligible time delays, $\Delta t \ll \tau_\nu - \tau_{\nu-1} \ll \gamma^{-1}$ for any $\nu$. Distinct coupling points collide with different, generally non-consecutive, time bins.

$$\hat{b}_n = \frac{1}{\sqrt{\Delta t}} \int_{t_{n-1}}^{t_n} dt\, \hat{b}_t \,. \tag{4.34}$$

It is easily checked that the commutation rules for the $\hat{b}_t$'s [cf. Eq. (4.5)] entail $[\hat{b}_n, \hat{b}_m^\dagger] = \delta_{nm}$ and $[\hat{b}_n, \hat{b}_m] = [\hat{b}_n^\dagger, \hat{b}_m^\dagger] = 0$. Thus the $\hat{b}_n$'s define a discrete collection of bosonic modes, which we will usually refer to in the remainder as "time-bin modes" or just "time bins".

Thus (4.27) in the present regime reduces to

$$\hat{\mathcal{H}}_n^{(0)} \simeq \hat{V}_n = \sqrt{\frac{\gamma}{\Delta t}}\, (\hat{\mathcal{A}}\, \hat{b}_n^\dagger + \text{H.c.}) \,, \tag{4.35}$$

where $\hat{\mathcal{A}} = \sum_\nu \hat{A}_\nu$ is a collective operator of the emitters. Note the characteristic scaling $\sim \Delta t^{-1/2}$ of the emitter-(time bin) coupling strength, which is a hallmark of collision models [7].

## Box 4: Terms $\hat{\mathcal{H}}^{(1)}_{\rm th}$ and $\hat{\mathcal{H}}^{(1)}_{\rm sq}$

As anticipated in the main text, for $\tau_\nu - \tau_{\nu-1} \ll \Delta t$ for all $\nu$'s (negligible time delays) and setting $\tau_1 = 0$, in Eqs. (4.30) and (4.31) all time delays can be neglected replacing $s - \tau_\nu$ ($s' - \tau_{\nu'}$) with $s$ ($s'$). This yields

$$\hat{\mathcal{H}}^{(1)}_{\rm th} \simeq \tfrac{i\gamma}{2\Delta t}\sum_{\nu\nu'}[\hat{\mathcal{A}}_\nu, \hat{\mathcal{A}}^\dagger_{\nu'}]\int_{t_{n-1}}^{t_n} ds \int_{t_{n-1}}^{t_n} ds' \mathrm{sgn}(s'-s)\hat{b}^\dagger_s \hat{b}_{s'}, \tag{4.36}$$

$$\hat{\mathcal{H}}^{(1)}_{\rm sq} \simeq \tfrac{i\gamma}{4\Delta t}\sum_{\nu\nu'}[\hat{\mathcal{A}}_\nu, \hat{\mathcal{A}}_{\nu'}]\int_{t_{n-1}}^{t_n} ds \int_{t_{n-1}}^{t_n} ds' \mathrm{sgn}(s'-s)\hat{b}^\dagger_s \hat{b}^\dagger_{s'} + \text{H.c.}\,, \tag{4.37}$$

where we introduced the sign function to get more compact expressions. The integral in $\hat{\mathcal{H}}^{(1)}_{\rm sq}$ vanishes identically, due to the antisymmetry of the integrand under the exchange $s \rightleftarrows s'$. The same argument applies for a bidirectional field [cf. Eqs. (4.63)], in which case the integrals in $\hat{\mathcal{H}}^{(1)}_{\rm sq}$ features extra terms with the same symmetry.

To evaluate $\hat{\mathcal{H}}^{(1)}_{\rm th}$, we expand the field $\hat{b}_t$ in terms of time-bin modes $\hat{b}_{n,k}$ [cf. Eqs. (4.42) and (4.43)]. This yields

$$\hat{H}_{\rm th} = -\gamma\sum_{\nu,\nu'}[\hat{\mathcal{A}}_\nu, \hat{\mathcal{A}}^\dagger_{\nu'}]\sum_{k\neq 0}\frac{\hat{b}^\dagger_{n,k}\hat{b}_{n,k} - \left(\hat{b}^\dagger_{n,k}\hat{b}_{n,0} + \text{H.c.}\right)}{2\pi k}\,. \tag{4.38}$$

As discussed in Section 4.5, for $\Delta t$ short enough, each mode $\hat{b}_{n,k\neq 0}$ is in its own vacuum state $|0\rangle_{n,k}$ [cf. Eq. (4.44)]. Thus, effectively, $\hat{H}_{\rm th} = 0$.

For a bidirectional field, we will additionally expand $\hat{b}'_t$ in terms of left-going time-bin modes $\hat{b}'_{n,k}$ [defined in full analogy with (4.43)]. This results in an expression similar to (4.38), featuring overall terms of type $\sim \hat{\beta}'^\dagger_{n,k}\hat{\beta}_{n',k'}$ with $\beta, \beta' = b, b'$ and where at least one among $k$ and $k'$ is non-zero. Thus $\hat{\mathcal{H}}^{(1)}_{\rm th}$ is negligible when modes $b_{n,k\neq 0}$ and $b'_{n,k\neq 0}$ are in the vacuum state.

In line with approximation (4.33), in Eqs. (4.30) and (4.31) all time delays can be neglected replacing $s - \tau_\nu$ ($s' - \tau_{\nu'}$) with $s$ ($s'$). Based on this, in Box 4 we show that both $\hat{\mathcal{H}}^{(1)}_{\rm th}$ and $\hat{\mathcal{H}}^{(1)}_{\rm sq}$ can be *neglected* (note that Box 4 refers to Section 4.5 to be discussed shortly).

Thus we are left only with the vacuum contribution $\hat{\mathcal{H}}^{(1)}_{\rm vac}$. To work this out, we first note that the each double integral in Eq. (4.29) runs over the shaded triangle sketched in Fig. 4.4. For a given pair $(\nu, \nu')$, the two-variable $\delta$ function

$$\delta(s' - \tau_{\nu'} - s + \tau_\nu) = [\hat{b}_{s'-\tau_{\nu'}}, \hat{b}^\dagger_{s-\tau_\nu}] \tag{4.39}$$

is peaked on the line $s' = s - (\tau_\nu - \tau_{\nu'})$. As shown in Fig. 4.4, this line falls within the triangle for $\nu > \nu'$ and outside of it for $\nu < \nu'$ (since $\tau_\nu - \tau_{\nu'} > 0$ for $\nu > \nu'$). Hence, only terms $\nu > \nu'$ contribute to $\hat{\mathcal{H}}^{(1)}_{\rm vac}$ and we conclude that $\hat{\mathcal{H}}^{(1)}_{\rm vac} \equiv \hat{H}_{\rm vac}$ :

$$\hat{H}_{\rm vac} = i\tfrac{\gamma}{2}\sum_{\nu>\nu'}\left(\hat{\mathcal{A}}^\dagger_{\nu'}\hat{\mathcal{A}}_\nu - \hat{\mathcal{A}}^\dagger_\nu\hat{\mathcal{A}}_{\nu'}\right)\,. \tag{4.40}$$

Note that this dipole-dipole Hamiltonian has a chiral origin: it arises because each

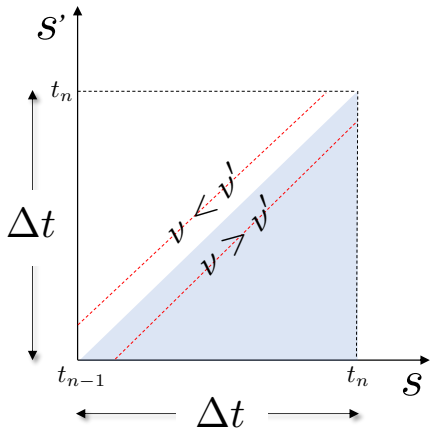


FIGURE 4.4: Calculation of double integrals appearing in the vacuum term (4.29). The shaded region (triangle) represents the domain of integration. The integrand $\delta(s' - s + (\tau_\nu - \tau_{\nu'}))$ vanishes everywhere except on the red line $s' = s - (\tau_\nu - \tau_{\nu'})$. This line lies within the triangular domain for $\nu > \nu'$ and outside of it for $\nu < \nu'$. Thereby, the integral is equal to $\Delta t$ in the former case and vanishes in the latter.

time bin (see Fig. 1) collides *first* with coupling point $\nu = 1$, *then* $\nu = 2$ and so on. Indeed if all the coupling points had the same location, $\hat{V}_n$ would still be present but $\hat{H}_{\rm vac} = 0$. Eq. (4.40) shows that, for delays negligible with respect to $\Delta t$, which in turn is much shorter than the interaction characteristic time scale $\gamma^{-1}$, in Eq. (4.24) we can approximate $\hat{\mathcal{H}}_n^{(0)} \simeq \hat{V}_n$ and $\hat{\mathcal{H}}_n^{(1)} \simeq \hat{H}_{\rm vac}$. Thereby,

$$\hat{U}_n \simeq \mathbb{1} - i\,(\hat{H}_{\rm vac} + \hat{V}_n)\,\Delta t - \tfrac{1}{2}\hat{V}_n^2\,\Delta t^2\,, \tag{4.41}$$

showing that in this regime the joint emitter-field dynamics can be effectively pictured as a sequence of short pairwise interactions (collisions) of duration $\Delta t$ (collision time), as sketched in Figs. 4.1 and 4.3(a). In each interaction the emitters collectively couple to a fresh time bin (only one) according to the coupling Hamiltonian $\hat{V}_n$ and at the same time coherently interact with one another through the second-order many-body Hamiltonian $\hat{H}_{\rm vac}$. Note that time bins are uncoupled from one another and that each collides with the emitter only once in a "conveyor-belt" fashion (see Fig. 4.1).

As said, to arrive at Eq. (4.41), all time delays $\tau_\nu - \tau_{\nu'}$ were neglected. We point out that this is different from setting $\tau_\nu - \tau_{\nu'} = 0$. Instead, it corresponds to performing the limit $\tau_\nu - \tau_{\nu'} \to 0^+$ for all pairs $(\nu, \nu')$ with $\nu > \nu'$. Indeed, it is easily checked that setting $\tau_\nu - \tau_{\nu'} = 0$ entails $\hat{\mathcal{H}}_{\rm vac}^{(1)} = 0$ since in this case both terms $\nu > \nu'$ and $\nu < \nu'$ exactly cancel out (the two dashed lines in Fig. 4.4 now both reduce to $s' = s$). Physically, this means that the effective Hamiltonian $\hat{H}_{\rm vac}$ stems from the fact that, while traveling from left to right [see Fig. 4.3(a)], the $n$th time bin interacts *first* with the coupling point $\nu$ and only *afterwards* with $\nu + 1$, no matter how short the delay $\tau_{\nu+1} - \tau_\nu$ is. This is in line with similar observations made in derivations of cascaded MEs through other methods (see e.g. [101]). Interestingly, the collisional

picture allows for a complementary interpretation of this phenomenon in terms of far-detuned time-bin modes $\hat{b}_{n,k}$, which we introduce next.

## 4.5 Time-bin modes $\hat{b}_{n,k}$

It should be clear from their definition (4.34) that, for a finite $\Delta t$, modes $\hat{b}_n$ generally capture only part of the field degrees of freedom. Formally, this can be seen by expanding the continuous time modes as [17]

$$\hat{b}_t = \tfrac{1}{\sqrt{\Delta t}} \sum_n \sum_{k=-\infty}^{\infty} \Theta_n(t) e^{-i2\pi kt/\Delta t}\, \hat{b}_{n,k}\,, \tag{4.42}$$

with $\Theta_n(t) = 1$ for $t \in [t_{n-1}, t_n]$ and 0 otherwise, and where

$$\hat{b}_{n,k} = \tfrac{1}{\sqrt{\Delta t}} \int_{t_{n-1}}^{t_n} dt\, e^{i2\pi kt/\Delta t}\, b_t\,. \tag{4.43}$$

The ladder operators $\hat{b}_{n,k}$ fulfill $[\hat{b}_{n,k}, \hat{b}^\dagger_{n',k'}] = \delta_{n,n'}\delta_{k,k'}$, $[\hat{b}_{n,k}, \hat{b}_{n',k'}] = [\hat{b}^\dagger_{n,k}, \hat{b}^\dagger_{n',k'}] = 0$. Moreover, for $k = 0$ we retrieve modes $\hat{b}_n$ [cf. Eq. (4.34)], i.e., $\hat{b}_{n,0} \equiv \hat{b}_n$. A straightforward Fourier analysis shows that time-bin modes $\hat{b}_{n,k\neq 0}$ are dominated by field normal modes whose detunings from the emitter grow as $\sim |k|/\Delta t$, (while modes $\hat{b}_{n,0}$ contain field frequencies quasi-resonant with the emitter) [17]. In the continuous-time limit of the dynamics, which corresponds to the limit $\Delta t \to 0$, these frequencies become divergent. Accordingly, it is reasonable to assume there are no photons populating modes $\hat{b}_{n,k\neq 0}$. This is equivalent to stating that the most general field state is of the form

$$\rho_f = \eta_{\text{bins}} \bigotimes_{n,k\neq 0} |0\rangle_{n,k}\langle 0| \tag{4.44}$$

with $\eta_{\text{bins}}$ the (generally mixed) state of modes $\hat{b}_n \equiv \hat{b}_{n,0}$ and $|0\rangle_{n,k}$ the vacuum state of mode $\hat{b}_{n,k}$.

For a *single* coupling point ($\mathcal{N} = 1$) $\hat{H}_{\text{vac}}$ cannot arise and we are only left with $\hat{V}_n$ (containing only $\hat{b}_n \equiv \hat{b}_{n,0}$), meaning that the coupling to time-bin modes $k \neq 0$ is negligible. Yet, for two or more coupling points ($\mathcal{N} \geq 2$), these off-resonant modes yield non-negligible effects despite they do not explicitly appear in $\hat{H}_{\text{vac}}$ (not even in $\hat{V}_n$, of course). Indeed, they are in fact responsible for the emergence of $\hat{H}_{\text{vac}}$. This can be seen from Eq. (4.29) featuring a singularity in the integrand function due to the field commutator. Such a singular behavior forbids to retaining only $k = 0$ terms in expansion (4.42) no matter how small $\Delta t$ (indeed it is easily checked that expanding each field operator entering Eq. (4.29) and retaining only modes $\hat{b}_{n,0} = \hat{b}_n$ would yield a vanishing $\hat{H}_{\text{vac}}$).

Thus all time-bin modes $\hat{b}_{n,k}$ in fact contribute to the dynamics for $\mathcal{N} > 1$. However, unlike $k = 0$ modes, off-resonant modes $k \neq 0$ are only virtually excited, explaining why they do not explicitly appear in $\hat{H}_{\text{vac}}$.

## 4.6 Non-negligible time delays

A comprehensive treatment of the regime of non-negligible delays is beyond our scope. Yet, we wish to highlight a major difference from the negligible delays regime, this being that at each time step the emitters collide with as many time bins as the number of coupling points (instead of only one). To illustrate this, we work out next $\hat{\mathcal{H}}_n^{(0)}$ [cf. Eq. (4.25) and its equivalent expression (4.27)].

In contrast with the negligible delays regime, now one can take a time step negligible compared with all the system's time delay, i.e., $\Delta t \ll \tau_\nu - \tau_{\nu-1}$ for all $\nu$ (note that this is compatible with condition $\Delta t \ll \gamma^{-1}$ that we assume throughout). For sufficiently short $\Delta t$, the coupling points coordinates can be discretized as $\tau_\nu = m_\nu \Delta t$, where $\{m_\nu\}$ are $\mathcal{N}$ integers such that $m_1 < m_2 < ... < m_\mathcal{N}$, and set $\tau_1 = m_1 = 0$. Accordingly, (4.27) becomes [recall that $t_n = n\Delta t$]

$$\hat{\mathcal{H}}_n^{(0)} = \sqrt{\tfrac{\gamma}{\Delta t}} \sum_\nu (\hat{\mathcal{A}}_\nu \, \hat{b}^\dagger_{n-m_\nu} + \text{H.c.}) \,, \tag{4.45}$$

showing that, during a given time interval $[t_{n-1}, t_n]$, each coupling point $\nu$ interacts with a different time bin $n - m_\nu$ [see Fig. 4.3(b)].

In the presence of giant emitters (even a single one), this dynamics is tough to tackle analytically. Through an elegant diagrammatic technique, Grimsmo found an analytical solution for the open dynamics of a driven giant atom with two coupling points [12], while Pichler and Zoller found an efficient matrix-product-state approach which they applied to a pair of driven normal atoms coupled to a bidirectional field [11] A major reason behind the complexity of this dynamics lies in its generally non-Markovian nature (conditions for Markovian behaviour are discussed in Section 4.7).

## 4.7 Master equation for negligible time delays

In section 4.4, we focused on the total propagator showing that for negligible time delays it can be decomposed as a sequence of collisions between the emitters (jointly) and a field time bin, each described by the two-body elementary unitary $\hat{U}_n$ in Eq. (4.41), which is fully specified by $\hat{H}_{\text{vac}}$ and $\hat{V}_n$. In this section, we derive master equations for the emitters and time bin in the regime of negligible time delays.

Based on (4.44) and related discussion, from now on time-bin modes $\hat{b}_{n,k\neq 0}$ will be ignored. The joint state of the emitters and *all* time bins (modes $\hat{b}_n \equiv \hat{b}_{n,0}$) evolves at each time step as $\sigma_n = \hat{U}_n \sigma_{n-1} \hat{U}_n^\dagger$ with $\sigma_n = \sigma_{t=t_n}$. A corresponding finite-difference equation of motion is worked out by replacing $\hat{U}_n$ with (4.41) and retaining only terms up to second order in $\Delta t$

$$\frac{\Delta \sigma_n}{\Delta t} = -i \, [\hat{H}_{\text{vac}} + \hat{V}_n, \sigma_{n-1}] + \Delta t \Big( \hat{V}_n \sigma_{n-1} \hat{V}_n - \tfrac{1}{2} \, [\hat{V}_n^2, \sigma_{n-1}]_+ \Big) \,, \tag{4.46}$$

where $\Delta\sigma_n = \sigma_n - \sigma_{n-1}$ (recall that $\hat{V}_n \sim 1/\sqrt{\Delta t}$). Under the usual assumption of zero initial correlations between the emitters and the field, the initial condition reads $\sigma_0 = \rho_0 \otimes \eta_{\text{bins}}$, where $\rho_0$ and $\eta_{\text{bins}}$ are the initial states of all emitters and all time bins, respectively.

We next ask whether or not the reduced dynamics of the emitters $\rho_n = \text{Tr}_{\text{bins}}\{\sigma_n\}$ is Markovian and describable by a Lindblad master equation. We note that this is generally not the case when time bins are initially correlated, namely $\eta_{\text{bins}}$ is *not* a product state, since in these conditions the emitters can get correlated with a time bin even before colliding with it [35, 7]. This indeed rules out that that the evolution of the emitters (open system) at each elementary collision be described by a completely positive and trace preserving (CPT) quantum map [3], which is the key requirement in order for a Lindblad master equation to hold. A typical instance is a single-photon wavepacket of bandwidth comparable with $\gamma$ [19, 20, 21, 22, 102].

We thus consider the case in which the time bins are initially uncorrelated, that is

$$\eta_{\text{bins}} = \bigotimes_n \eta_n \tag{4.47}$$

with $\eta_n$ the reduced state of the $n$th time bin mode having ladder operator $\hat{b}_n = \hat{b}_{n.0}$. Note that time bins define a set of ancillae fulfilling hypotheses 2.1. This entails

$$\rho_n = \text{Tr}_{\text{bins}}\left\{\hat{U}_n \sigma_{n-1} \hat{U}_n^\dagger\right\} = \text{Tr}_{\text{n}}\left\{\hat{U}_n \rho_{n-1} \eta_n \hat{U}_n^\dagger\right\}, \tag{4.48}$$

where $\text{Tr}_{\text{n}}$ is the partial trace over the time bin $n$ (mode $\hat{b}_n \equiv \hat{b}_{n,0}$). This defines a CPT map describing how the emitters' state $\rho_n$ is changed by the $n$th collision. Likewise, the $n$th time bin evolves according to

$$\eta_n' = \text{Tr}_S\left\{\hat{U}_n \rho_{n-1} \eta_n \hat{U}_n^\dagger\right\} \tag{4.49}$$

with $\text{Tr}_S$ the partial trace over the emitters. This is a CPT map describing the change of the single time bin state due to collision with the emitters (after the collision this state will no longer change since time bins are non-interacting). Note that map (4.49) depends parametrically on the current reduced state of emitters (updated at each collision).

### 4.7.1 Master equation for the emitters

To work out the Lindblad master equation of the emitters corresponding to map (4.48) we simply trace off all time bins from Eq. (4.46), which yields

$$\frac{\Delta\rho_n}{\Delta t} = -i[\hat{H}_{\text{vac}} + \langle \hat{V}_n \rangle, \rho_{n-1}] + \mathcal{D}[\rho_{n-1}] \tag{4.50}$$

with $\langle ... \rangle = \text{Tr}_n\{... \eta_n\}$, $\Delta\rho_n = \rho_n - \rho_{n-1}$ and

$$\mathcal{D}[\rho_{n-1}] = \Delta t \text{Tr}_n\left\{\hat{V}_n \rho_{n-1} \eta_n \hat{V}_n - \tfrac{1}{2}\left[\hat{V}_n^2, \rho_{n-1}\eta_n\right]_+\right\}. \tag{4.51}$$

Although not explicit, this equation is in Lindblad form as is easily checked by spectrally decomposing $\eta_n$ [103]. The Linbdlad form is a guaranteed by the fact that the emitters evolution at each collision is described by a CPT map [last identity in Eq. (4.48)].

Using (4.35) the first-order Hamiltonian and second-order dissipator can be put in the more explicit form

$$\begin{aligned} \langle \hat{V}_n \rangle &= \sqrt{\tfrac{\gamma}{\Delta t}} \left( \langle \hat{b}_n \rangle \, \hat{\mathcal{A}}^\dagger + \text{H.c.} \right) \\ \mathcal{D}[\rho_{n-1}] &= \gamma \sum_{\mu\mu'} \langle \hat{c}_\mu \hat{c}_{\mu'} \rangle \left( \hat{\mathcal{C}}_{\mu'} \rho_{n-1} \hat{\mathcal{C}}_\mu - \tfrac{1}{2} \left[ \hat{\mathcal{C}}_\mu \hat{\mathcal{C}}_{\mu'}, \rho_{n-1} \right]_+ \right) . \end{aligned} \tag{4.52}$$

with $\mu, \mu' = 1, 2$ and where we set

$$\hat{c}_1 = \hat{b}_n \,, \;\; \hat{c}_2 = \hat{b}_n^\dagger \,, \;\; \hat{\mathcal{C}}_1 = \hat{\mathcal{A}}^\dagger \,, \;\; \hat{\mathcal{C}}_2 = \hat{\mathcal{A}} \,. \tag{4.53}$$

Now Eq. (4.50) is expressed fully in terms of the time-bin moments $\langle \hat{b}_n \rangle$, $\langle \hat{b}_n^\dagger \hat{b}_n \rangle$ and $\langle \hat{b}_n^2 \rangle$, which depend on $\eta_n$ in turn dependent on the initial field state [cf. Eq. (4.47)].

The time-bin moments can be determined for the most general white-noise Gaussian state of the field, which is fully specified by the 1st and 2nd moments [80]

$$\langle d\hat{b}_t \rangle = \alpha_t \, dt \,, \;\; \langle d\hat{b}_t^\dagger \, d\hat{b}_t \rangle = N \, dt \,, \;\; \langle d\hat{b}_t \, d\hat{b}_t \rangle = M \, dt \,. \tag{4.54}$$

with $d\hat{b}_t = \int_t^{t+dt} ds \, \hat{b}_s$ the well-known quantum noise increment. Correspondingly, the most general Gaussian, uncorrelated state of the time bins is fully specified by the moments

$$\langle \hat{b}_n \rangle = \alpha_n \sqrt{\Delta t}, \; \langle \hat{b}_n^\dagger \, \hat{b}_{n'} \rangle = \delta_{n,n'} \, N, \; \langle \hat{b}_n \, \hat{b}_{n'} \rangle = \delta_{n,n'} \, M \,. \tag{4.55}$$

with $\alpha_n = \alpha_{t=t_n}$, $N \geq 0$ and $|M|^2 \leq N(N+1)$.

Noting that $\hat{b}_n = \int_{t_{n-1}}^{t_n} db_t / \sqrt{\Delta t}$, it is evident that for such a field state, $\langle \hat{b}_n^\dagger \hat{b}_{n'} \rangle = \langle \hat{b}_n \hat{b}_{n'} \rangle = 0$ for $n \neq n'$. This, because of the Gaussianity hypothesis, is equivalent to Eq. (4.47). Thus time bins are initially uncorrelated. Their 1st and 2nd moments are given by (4.55), where $\alpha_n = \int_{t_{n-1}}^{t_n} dt \, \alpha_t / \Delta t$ (for $\Delta t$ short enough, this reduces to $\alpha_n \simeq \alpha_{t_n}$). Note that $\langle \hat{b}_n \rangle \propto \sqrt{\Delta t}$, which cancels the $1/\sqrt{\Delta t}$ factor in Eq. (4.52).

Plugging moments (4.55) into the finite-difference Eq. (4.50) and taking the continuous-time limit such that $\gamma \Delta t \to 0$, $t_n \to t$, $\rho_{n-1} \to \rho_t$, $\Delta \rho_n / \Delta t \to d\rho/dt$ we end up with the general master equation

$$\begin{aligned} \frac{d\rho}{dt} = &- i \left[ \hat{H}_{\text{vac}} + \sqrt{\gamma} \, (\alpha_t^* \hat{\mathcal{A}} + \text{H.c.}), \rho \right] + \gamma(N+1) \mathcal{D}_{\hat{\mathcal{A}}}[\rho] + \gamma N \mathcal{D}_{\hat{\mathcal{A}}^\dagger}[\rho] \\ &+ \gamma \left( M(\hat{\mathcal{A}}^\dagger \rho \hat{\mathcal{A}}^\dagger - \tfrac{1}{2} [\hat{\mathcal{A}}^{\dagger 2}, \rho]_+) + \text{H.c.} \right) . \end{aligned} \tag{4.56}$$

This can be expressed in terms of original ladder operators $\hat{A}_j$ using (4.7) and recalling $\hat{\mathcal{A}} = \sum_\nu \hat{\mathcal{A}}_\nu$.

### Time bin master equation

An equation for the rate of change of the single time bin state, $\Delta\eta_n/\Delta t$ with $\Delta\eta_n = \eta'_n - \eta_n$, can be similarly worked out. We again start from Eq. (4.46) but now trace over all emitters and all time bins $n' \neq n$, obtaining

$$\frac{\Delta\eta_n}{\Delta t} = -i[\langle \hat{V}_n \rangle_\rho, \eta_n] + \mathcal{D}_\rho[\eta_n] \tag{4.57}$$

with $\langle ... \rangle_\rho = \mathrm{Tr}_S\{... \rho\}$ and

$$\mathcal{D}_\rho[\eta_n] = \Delta t\, \mathrm{Tr}_S\left\{\hat{V}_n \rho_{n-1} \eta_n \hat{V}_n - \tfrac{1}{2}\left[\hat{V}_n^2, \rho_{n-1}\eta_n\right]_+\right\} \tag{4.58}$$

where $\mathrm{Tr}_S\{...\}$ is the partial trace over the system. Note that this equation parametrically depends on the state of the emitters, $\rho_{n-1}$, which changes at each time step. Eq. (4.57) expresses map (4.49) in the short-collision-time limit.

## 4.8 Generalization to bidirectional field and examples

For a bidirectional field unitaries $\hat{\mathcal{U}}_t$ and $\hat{U}_n$ are formally the same as (4.22) and (4.23), respectively, but $\hat{V}_t$ is now given by Eq. (4.20). The $\hat{U}_n$'s lowest-order expansion (4.24) is formally unchanged. Through a reasoning analogous to that in Section 4.3, in light of (4.20), Eqs. (4.27) and (4.28) are generalized as

$$\hat{\mathcal{H}}_n^{(0)} = \sqrt{\tfrac{\gamma}{\Delta t}} \sum_\nu \hat{\mathcal{A}}_\nu \left(\tfrac{1}{\sqrt{\Delta t}} \int_{t_{n-1}}^{t_n} ds\ \hat{b}^\dagger_{s-\tau_\nu}\right) + \sqrt{\tfrac{\gamma'}{\Delta t}} \sum_\nu \hat{\mathcal{A}}'_\nu \left(\tfrac{1}{\sqrt{\Delta t}} \int_{t_{n-1}}^{t_n} ds\ \hat{b'}^\dagger_{s+\tau_\nu}\right) + \text{H.c.}\,, \tag{4.59}$$

$$\hat{\mathcal{H}}_n^{(1)} = \hat{\mathcal{H}}_{\mathrm{sq}}^{(1)} + \hat{\mathcal{H}}_{\mathrm{th}}^{(1)} + \hat{\mathcal{H}}_{\mathrm{vac}}^{(1)} \tag{4.60}$$

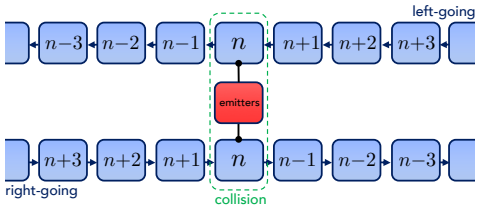


FIGURE 4.5: Collision-model description for a bidirectional field. Each time bin is now bipartite, comprising a right-going mode (bottom) and a left-going mode (top). At each collision the emitters jointly collide with the two-mode time bin according to the coupling Hamiltonian (4.64) and, additionally, are subject to an internal coherent dynamics corresponding to the dipole-dipole Hamiltonian (4.66).

with $\hat{\mathcal{A}}'_\nu$ is defined as in (4.21) and

$$\hat{\mathcal{H}}^{(1)}_{\rm vac} = \tfrac{i}{2\Delta t}\sum_{\nu,\nu'}\hat{\mathcal{A}}^\dagger_{\nu'}\hat{\mathcal{A}}_\nu\int_{t_{n-1}}^{t_n}ds\int_{t_{n-1}}^{s}ds'\left(\gamma\,[\hat{b}_{s'-\tau_{\nu'}},\hat{b}^\dagger_{s-\tau_\nu}]+\gamma'\,[\hat{b}'_{s'+\tau_{\nu'}},\hat{b}'^\dagger_{s+\tau_\nu}]-\text{H.c.}\right), \tag{4.61}$$

$$\hat{\mathcal{H}}^{(1)}_{\rm th} = \tfrac{i}{2\Delta t}\sum_{\nu\nu'}\int_{t_{n-1}}^{t_n}ds\int_{t_{n-1}}^{s}ds'\left(\gamma\,[\hat{\mathcal{A}}^\dagger_{\nu'},\hat{\mathcal{A}}_\nu]\,\hat{b}^\dagger_{s-\tau_\nu}\hat{b}_{s'-\tau_{\nu'}}+\gamma'[\hat{\mathcal{A}}'^\dagger_{\nu'},\hat{\mathcal{A}}'_\nu]\,\hat{b}'^\dagger_{s+\tau_\nu}\hat{b}'_{s'+\tau_{\nu'}}-\text{H.c.}\right)$$
$$+\tfrac{i}{2\Delta t}\sqrt{\gamma\gamma'}\sum_{\nu\nu'}\int_{t_{n-1}}^{t_n}ds\int_{t_{n-1}}^{s}ds'\left([\mathcal{A}^\dagger_\nu,\mathcal{A}'_{\nu'}]\,\hat{b}_{s-\tau_\nu}\hat{b}'^\dagger_{s'+\tau_{\nu'}}+[\mathcal{A}'^\dagger_\nu,\mathcal{A}_{\nu'}]\,\hat{b}^\dagger_{s'-\tau_{\nu'}}\hat{b}'_{s+\tau_\nu}-\text{H.c.}\right), \tag{4.62}$$

$$\hat{\mathcal{H}}^{(1)}_{\rm sq} = \tfrac{i}{2\Delta t}\sum_{\nu\nu'}\int_{t_{n-1}}^{t_n}ds\int_{t_{n-1}}^{s}ds'\left(\gamma\,[\hat{\mathcal{A}}_{\nu'},\hat{\mathcal{A}}_\nu]\,\hat{b}^\dagger_{s-\tau_\nu}\hat{b}^\dagger_{s'-\tau_{\nu'}}+\gamma'\,[\hat{\mathcal{A}}'_{\nu'},\hat{\mathcal{A}}'_\nu]\,\hat{b}'^\dagger_{s+\tau_\nu}\hat{b}'^\dagger_{s'+\tau_{\nu'}}-\text{H.c.}\right)$$
$$+\tfrac{i}{2\Delta t}\sqrt{\gamma\gamma'}\sum_{\nu\nu'}\int_{t_{n-1}}^{t_n}ds\int_{t_{n-1}}^{s}ds'\left([\mathcal{A}'^\dagger_{\nu'},\mathcal{A}^\dagger_\nu]\,\hat{b}_{s-\tau_\nu}\hat{b}'_{s'+\tau_{\nu'}}+[\mathcal{A}^\dagger_{\nu'},\mathcal{A}'^\dagger_\nu]\,\hat{b}_{s'-\tau_{\nu'}}\hat{b}'_{s+\tau_\nu}-\text{H.c.}\right). \tag{4.63}$$

In the present regime, an argument analogous to that leading to (4.35) yields $\hat{\mathcal{H}}^{(0)}_n \simeq \hat{V}_n$ with $\hat{V}_n$ given by

$$\hat{V}_n = \tfrac{1}{\sqrt{\Delta t}}\left(\sqrt{\gamma}\,\hat{\mathcal{A}}^\dagger\hat{b}_n+\sqrt{\gamma'}\,\hat{\mathcal{A}}'^\dagger\hat{b}'_n+\text{H.c.}\right). \tag{4.64}$$

with

$$\hat{\mathcal{A}}=\sum_\nu\hat{\mathcal{A}}_\nu\,,\quad \hat{\mathcal{A}}'=\sum_\nu\hat{\mathcal{A}}'_\nu\,. \tag{4.65}$$

As in the unidirectional case, the terms $\hat{\mathcal{H}}^{(1)}_{\rm th}$ and $\hat{\mathcal{H}}^{(1)}_{\rm sq}$ are also negligible in the limit of vanishing delays (see Box 4). Compared to the unidirectional case [cf. Eq. (4.29)], $\hat{\mathcal{H}}^{(1)}_{\rm vac}$ has an extra term, due to the left-going modes, featuring the $\delta$ function $[\hat{b}'_{s'+\tau_{\nu'}},\hat{b}'^\dagger_{s+\tau_\nu}]$. This peaks on the line $s'=s-(\tau_{\nu'}-\tau_\nu)$, which differs from the $\delta$ function coming from right-going modes [cf. Eq. (4.39)] for the exchange $\nu\leftrightarrow\nu'$. Accordingly, in Fig. 4.4, the lines corresponding to $\nu<\nu'$ and $\nu>\nu'$ are swapped, hence now only terms $\nu<\nu'$ (instead of $\nu>\nu'$) contribute to $\hat{\mathcal{H}}^{(1)}_{\rm vac}$. Thus we end up with $\hat{\mathcal{H}}^{(1)}_{\rm vac}\equiv\hat{H}_{\rm vac}$

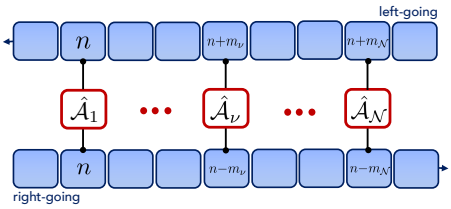


FIGURE 4.6: Bidirectional field for non-negligible time delays. Left-going time bins (top) and right-going time bins (bottom). We set $\tau_1 = m_1 = 0$.

with $\hat{H}_{\text{vac}}$ given by

$$\hat{H}_{\text{vac}} = \tfrac{i}{2} \sum_{\nu>\nu'} \left( \gamma \hat{\mathcal{A}}^\dagger_{\nu'} \hat{\mathcal{A}}_\nu + \gamma' \hat{\mathcal{A}}'^\dagger_{\nu} \hat{\mathcal{A}}'_{\nu'} - \text{H.c.} \right) , \tag{4.66}$$

Thereby, for $\tau_\mathcal{N} - \tau_1 \ll \Delta t \ll (1/\gamma, 1/\gamma')$, the joint dynamics can be be represented by an effective collision model (see Fig. 4.5), where at each collision the emitters jointly collide with a right-going and a left-going time bin, at once being subject to an internal coherent dynamics governed by the second-order Hamiltonian (4.66). Note that, formally, this can still be thought as a collision model featuring a single stream of time bins [like Fig. 4.1] provided that one defines a two-mode time bin $(\hat{b}_n, \hat{b}'_n)$.

An argument analogous to that used in Section 4.6 generalizes Eq. (4.45) as

$$\hat{\mathcal{H}}^{(0)}_n = \tfrac{1}{\sqrt{\Delta t}} \sum_\nu \left( \sqrt{\gamma}\, \hat{\mathcal{A}}_\nu\, \hat{b}^\dagger_{n-m_\nu} + \sqrt{\gamma'} \hat{\mathcal{A}}'_\nu\, \hat{b}'_{n+m_\nu} + \text{H.c.} \right) . \tag{4.67}$$

In the case of a bidirectional field, the time bin is now bipartite (see Fig. 4.5) having associated ladder operators $\hat{b}_n$ [cf. Eq. (4.34)] and $\hat{b}'_n$, the latter given by

$$\hat{b}'_n = \tfrac{1}{\sqrt{\Delta t}} \int_{t_{n-1}}^{t_n} dt\, \hat{b}'_t \, , \tag{4.68}$$

defining a discrete collection of left-going bosonic modes analogous to $\hat{b}_n$ (commuting with them).

Note the different subscripts in $\hat{b}_{n-m_\nu}$ and $\hat{b}'_{n+m_\nu}$, reflecting that right- and left-going time bins travel in opposite directions as sketched in Fig. 4.6.

Similarly to the unidirectional case discussed in Section 4.6, analytical descriptions of this dynamics are demanding [11, 104, 105].

With the extended definitions of $\hat{H}_{\text{vac}}$ and $\hat{V}_n$ for a bidirectional field the finite-difference equation of motion (4.46) for the joint dynamics still holds. The initial state of the time bins $\eta_{\text{bins}}$ is obtained from the initial field state by using (4.42) and tracing off time-bin modes $k \neq 0$ (with left-going time-bin modes $\hat{b}'_{n,k}$ also accounted for).

Also in the bidirectional case, when the field state are assumed uncorrelated state of the time bins, the collisional picture give rise to a Markovian open dynamics.

Specifically, when

$$\eta_{\text{bins}} = \bigotimes_n (\eta_{r,n} \otimes \eta_{l,n}) \tag{4.69}$$

with $\eta_{r,n}$ ($\eta_{l,n}$) the reduced state of the $n$th right-going (left-going) time bin. Under this assumption, the emitters evolve at each collision according to a CPT map [cf. Eq. (4.48)] and so do time bins [see Eq. (4.49)].

The finite-difference master equation of the emitters (4.50) holds, where $\langle \hat{V}_n \rangle$ and $\mathcal{D}[\rho_{n-1}]$ are now given by

$$\langle \hat{V}_n \rangle = \sqrt{\tfrac{1}{\Delta t}} \left( \sqrt{\gamma} \langle \hat{b}_n \rangle \hat{\mathcal{A}}^\dagger + \sqrt{\gamma'} \langle \hat{b'}_n \rangle \hat{\mathcal{A}'}^\dagger + \text{H.c.} \right), \tag{4.70}$$

$$\mathcal{D}[\rho_{n-1}] = \mathcal{D}_r[\rho_{n-1}] + \mathcal{D}_l[\rho_{n-1}] \tag{4.71}$$

with $\mathcal{D}_r[\dots]$ the same as (4.53) and $\mathcal{D}_l[\dots]$ obtained from (4.53) through the replacements $\gamma \to \gamma'$, $\hat{b}_n \to \hat{b'}_n$, $\hat{\mathcal{A}} \to \hat{\mathcal{A}}'$. The master equation is expressed in terms of first and second moments of right-going and left-going time bins, respectively depending on $\eta_{r,n}$ and $\eta_{l,n}$ [cf. Eq. (4.69)].

The most general white-noise Gaussian state of the field is now specified by right-going moments (4.54) plus the analogously defined left-going moments $\alpha'_t$, $N'$ and $M'$. The latter determine the time-bin moments $\langle \hat{b'}_n \rangle = \alpha'_n \sqrt{\Delta t}$, $\langle \hat{b'}^\dagger_n \hat{b'}_n \rangle = N'$ and $\langle \hat{b'}^2_n \rangle = M'$. Plugging these into the finite-difference Eq. (4.50) and taking next the continuous-time limit as done in the unidirectional case, we end up with master equation

$$\begin{aligned} \frac{d\rho}{dt} =& -i\,[\hat{H}_{\text{vac}} + \sqrt{\gamma}\,(\alpha^*_t \hat{\mathcal{A}} + \alpha'^*_t \hat{\mathcal{A}}' + \text{H.c.}), \rho] + \gamma(N+1)\mathcal{D}_{\hat{\mathcal{A}}}[\rho] + \gamma N \mathcal{D}_{\hat{\mathcal{A}}^\dagger}[\rho] \\ &+ \gamma'(N'+1)\mathcal{D}_{\hat{\mathcal{A}}'}[\rho] + \gamma' N' \mathcal{D}_{\hat{\mathcal{A}}'^\dagger}[\rho] + \gamma \left( M(\hat{\mathcal{A}}^\dagger \rho\, \hat{\mathcal{A}}^\dagger - \tfrac{1}{2}[\hat{\mathcal{A}}^{\dagger 2}, \rho]_+) + \text{H.c.} \right) \\ &+ \gamma' \left( M'(\hat{\mathcal{A}}'^\dagger \rho\, \hat{\mathcal{A}}'^\dagger - \tfrac{1}{2}[\hat{\mathcal{A}}'^{\dagger 2}, \rho]_+) + \text{H.c.} \right). \end{aligned} \tag{4.72}$$

where $\mathcal{D}_{\hat{J}}[\rho] = \hat{J}\rho\hat{J}^\dagger - \frac{1}{2}[\hat{J}^\dagger \hat{J}, \rho]_+$ and we recall (4.66). This can be expressed in terms of original ladder operators $\hat{A}_j$ through (4.7), (4.21) and (4.65). Master equation (4.56) for a unidirectional field is retrieved for $\gamma' = 0$.

The aim of this section is to illustrate how (4.72) encompasses and generalizes various quantum optics and waveguide QED master equations with a special focus on giant atoms and decoherence-free Hamiltonians. As such, it could be skipped by a reader solely interested in the collision-model derivation.

For a single normal emitter, $N_e = \mathcal{N} = 1$, $\hat{\mathcal{A}}_1 \equiv \hat{\mathcal{A}}$ (setting $x_1 = \tau_1 = 0$) and $\hat{H}_{\text{vac}} = 0$. Thus ME (4.56) [or (4.72) for $\gamma' = 0$] reduces to the well-known general ME of quantum optics for a point-like atom or harmonic oscillator [80].

For a pair of normal emitters coupled to a unidirectional field, we have: $N_e = \mathcal{N} = 2$ and $\hat{\mathcal{A}}_\nu \equiv e^{-i\omega_0 \tau_\nu} \hat{A}_\nu = e^{-ik_0 x_\nu} \hat{A}_\nu$ with $\nu = 1, 2$ (operators with different $\nu$'s in this case commute). Hence, $\hat{H}_{\text{vac}} = i\frac{\gamma}{2}(\hat{\mathcal{A}}_1^\dagger \hat{\mathcal{A}}_2 - \hat{\mathcal{A}}_2^\dagger \hat{\mathcal{A}}_1)$ and $\hat{\mathcal{A}} = \hat{\mathcal{A}}_1 + \hat{\mathcal{A}}_2$ so that for $\alpha_t = N = M = 0$ (vacuum) (4.56) [or (4.72) for $\gamma' = 0$] reduces to the well-known ME of a pair of cascaded emitters in vacuum [101, 106].

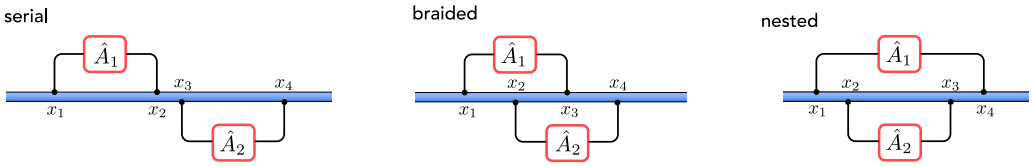


FIGURE 4.7: Possible topologies for the pattern of coupling points of two giant emitters: serial, nested and braided.

For $N_e = \mathcal{N}$ normal emitters coupled to a bidirectional field (such that $\gamma' = \gamma = \Gamma/2$) Eq. (4.72) reduces to

$$\begin{aligned}\dot{\rho} =& -i\tfrac{\Gamma}{2}\sum_{i\neq j}\sin(k_0 x_{ij}^-)[\hat{A}_i^\dagger \hat{A}_j,\rho] + \Gamma(N+1)\sum_{ij}\cos(k_0 x_{ij}^-)\Big(\hat{A}_i\rho\hat{A}_j^\dagger - \tfrac{1}{2}[\hat{A}_j^\dagger\hat{A}_i,\rho]_+\Big)\\ &+\Gamma N\sum_{ij}\cos(k_0 x_{ij}^-)\Big(\hat{A}_i^\dagger\rho\hat{A}_j - \tfrac{1}{2}[\hat{A}_j\hat{A}_i^\dagger,\rho]_+\Big)\\ &+\Gamma\sum_{ij}\cos(k_0 x_{ij}^+)\Big(M(\hat{A}_i^\dagger\rho\hat{A}_j^\dagger - \tfrac{1}{2}[\hat{A}_j^\dagger\hat{A}_i^\dagger,\rho]_+) + \text{H.c.}\Big)\end{aligned} \tag{4.73}$$

with $x_{ij}^\pm = x_j \pm x_i$ and where we used that $\hat{\mathcal{A}}_j = \hat{A}_j e^{-ik_0 x_j}$, $\hat{\mathcal{A}}'_j = \hat{A}_j e^{ik_0 x_j}$ (atom and coupling-point indexes coincide). For $N = N' = \sinh^2(|\xi|)$ and $M = M' = e^{-i\theta}\sinh(|\xi|)\cosh(|\xi|)$ Eq. (4.73) reduces to the master equation found through standard methods in Ref. [107] ($\xi = |\xi|e^{-i\theta}$ is the squeezing parameter, where $\theta$ can include contributions depending on the distance from the source).

For zero squeezing, $\xi = N = M = 0$, Eq. (4.73) reduces to the standard waveguide-QED master equation of a set of atoms [108, 109].

Thus Eq. (4.72) generalizes the squeezed-bath master equation to giant emitters.

For a single giant emitter with two coupling points in a bidirectional waveguide: $\gamma' = \gamma = \Gamma/2$ (with $\Gamma$ the total decay rate), $N_e = 1$, $\mathcal{N} = 2$, $\hat{\mathcal{A}}_1 = \hat{\mathcal{A}}'_1 = \hat{A}_1 = \hat{A}$, $\hat{\mathcal{A}}_2 = e^{-i\varphi}\hat{A}$, $\hat{\mathcal{A}}'_2 = e^{i\varphi}\hat{A}$, where we set $x_1 = \tau_1 = 0$ and $\varphi = k_0 x_2 = \omega_0 \tau_2$ ($\hat{A}$ could be a spin-1/2 or bosonic ladder operator). The collective operators (4.65) thus read

$$\hat{\mathcal{A}} = (1 + e^{-i\varphi})\,\hat{A}\,, \quad \hat{\mathcal{A}}' = (1 + e^{+i\varphi})\,\hat{A}\,. \tag{4.74}$$

Plugging these into Eq. (4.72), for $\alpha_t = \alpha'_t = N = N' = M = M' = 0$ we retrieve the vacuum master equation [110, 53]

$$\dot{\rho} = -i\,\tfrac{\Gamma}{2}\sin\varphi\,[\hat{A}^\dagger\hat{A},\rho] + \Gamma(1+\cos\varphi)\mathcal{D}_{\hat{A}}[\rho]\,. \tag{4.75}$$

For a pair of giant emitters with two coupling points each and a bidirectional waveguide: $\gamma' = \gamma = \Gamma/2$, $N_e = 2$, $\mathcal{N} = 4$. The $\hat{\mathcal{A}}_\nu$'s and $\hat{\mathcal{A}}'_\nu$'s depend on the pattern of coupling points, for which three different topologies are possible: serial, nested and braided (see Fig. 4.7). Setting $\varphi_\nu = k_0 x_\nu = \omega_0 \tau_\nu$ and as usual $x_1 = \tau_1 = 0$, in the braided configuration in particular one gets $\hat{\mathcal{A}}_1 = \hat{A}_1$, $\hat{\mathcal{A}}_2 = \hat{A}_2 e^{-i\varphi_2}$, $\hat{\mathcal{A}}_3 =$

$\hat{A}_1 e^{-i\varphi_3}$ and $\hat{\mathcal{A}}_4 = \hat{A}_2 e^{-i\varphi_4}$. Hence [cf. Eq. (4.65)],

$$\hat{\mathcal{A}} = (1 + e^{-i\varphi_3})\hat{A}_1 + (e^{-i\varphi_2} + e^{-i\varphi_4})\hat{A}_2\,, \tag{4.76}$$

while $\hat{\mathcal{A}}'$ has an analogous expression with $\varphi_\nu \to -\varphi_\nu$. Plugging these into (4.72), for $\varphi_\nu = \nu\varphi$ (uniform spacings) and the field vacuum state, one gets

$$\begin{aligned}\dot{\rho} = &-\tfrac{i\Gamma}{2}\,(3\sin\varphi + \sin 3\varphi)\left[\hat{A}_2^\dagger\hat{A}_1 + \hat{A}_1^\dagger\hat{A}_2, \rho\right] + 2\Gamma\,(1+\cos 2\varphi)\left(\mathcal{D}_{\hat{A}_1}[\rho] + \mathcal{D}_{\hat{A}_2}[\rho]\right)\\ &+ \Gamma\,(3\cos\varphi + \cos 3\varphi)\sum_{i\neq j}\left(\hat{A}_i\rho\hat{A}_j^\dagger - \tfrac{1}{2}[\hat{A}_j^\dagger\hat{A}_i, \rho]_+\right)\,,\end{aligned} \tag{4.77}$$

which was derived through the SLH formalism in Ref. [53] alongside other master equations for different configurations and number of atoms [these can all be retrieved from (4.72) likewise].

## 4.9 Mechanism of decoherence-free coupling between giant atoms

While a longstanding way for matching the Decoherence-Free (DF) condition in quantum optics is coupling atoms to single- or multi-mode photonic environment dispersively (off-resonantly), Decoherence-free Hamiltonians via giant atoms work in the regime in which the atomic frequency $\omega_0$ is well within a photonic band which can thus be approximated as infinite. This is possible due to *non-local* coupling (the hallmark of giant atoms) as will become clear later.

## Box 5: General scheme for Decoherence-Free Hamiltonians

The averaged interaction $\overline{V}_n = \hat{\mathcal{H}}_n^{(0)}$ and Hamiltonian $\hat{\mathcal{H}}_n^{(1)}$ (Eqs. (4.25) and (4.26)) are the two central quantities to consider for implementing DF Hamiltonians. In sketchy terms, one seeks to fulfill $\overline{V}_n = 0$ (henceforth referred to as the "DF condition") in a way that $\hat{\mathcal{H}}_n$ yields (upon partial trace) a dissipationless effective Hamiltonian of $S$, $\hat{H}_{\rm eff}$. This is formalized in detail in the following.

Let $\sigma_n$ be the joint $S$-$E$ state at time $t_n$ and $\rho_n = \mathrm{Tr}_E\{\sigma_n\}$ the reduced state of the system at the same time. We will consider a coarse-grained time scale defined by $\Delta t$ short enough that (4.24) holds. In the corresponding continuous-time limit, $t_n \to t$, $\sigma_n \to \sigma_t$, $\dot{\sigma} \simeq \Delta\sigma_n/\Delta t$ where we set $\Delta\sigma_n = \sigma_n - \sigma_{n-1}$ (analogously for $\rho_n$). We also define

$$\langle \hat{\mathcal{H}}_n^{(1)} \rangle_{\rho_0} = \mathrm{Tr}_S \left\{ \hat{\mathcal{H}}_n^{(1)} \rho_0 \otimes \mathbb{1}_E \right\}, \tag{4.78}$$

$$\hat{H}_{\rm eff} = \mathrm{Tr}_E \left\{ \hat{\mathcal{H}}_n^{(1)} \mathbb{1}_S \otimes \rho_E \right\} \tag{4.79}$$

with $\mathrm{Tr}_{S(E)}\{\}$ the partial trace over $S$ ($E$). These are effective Hamiltonians on $E$ and $S$, respectively. When $S$ is multipartite, in particular, $\hat{H}_{\rm eff}$ will generally feature mutual couplings between subsystems of $S$.

The following property holds.

**Property.** *Let the system and environment be initially in the uncorrelated state $\rho_0 \otimes \rho_E$ with $\rho_0$ ($\rho_E$) the initial state of the system (environment). If*

$$\overline{V}_n = 0 \tag{4.80}$$

*in each time interval $[t_{n-1}, t_n]$, and*

$$[\hat{\mathcal{H}}_n, \mathbb{1}_S \otimes \rho_E] = 0 \tag{4.81}$$

*then in the continuous-time limit*

$$\dot{\rho} = -i\,[\hat{H}_{\rm eff}, \rho]\,. \tag{4.82}$$

This embodies a rather general working principle for realizing DF effective Hamiltonians: conditions (4.80) and (4.81) entail a *unitary* reduced dynamics of $S$ generated by the effective Hamiltonian $\hat{H}_{\rm eff}$. Among (4.80) and (4.81), the former (DF condition) is the most relevant: it means that the interaction Hamiltonian $\hat{V}_t$ *averages* to zero over the coarse-grained time scale $\Delta t$.

The above property is easily shown (see [88] for further details), from which in particular it turns out that $\sigma_n = \rho_n \otimes \rho_E$ namely $E$ remains in its initial state, uncorrelated with $S$.

A typical case where (4.81) occurs is when $\hat{\mathcal{H}}_n$ acts trivially on $E$, then (4.81) is matched for any $\rho_E$ and $\hat{\mathcal{H}}_n \equiv \hat{H}_{\rm eff}$ (this happens with giant atoms as we will see). Another instance is when $S$ is a two-level system and $E$ a harmonic oscillator with $\hat{\mathcal{H}}_n \sim \hat{\sigma}_z\,\hat{b}^\dagger\hat{b}$ (dispersive regime of the Jaynes-Cummings model [4]; see next section). Then (4.81) holds when $\rho_E$ is any mixture of Fock states.

A paradigmatic instance is the braided configuration in Fig. 4.7. By adjusting a $\pi$-phase shift between the coupling points of the same emitter, e.g., setting $\varphi = \pi/2$, all the dissipative terms in Eq. (4.77) vanish but the Hamiltonian $\hat{H}_{\rm vac}$, which effectively seeds a dissipationless coherent interaction [53].

As illustrated in Box 5, in the collisional picture this phenomenon can be predicted without working out the master equation, making clear at once that it occurs

regardless of the field state [thus being not limited to the vacuum state assumed in the derivation of Eq. (4.77)]. Indeed, we can easily anticipate that the condition that collective operators (4.65) vanish,

$$\hat{\mathcal{A}} = \hat{\mathcal{A}}' = 0 \tag{4.83}$$

(or just $\hat{\mathcal{A}} = 0$ with a unidirectional field), guarantees that the joint emitters-field propagator reduces to $\hat{\mathcal{U}}_t = \exp(-i\hat{H}_{\rm vac}t)$. This is because (4.83) effectively decouples the emitters from the field time bins in light of Eqs. (4.22), (4.66) and (4.64), thus inhibiting dissipation. Having giant emitters is clearly indispensable since for normal emitters there is no way for $\hat{\mathcal{A}}$ and $\hat{\mathcal{A}}'$ to identically vanish in the entire Hilbert space. The question is now whether or not (4.83) yields a null $\hat{H}_{\rm vac}$ (if so no evolution takes place). In the rest of this chapter this problem will be addressed by formulating a collision model-based microscopic theory of DF coupling.

### 4.9.1 Giant atoms in a broadband waveguide

We study now in detail the occurrence of DF Hamiltonians for giant atoms. Consider a set of giant two-level atoms weakly coupled to a one-dimensional waveguide with $\omega_0$ inside a band of the waveguide field. For the sake of clarity, but without loss of generality, in this section we address the one-directional field configuration.

We report the interaction Hamiltonian in the interaction picture (see Box 3)

$$\hat{V}_t = g_{k_0} \sum_{j,\ell} e^{-i\varphi_{j\ell}} \hat{\sigma}_j \sum_k e^{-i\omega_k(t-\tau_{j\ell})}\, \hat{b}_k^\dagger + \text{H.c.}\,. \tag{4.84}$$

where $\hat{A}_j \to \hat{\sigma}_j = |g\rangle_j\langle e|$ and $\varphi_{j\ell} = k_0\, x_{j\ell}$.

Averaging (4.84) over a time interval $[t_{n-1}, t_n]$ yields

$$\overline{V}_n = g_{k_0} \sum_j \left( \sum_\ell e^{-i\varphi_{j\ell}} \right) \hat{\sigma}_j \int_{t_{n-1}}^{t_n} ds \sum_k e^{-i\omega_k(s-\tau_{j\ell})}\, \hat{b}_k^\dagger + \text{H.c.} \tag{4.85}$$

(we have also split the sum over $j$ and $\ell$). If all these time delays are negligible compared to $\Delta t$, then (4.85) can be approximated as

$$\overline{V}_n \simeq g_{k_0} \sum_j \left( \sum_\ell e^{-i\varphi_{j\ell}} \right) \hat{\sigma}_j \int_{t_{n-1}}^{t_n} ds \sum_k e^{-i\omega_k s}\, \hat{b}_k^\dagger + \text{H.c.} \tag{4.86}$$

Now, the key point is that each atomic operator $\hat{\sigma}_j$ comes with a pre-factor $\sum_\ell e^{i\varphi_{j\ell}}$, which – due to non-local coupling – can vanish for all atoms at the same time. This occurs when the coupling point phases are adjusted so as to match the condition

$$\sum_{\ell=1}^{\mathcal{N}_j} e^{-i\varphi_{j\ell}} = 0 \quad \text{for any } j\,, \tag{4.87}$$

which is the DF condition (4.80) for giant atoms equivalent to Eq. (4.83). Note that this cannot be satisfied by normal atoms: *each* atom must have at least *two* coupling points ($\mathcal{N}_j \geq 2$).

### 4.9.2 Effective Hamiltonian

When $\overline{V}_n = 0$, atoms will evolve unitarily with effective Hamiltonian [recall Eq. (4.79)] $\hat{H}_{\text{eff}} = \hat{\mathcal{H}}_n^{(1)}$ (which acts trivially on the field).

We write now more explicitly the effective Hamiltonian $\hat{H}_{\text{eff}} = \hat{\mathcal{H}}_n^{(1)}$ for generic two-dimensional bath as [cf. Eqs. (4.7) and (4.66)]

$$\hat{H}_{\text{eff}} = \frac{i}{2} \sum_{\nu > \nu'} \left( \gamma \, e^{i(\varphi_{j'\ell'} - \varphi_{j\ell})} \hat{\sigma}_{j'}^\dagger \hat{\sigma}_j + \gamma' \, e^{i(\varphi_{j'\ell'} - \varphi_{j\ell})} \hat{\sigma}_j^\dagger \hat{\sigma}_{j'} - \text{H.c.} \right) , \tag{4.88}$$

where $(j, \ell)$ are understood as the pair of indexes corresponding to $\nu$ [and likewise $(j', \ell')$ with respect to $\nu'$]. This in turn can be expressed in the compact form

$$\hat{H}_{\text{eff}} = \sum_{jj'} J_{jj'} \, \hat{\sigma}_j^\dagger \hat{\sigma}_{j'} + \text{H.c.} \tag{4.89}$$

with

$$J_{jj'} = \sum_{\nu_{j'\ell'} > \nu_{j\ell}} \left[ \tfrac{\gamma + \gamma'}{2} \sin(\varphi_{j'\ell'} - \varphi_{j\ell}) + i \, \tfrac{\gamma - \gamma'}{2} \cos\left(\varphi_{j'\ell'} - \varphi_{j\ell}\right) \right] , \tag{4.90}$$

and where $\nu_{j\ell}$ is the (previously introduced) discrete map returning the coupling point index for each pair $(j, \ell)$. Note that for isotropic coupling ($\gamma = \gamma'$), each $J_{jj'}$ (for given $j$ and $j'$) reduces to a sum of sines, where the argument of each sine is the phase shift associated to a pair of coupling points (one of atom $j$ one of $j'$). Alternatively, $J_{jj'}$ can be expressed by separating the right- and left-going contributions as

$$J_{jj'} = \gamma K_{jj'} + \gamma' K_{jj'}^* \tag{4.91}$$

with

$$K_{jj'} = \tfrac{1}{2} \sum_{\nu_{j'\ell'} > \nu_{j\ell}} e^{i(\varphi_{j\ell} - \varphi_{j'\ell'} + \frac{\pi}{2})} . \tag{4.92}$$

The issue is now raised as to whether or not $\hat{H}_{\text{eff}} \neq 0$ when decoherence is inhibited [condition (4.87)]. It turns out that there generally exist patterns of coupling points such that $\hat{H}_{\text{eff}} = 0$ and patterns for which $\hat{H}_{\text{eff}} \neq 0$, where the former yield a trivial dynamics (the system just does not evolve) and are thus unwanted. The best instance for illustrating this is a pair of giant atoms 1 and 2, such that $\mathcal{N}_1 = \mathcal{N}_2 = 2$, with equally-spaced coupling points

$$k_0 x_\nu = (\nu - 1)\varphi \quad \text{with} \quad \nu = 1, 2, 3, 4 , \tag{4.93}$$

the field being unidirectional ($\gamma' = 0$). Three different types of patterns are then possible: serial, nested and braided [see Fig. 4.7(a), (c), (e)]. For the serial and nested topology, we choose $\varphi = \pi$ while in the braided case we take $\varphi = \pi/2$. Each of these settings ensures that there is $(2n+1)\pi$-phase-shift between the two coupling points of each giant atom, thus matching the DF condition [recall Eq. (4.87)]. Using (4.89), in the serial and nested topologies we get $H_{\text{eff}} = 0$, while the braided yields [53]

$$\hat{H}_{\text{eff}} = \gamma\,(\hat{\sigma}_1\hat{\sigma}_2^\dagger + \hat{\sigma}_1^\dagger\hat{\sigma}_2)\,, \tag{4.94}$$

(we absorbed a phase factor $e^{-i\pi/2}$ in the definition of $\hat{\sigma}_2$). Analogous conclusions hold for isotropic coupling ($\gamma' = \gamma = \Gamma/2$), in which case (4.94) is generalized by replacing $\gamma$ with $\Gamma$.

### 4.9.3 Mapping into a cascaded collision model

While, as pointed out in the previous section, the collision $\hat{U}_n$ formally describes a simultaneous collision with all the atoms (recall Fig. 4.5), we show next that it can be effectively decomposed as a *cascade* of sub-collisions each involving only *one* coupling point. Cascaded collision models (for normal atoms) were introduced in Refs. [8, 111] (see also Ref. [112]).

For each coupling point $\nu$, let us define the interaction Hamiltonian

$$\hat{V}_{n\nu} = \sqrt{\tfrac{\gamma}{\Delta t}}\,\left(\hat{A}_\nu\,\hat{b}_n^\dagger + \text{H.c.}\right) \tag{4.95}$$

coupling the $n$th time bin to atom $j$ with phase $\varphi_{j\ell}$ [cf. Eq. (4.7)], where $(j,\ell)$ is the pair correspond to coupling point $\nu$ (in the remainder we introduce a convenient terminology and say that the time bin "interacts with the coupling point"). Using (4.76), (4.64) and (4.95), it is easily immediately checked that the average interaction Hamiltonian is just the sum of the $\hat{V}_{n\nu}$'s

$$\overline{V}_n = \sum_\nu \hat{V}_{n\nu}\,. \tag{4.96}$$

More importantly, as shown in the remainder, it turns out that, when the DF condition (4.87) is matched, the unitary collision $\hat{U}_n$ can be decomposed as

$$\hat{U}_n = e^{-i\hat{V}_{n\mathcal{N}}\Delta t}\cdots e^{-i\hat{V}_{n1}\Delta t}\,. \tag{4.97}$$

Thereby, one can think of each collision (see Fig. 4.8) as the result of $\mathcal{N}$ cascaded sub-collisions in each of which the time bin "collides" with one of the coupling points according to unitary $e^{-i\hat{V}_{n\nu}\Delta t}$ with $\hat{V}_{n\nu}$ given by (4.95) . Of course, this in particular entails that the same time bin collides with a given atom as many times as the number of respective coupling points $\mathcal{N}_j$. Yet, the sub-collisions with the same atom occur with different coupling Hamiltonians and are generally non-consecutive (i.e., between two sub-collisions with the same atom $j$ there may be sub-collisions with

atoms $j' \neq j$), which is key to the occurrence of a non-trivial DF Hamiltonian as we will see shortly.

To prove (4.97), we expand to second order each sub-collision unitary on the right hand side as $e^{-i\hat{V}_{n\nu}\Delta t} \simeq \mathbb{1} - i\hat{V}_{n\nu}\Delta t - \frac{1}{2}\hat{V}_{n\nu}^2\Delta t^2$. This yields (to leading order)

$$\prod_{\nu=1}^{\mathcal{N}} e^{-i\hat{V}_{n\nu}\Delta t} \simeq \mathbb{1} - i\left(\overline{V}_n + \tilde{\mathcal{H}}_n\right)\Delta t - \tfrac{1}{2}\,\overline{V}_n^2\,\Delta t^2 \tag{4.98}$$

with the order in the product understood as in (4.97) and

$$\tilde{\mathcal{H}}_n = i\,\tfrac{\Delta t}{2}\sum_{\nu>\nu'}\left[\hat{V}_{n\nu'}, \hat{V}_{n\nu}\right], \tag{4.99}$$

where we used (4.96). Using (4.87), it is easily shown that $\tilde{\mathcal{H}}_n = \hat{\mathcal{H}}_n^{(1)} \equiv \hat{H}_{\text{eff}}$. Indeed in the unidirectional case each commutator in (4.99) is explicitly worked out as

$$\left[\hat{V}_{n\nu'}, \hat{V}_{n\nu}\right] = \tfrac{\gamma}{\Delta t}\left(\left[\hat{A}_{\nu'}, \hat{A}_{\nu}^\dagger\right] - \text{H.c.}\right)\hat{b}_n^\dagger\hat{b}_n + \tfrac{\gamma}{\Delta t}\left(\hat{A}_{\nu'}^\dagger\hat{A}_{\nu} - \text{H.c.}\right). \tag{4.100}$$

Upon comparison with (4.66) , the proof thus reduces to showing that the sum over $\nu{>}\nu'$ of terms $\propto \hat{b}_n^\dagger\hat{b}_n$ vanishes.

Each commutator $\left[\hat{A}_{\nu'}, \hat{A}_{\nu}^\dagger\right]$ is non-zero only when coupling points $\nu$ and $\nu'$ belong to the same atom. Thus, in light of (4.7),

$$\begin{aligned}\sum_{\nu>\nu'}\left[\hat{A}_{\nu}, \hat{A}_{\nu'}^\dagger\right] - \text{H.c.} &= \sum_j\sum_{\ell>\ell'} e^{i(\varphi_{j\ell}-\varphi_{j\ell'})}\left[\hat{\sigma}_j, \hat{\sigma}_j^\dagger\right] - \text{H.c.} \\ &= \sum_j\left(\sum_{\ell>\ell'} e^{i(\varphi_{j\ell}-\varphi_{j\ell'})} - \text{c.c.}\right)\hat{\sigma}_{jz}\end{aligned} \tag{4.101}$$

(recall that $x_{j1} < x_{j2} < \ldots$ ). When (4.87) holds, the coefficient of $\hat{\sigma}_{jz}$vanishes for each $j$

$$\sum_{\ell>\ell'} e^{i(\varphi_{j\ell}-\varphi_{j\ell'})} - \text{c.c.} = \sum_{\ell=\ell'}^{\mathcal{N}_j} e^{i\varphi_{j\ell}}\sum_{\ell'=1}^{\mathcal{N}_j} e^{-i\varphi_{j\ell'}} - \text{c.c.} = 0\,. \tag{4.102}$$

Thus

$$\sum_{\nu>\nu'}\left[\hat{V}_{n\nu'}, \hat{V}_{n\nu}\right] = \tfrac{\gamma}{\Delta t}\sum_{\nu>\nu'}\left(\hat{A}_{\nu'}^\dagger\hat{A}_{\nu} - \text{H.c.}\right), \tag{4.103}$$

completing the proof.

Upon comparison with (4.24), we thus conclude that (4.97) holds true.

The decomposition in terms of cascaded sub-collisions in particular highlights the physical origin of effective Hamiltonian (4.66): if, instead of being sequential, the sub-collisions occurred simultaneously (corresponding to perfectly co-located coupling points) then the overall collision unitary would be $e^{-i(\sum_\nu \hat{V}_{n\nu})\Delta t} \equiv e^{-i\overline{V}_n\Delta t}$, the corresponding second-order expansion being just (4.98) *without* term $\tilde{\mathcal{H}}_n \equiv \hat{H}_{\text{eff}}$. Thus the effective Hamiltonian arises precisely because the time bin collides with

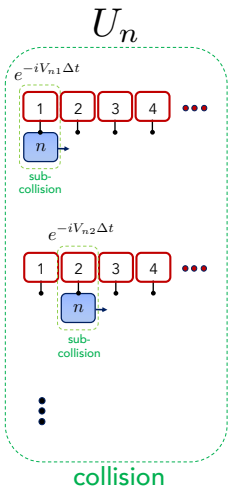


FIGURE 4.8: Under the DF condition (4.87), each collision in Fig. 4.5 (we address here the case $\gamma' = 0$) can be effectively decomposed into $\mathcal{N}$ cascaded sub-collisions according to Eq. (4.97). Each sub-collision is between the same time bin $n$ and a different coupling point corresponding to coupling Hamiltonian (4.95) (time grows from top to bottom).

the coupling points in a cascaded fashion. This is in fact the same mechanism underpinning emergence of effective Hamiltonians in chiral quantum optics with normal atoms [97], the difference yet being that decoherence cannot be suppressed in the latter case (because $\overline{V}_n$ cannot vanish with normal atoms).

The generalization for a bidirectional waveguide is straightforward: under the DF condition (4.87) the cascaded sub-collision decomposition takes the form

$$\hat{U}_n = e^{-i(\hat{V}_{n\mathcal{N}}+\hat{V}'_{n1})\Delta t} \cdots e^{-i(\hat{V}_{n1}+\hat{V}'_{n\mathcal{N}})\Delta t} . \tag{4.104}$$

with

$$\hat{V}'_{n\nu} = \sqrt{\frac{\gamma'}{\Delta t}} \left( \hat{S}'_\nu \, \hat{b}'^\dagger_n + \text{H.c.} \right) . \tag{4.105}$$

Thus $\tilde{\mathcal{H}}_n$ [cf. Eq. (4.99)] is now generally defined as

$$\tilde{\mathcal{H}}_n = i\tfrac{\Delta t}{2} \sum_{\nu>\nu'} \left[ \hat{V}_{n,\nu'} + \hat{V}'_{n,\mathcal{N}+1-\nu'}, \hat{V}_{n,\nu} + \hat{V}'_{n,\mathcal{N}+1-\nu} \right] . \tag{4.106}$$

Each commutator reads

$$\begin{aligned} \left[ \hat{V}_{n,\nu'} + \hat{V}'_{n,\mathcal{N}+1-\nu'}, \hat{V}_{n,\nu} + \hat{V}'_{n,\mathcal{N}+1-\nu} \right] = & \left[ \hat{V}_{n,\nu'}, \hat{V}_{n,\nu} \right] + \left[ \hat{V}'_{n,\mathcal{N}+1-\nu'}, \hat{V}'_{n,\mathcal{N}+1-\nu} \right] \\ & + \left[ \hat{V}_{n,\nu'}, \hat{V}'_{n,\mathcal{N}+1-\nu} \right] + \left[ \hat{V}'_{n,\mathcal{N}+1-\nu'}, \hat{V}_{n,\nu} \right] . \end{aligned} \tag{4.107}$$

The last line features terms $\propto [\hat{b}^\dagger_n, \hat{b}'_n]$ and $\propto [\hat{b}'^\dagger_n, \hat{b}_n]$, which vanish because left- and right-going time-bin operators commute. Additionally, there are terms $\propto \hat{b}^\dagger_n \hat{b}'_n$ (or $\propto \hat{b}'^\dagger_n \hat{b}_n$) featuring quantities like (4.101) where however one of the two phases is primed: these vanish as well since (4.102) holds even if $\varphi_{j\ell'} \to \varphi'_{j\ell'}$. We are thus only

left with terms analogous to (4.100) given by

$$\left[\hat{V}_{n,\nu'},\hat{V}_{n,\nu}\right]+\left[\hat{V}'_{n,\mathcal{N}+1-\nu'},\hat{V}'_{n,\mathcal{N}+1-\nu}\right]=\tfrac{\gamma}{\Delta t}\left(\hat{A}^\dagger_{\nu'}\hat{A}_\nu+\hat{A}'^\dagger_{\mathcal{N}+1-\nu'}\hat{A}'_{\mathcal{N}+1-\nu}-\text{H.c.}\right). \tag{4.108}$$

Summing this over $\nu > \nu'$ yields $\frac{\gamma}{\Delta t}\left(\hat{A}^\dagger_{\nu'}\hat{A}_\nu+\hat{A}'^\dagger_{\nu}\hat{A}'_{\nu'}-\text{H.c.}\right)$ (where we used that $\mathcal{N}+1-\nu' > \mathcal{N}+1-\nu$ for $\nu > \nu'$), yielding the complete Hamiltonian (4.89).

### 4.9.4 Mechanism behind emergence of non-trivial $\hat{H}_{\text{eff}}$

Occurrence of non-trivial (i.e., non-zero) DF Hamiltonians is simply interpreted in the cascaded-collision-model picture.

As in Section 4.9.2, throughout this and the next section we consider a *unidirectional* waveguide and giant atoms with *two coupling points* each, which captures most of the essential physics.

Let us consider first a single giant atom and set $x_1 = \tau_1 = 0$, $\varphi = k_0 x_2$. The DF condition $\overline{V}_n = 0$ then simply reads $\varphi = (2n+1)\pi$ with $n$ an integer number. Hence, $\hat{S}_1 = -\hat{S}_2 = \hat{\sigma}_1$ and [cf. Eq. (4.95)]

$$\hat{V}_{n1} = \sqrt{\tfrac{\gamma}{\Delta t}}\,(\hat{\sigma}_1\,\hat{b}^\dagger_n+\text{H.c.})\,,\ \ \hat{V}_{n2} = \sqrt{\tfrac{\gamma}{\Delta t}}\,(-\hat{\sigma}_1\,\hat{b}^\dagger_n+\text{H.c.})\,. \tag{4.109}$$

Thus $\hat{V}_{n1} = -\hat{V}_{n2}$ and [see Eq. (4.97)]

$$\hat{U}_n = e^{-i\hat{V}_{n2}\Delta t}\,e^{-i\hat{V}_{n1}\Delta t} = \mathbb{1}\,, \tag{4.110}$$

meaning that the collision has no effect overall. This, in particular, necessarily entails $\hat{H}_{\text{eff}} = 0$ [recall Eq. (4.24)]. In other words, the two sub-collisions are the *time-reversed* of one another (so that the net effect is null). To sum up, in order to ensure the DF condition $\overline{V}_n = 0$ for a single giant atom, one must adjust the phase shift so that $\hat{V}_{n2} = -\hat{V}_{n1}$. This yet brings about that one sub-collision is just the other one time-reversed, trivially yielding $\hat{U}_n = 0$ hence $\hat{H}_{\text{eff}} = 0$.

When it comes to a pair of giant atoms, instead, conditions $\overline{V}_n = 0$ and $\hat{U}_n \neq 0$ can be matched simultaneously. To see this, we reconsider uniformly-spaced atoms as in Eq. (4.93) and always set $\varphi$ so as to ensure a $(2n+1)\pi$-phase-shift between the pair of coupling points of each atom, hence $\overline{V}_n = 0$ (similarly to the single-atom instance just discussed).

For convenience, we define the coupling Hamiltonians

$$\hat{\mathcal{V}}_j = \sqrt{\tfrac{\gamma}{\Delta t}}\left(\hat{\sigma}_j\,\hat{b}^\dagger_n+\text{H.c.}\right) \tag{4.111}$$

with $j = 1,2$ (the dependence on $n$ is left implicit). No phase factor appears in this definition.

Consider first the serial scheme in Fig. 4.7, in which case we set $\varphi = \pi$. Then [see Fig. 4.7],

$$\hat{V}_{n1} = \hat{\mathcal{V}}_1\,,\ \hat{V}_{n2} = -\hat{\mathcal{V}}_1\,,\ \hat{V}_{n3} = \hat{\mathcal{V}}_2\,,\ \hat{V}_{n4} = -\hat{\mathcal{V}}_2\,. \tag{4.112}$$

This results in the collision unitary [cf. (4.97)]

$$\hat{U}_n = e^{i\hat{\mathcal{V}}_2\Delta t}e^{-i\hat{\mathcal{V}}_2\Delta t}e^{i\hat{\mathcal{V}}_1\Delta t}e^{-i\hat{\mathcal{V}}_1\Delta t} = \mathbb{1}\,, \tag{4.113}$$

that is a trivial dynamics such that $\hat{H}_{\rm eff} = 0$. This case is in fact an extension the single giant atom considered above.

For the nested case in Fig. 4.7, we set $\varphi = \pi$. Then [see Fig. 4.7(d)],

$$\hat{V}_{n1} = \hat{\mathcal{V}}_1\,,\ \hat{V}_{n2} = -\hat{\mathcal{V}}_2\,,\ \hat{V}_{n3} = \hat{\mathcal{V}}_2\,,\ \hat{V}_{n4} = -\hat{\mathcal{V}}_1\,, \tag{4.114}$$

Thus the second pair of sub-collisions is the first pair time-reversed

$$\hat{U}_n = e^{i\hat{\mathcal{V}}_1\Delta t}e^{-i\hat{\mathcal{V}}_2\Delta t}e^{i\hat{\mathcal{V}}_2\Delta t}e^{-i\hat{\mathcal{V}}_1\Delta t} = \mathbb{1}\,, \tag{4.115}$$

ensuing again a trivial dynamics and $\hat{H}_{\rm eff} = 0$. Equivalently, the pair of central sub-collisions, both involving atom 2, are the time-reversed of one another. Thus atom 2 simply disappears from $\hat{U}_n$, which reduces to $\hat{U}_n = e^{i\hat{\mathcal{V}}_1\Delta t}e^{-i\hat{\mathcal{V}}_1\Delta t} = \mathbb{1}$.

For the braided arrangement of Fig. 4.7(e), we set $\varphi = \pi/2$. Then [see Fig. 4.7],

$$\hat{V}_{n1} = \hat{\mathcal{V}}_1\,,\ \hat{V}_{n2} = \hat{\mathcal{V}}_2\,,\ \hat{V}_{n3} = -\hat{\mathcal{V}}_1\,,\ \hat{V}_{n4} = -\hat{\mathcal{V}}_2 \tag{4.116}$$

[with $\hat{\mathcal{V}}_2$ now defined by (4.111) for $j = 2$ under the replacement $\hat{\sigma}_2 \to -i\hat{\sigma}_2$]. The collision unitary is given by

$$\hat{U}_n = e^{i\hat{\mathcal{V}}_2\Delta t}e^{i\hat{\mathcal{V}}_1\Delta t}e^{-i\hat{\mathcal{V}}_2\Delta t}e^{-i\hat{\mathcal{V}}_1\Delta t} = e^{-i\gamma(\hat{\sigma}_1\hat{\sigma}_2^\dagger + \hat{\sigma}_1^\dagger\hat{\sigma}_2)\Delta t} \neq \mathbb{1}\,. \tag{4.117}$$

Therefore, $\overline{V}_n = 0$ is fulfilled but now $\hat{H}_{\rm eff} \neq 0$.

The above shows that, while being irrelevant for realizing the DF condition $\overline{V}_n = 0$, the coupling points topology is crucial in order to have a non-vanishing effective Hamiltonian. In terms of propagators [cf. Eqs. (4.22) and (4.24)], this is ultimately due to the fact that the second-order term $\hat{\mathcal{H}}_n$ is affected by the time-ordering operator, while $\overline{V}_n$ and (of course) $\overline{V}_n^2$ are fully insensitive to it.

### 4.9.5 More than two coupling points

The discussion in Section 4.9.4 in many respects relied on the property that a single giant atom with a $\pi$-phase shift between its two coupling points (i.e., the DF condition) fully decouples from the field, i.e., $\hat{U}_n = \mathbb{1}$ [cf. Eq. (4.110)]. For more than two coupling points, the DF condition for a single giant atom does not necessarily entail $\hat{U}_n = \mathbb{1}$. The simplest example to see this is a single giant atom with three coupling points ($\mathcal{N} \equiv \mathcal{N}_1 = 3$). The DF condition (4.87) occurs for (we drop subscript $j$ since

there is only one atom; also we set $\varphi_1 = 0$)

$$\varphi_2 = \tfrac{2\pi}{3} + 2n\pi,\ \varphi_3 = \tfrac{4\pi}{3} + 2m\pi \tag{4.118}$$

with $n$, $m$ integers. Plugging these into the effective Hamiltonian (4.89) for $\gamma' = 0$ we get

$$\hat{H}_{\text{eff}} = \tfrac{\gamma}{2}\left(2\sin(\tfrac{2\pi}{3}) + \sin(\tfrac{4\pi}{3})\right)\hat{\sigma}_z \neq 0 \tag{4.119}$$

(the sum of the three sines is $\simeq 0.87$).

For an atom $j$ such that $x_{j'\neq j,\ell'} \notin [x_{j,1}, x_{j,\mathcal{N}_j}]$ and fulfilling the DF condition $\sum_\ell \hat{V}_{n,\nu_{j,\ell}} = 0$, in general

$$e^{-i\hat{V}_{n,\nu_{j,\mathcal{N}_j}}\Delta t} \dots e^{-i\hat{V}_{n,\nu_{j,1}}\Delta t} \neq \mathbb{1}\,, \tag{4.120}$$

where $\mathcal{N}_j > 2$ (if $\mathcal{N}_j = 2$, the identity holds). However, (4.120) is anyway of the form $e^{-i\delta_j\hat{\sigma}_z\Delta t}$ (with $\delta_j$ a frequency shift), hence all terms of $\hat{H}_{\text{eff}}$ coupling $j$ to any other atom will vanish, i.e., in (4.89) $J_{jj'} \neq 0$ only for $j' = j$. Thus, if the only focus is coupling the atoms, then the braided topology remains the only one yielding a non-trivial $\hat{H}_{\text{eff}}$. This remains true for a chiral waveguide ($\gamma' \neq 0$) since (4.91) shows that if $J_{jj'} = 0$ for $\gamma' = 0$ then it vanishes also for $\gamma' \neq 0$.

## 4.10 Summary

In this chapter, we formulated the collision-model-based description of quantum optics dynamics in the presence of many quantum emitters, each able to interact with a generally chiral field at many coupling points. We focused on the regime of negligible time delays, in which the dynamics is effectively represented as a sequence of pairwise collisions each between a field time bin and all the emitters collectively. These at once undergo an internal dynamics ruled by an effective second-order Hamiltonian describing dipole-dipole interaction originating from the fact that the traveling time bin reaches the system's coupling points in sequence, no matter how short the delays. As such, the effective Hamiltonian depends on the coupling points topology. We then derived a general master equation for system of giant emitters coupled to a generally chiral waveguide.

We finally investigated the physical mechanism underpinning implementation of DF Hamiltonians with giant atoms. We introduced a general framework for obtaining DF Hamiltonians through second-order interactions mediated by an environment and showed that collision models allow an intuitive understanding of the origin of the effective Hamiltonian.

# Chapter 5

# Large deviations in open quantum systems

As anticipated in Chapter 3, we show here some original applications of thermodynamics of quantum trajectories to problems of particular interest in the theory of open quantum systems.

In Sec. 5.1 we exploit the predictive power of large deviation theory in order to put forward a method for witnessing non-classicality of the output field from a generic quantum optical setup via the statistics of time-integrated photo currents. Specifically, exploiting the thermodynamics of quantum trajectories, we express a known non-classicality witness for bosonic fields fully in terms of the source master equation, thus bypassing the explicit calculation of the output light state. Further details can be found in [113]. Sec. 5.2 summarizes the main results in [114]. We present a microscopic (collisional) framework for the statistical characterization of quantum trajectories in discrete-time processes. We formulate a protocol to turn a preselected set of rare quantum trajectories into typical upon addition of extra collisions between the system and each probe. This provides a quantitative tool for studying dynamical fluctuations beyond the standard continuous-time regime corresponding to the Lindblad master equation.

## 5.1 Witnessing non-classicality through large deviations in quantum optics

### 5.1.1 Introduction

During the last decades, several platforms have been proposed for implementing efficiently quantum computing tasks [115, 116, 117]: all of them suffer from the effect of decoherence given by the coupling to the environment [5], which ultimately deteriorates the non-classical properties of the considered systems. In fact, for a quantum computational scheme to outperform a classical one, one requires that at least one of its components exhibits genuinely quantum features [118]. When the environment is the electromagnetic vacuum causing photon emission, as in dissipative

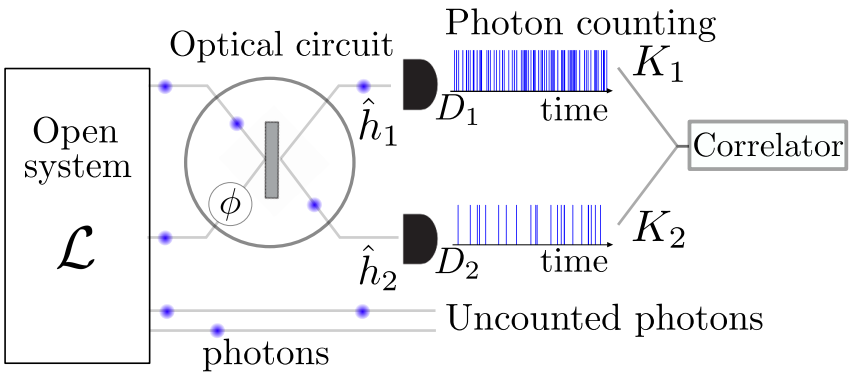


FIGURE 5.1: **Sketch of dissipative quantum optical network.** A generic quantum network is composed of a series of interconnected elements (system) emitting continuously detected radiation in the environment. The emitted fields can be manipulated and transformed via a series of unitary operations in an optical circuit using beam splitters and phase shifters. The photo-detectors ($D_1$ and $D_2$) allow the simultaneous reconstruction of the quantum trajectories for two emission channels. Their correlation properties are studied to uncover quantum non-classicality of the emitted radiation.

optical networks [119], the statistical analysis of the output light contains the information about the dynamical features of the open quantum systems [6]. In particular, the emitted photons can be used as a resource for quantum information processing [120]. Hence, the detection and optimization of non-classical correlations in the photons emitted by a general optical setup is of primary relevance for a variety of technological applications.

Specifically, the type of setups we consider includes an open quantum system, which is the source of photons, and an optical circuit used to manipulate the emission, as shown in Fig. 5.1. To obtain the statistical properties of the photons arriving at the detectors we make use of the *large deviations* approach (see Chapter 3).This allows to access the joint probability distribution of the photon counting at long times, together with relevant statistical quantities such as the fluctuations of the counting fields and corresponding cross-correlation functions. In this way a non-classicality criterion is formulated based on the time-integrated observables of the detection [10, 61, 121, 122].

From the theoretical point of view this establishes a natural link between the statistical-physics approach for analyzing the dynamics of open quantum systems [10], and a general class of non-classicality measures in quantum optics. We provide simple but instructive examples, where non-classical correlations are witnessed in different dynamical regimes of the sources, and for a broad range of parameters. Our theoretical scheme is effective in predicting the outcomes of quantum optics experiments that make use of photon countings to witness non-classicality [123, 124, 72, 125, 126, 127].

### 5.1.2 Open quantum systems and Large Deviation

Our goal is to infer the statistical properties of the output light of an open quantum system emitting into $N_L$ different modes called $\mathcal{B}_\mu$, with $\mu = 1, ..., N_L$. The photon counting statistics at the detectors (see Fig. 5.1) provides information about the state of the open system and about the properties of the optical circuit [6].

The counting statistics is fully characterized by the cumulants of the associated photon counting probability distribution which are encoded in the cumulant generating function (see Chapter 3).

The evolution of the reduced density operator of the open system $\rho$ in the Markovian approximation, is given by the Lindblad ME

$$\dot{\rho} = -i[\hat{H}, \rho] + \sum_{\mu=1}^{N_J} \mathcal{D}(\hat{L}_\mu)\rho \equiv \mathcal{L}[\rho], \tag{5.1}$$

where the jump operator $\hat{L}_\mu$ corresponds to the interaction with the field mode $\mathcal{B}_\mu$. Let us divide our jump operators in $N$ subsets, $\mathcal{J}_i$, each of size $n_i$, with $i = 1, ..., N$, such that $\sum_{i=1}^{N} n_i = N_L$. Suppose we record the occurrence of jump events due to the action of the operators in the first $M$ subsets ($M < N$), and let $K_m$ be the number of detected jumps corresponding to each subset $\mathcal{J}_m$ with $m = 1, 2..., M$. Furthermore we assume that the action of these jump operators induces photoemission. Introducing a short notation, let the vector $\mathbf{K} = (K_1, K_2, ..., K_M)$ be the collection of the photon counts associated with each $\mathcal{J}_m$. The probability to observe $\mathbf{K}$ counts from each decay channel after a time $t$ is $P_t(\mathbf{K}) = \mathrm{Tr}\{\rho^{\mathbf{K}}(t)\}$, where $\rho^{\mathbf{K}}(t)$ is the un-normalized reduced density operator conditioned to $\mathbf{K}$ [60]. The moment generating function associated with $P_t(\mathbf{K})$ reads $Z_t(\mathbf{s}) = \sum_{K=0}^{\infty} P_t(\mathbf{K}) e^{-\mathbf{s}\cdot\mathbf{K}}$ with $\mathbf{s} = (s_1, ..., s_M)$. Here $s_m$ is the conjugated field corresponding to $K_m$. The outcomes of photocount experiments are time-integrated photocurrents given by

$$\langle k_i \rangle = \frac{1}{t} \sum_{j=1}^{n_i} \mathrm{Tr}\left\{ \int_0^t d\tau \hat{L}_j^\dagger \hat{L}_j \rho(\tau) \right\}, \tag{5.2}$$

with $i = 1, 2, ..., M$. For $t$ much greater than the typical timescale of the system $\tau_c$, the probability distribution associated to the photon counting measurements takes a large deviation form. Specifically, at long times the moment generating function can be asymptotically approximated in virtue of large deviation theory as an exponential function of time

$$Z_t(\mathbf{s}) \sim e^{t\theta(\mathbf{s})}. \tag{5.3}$$

The analogue for the count probability reads $P_t(\mathbf{K}) \sim e^{t\varphi(\mathbf{K}/t)}$, where $\varphi(x) = -\min_s\{xs + \theta(s)\}$. The function $\theta(\mathbf{s}) = \frac{1}{t} \ln Z_t(\mathbf{s})$ is the scaled cumulant generating function. It

can be proven [63, 86] that this is given by the maximum real eigenvalue of the deformed superoperator

$$\mathcal{L}_s[\rho] = \mathcal{L}[\rho] - \sum_{i=1}^{M}(1-e^{-s_i})\sum_{\mu_i=0}^{n_i}\hat{L}_{\mu_i}\rho\hat{L}_{\mu_i}^{\dagger}, \tag{5.4}$$

which features the standard Liouvillian $\mathcal{L}$ and the dissipator $\mathcal{D}$, with the jump parts corresponding to each subset $\mathcal{J}_i$, the latter being weighted by the factor $e^{-s_i}$. Note that Eqs. (5.3) and (5.4) are the direct generalization of Eqs. (3.28) and (3.33) for vectors $\mathbf{s}$ and $\mathbf{K}$. The cumulants of the distribution $P_t(\mathbf{K})$ at long times are given by the derivative of $\theta(\mathbf{s})$ at $\mathbf{s} = 0$: cumulants give direct access to the moments of the associated distribution [85].

For the sake of argument, we consider the case $M = 2$ and $n_1 = n_2 = 1$, i.e. , two distinct counting fields each associated with a single jump operator, as shown in Fig. 5.1. Then Eq. (5.4) takes the form

$$\mathcal{L}_{s_1,s_2}[\rho] = \mathcal{L}[\rho] - \sum_{\mu=1}^{2}(1-e^{-s_\mu})\hat{L}_\mu\rho\hat{L}_\mu^{\dagger} \tag{5.5}$$

and the maximum real eigenvalue of $\mathcal{L}_{s_1,s_2}$ is $\theta(s_1,s_2) = \frac{1}{t}\ln Z_t(s_1,s_2)$, with $Z_t(s_1,s_2)$ the moment generating function of the probability distribution $P_t(K_1,K_2)$ associated with the photocount measurement described by the jump operators $\hat{L}_\mu$ in the long-time limit. In particular, we recover the moments of the marginal distributions $P(K_1)$ and $P(K_2)$ by setting $s_1 = 0$ or $s_2 = 0$. By exploiting the double weighting it is possible to access the correlations between the counting fields at the detectors. In particular the covariance reads

$$\mathrm{cov}(k_1,k_2) = \langle k_1k_2\rangle - \langle k_1\rangle\langle k_2\rangle = \partial_{s_1}\partial_{s_2}\theta(s_1,s_2)|_{s_1=s_2=0}. \tag{5.6}$$

All the other moments can be easily recovered in terms of higher order derivatives of $\theta(s_1,s_2)$. The possibility of accessing the full statistics of the joint probability distribution, as we shall see in the following, allows to make use of non-classicality measures on the bath operators, with the idea of finding possible signatures of quantum correlations between the detection events (in the long-time limit).

### 5.1.3 Vogel's non-classicality criterion (VC)

This criterion [70, 71] gives a necessary and sufficient condition to establish whether correlations in a stationary radiation field are nonclassical or not. It consists of a rephrasing of the well-known non-classicality criterion based on the negativity of the Glauber-Sudarshan distribution (or *$\mathcal{P}$-distribution*) [128, 129] in terms of photon counting detection. Referring to the setup in Fig. 5.1, let us consider the generic bosonic operators $\hat{h}_i$, $(i = 1,2)$, of the two output fields, and assume they are normally-ordered functions of the associated destruction and creation operators $\hat{a}_i$

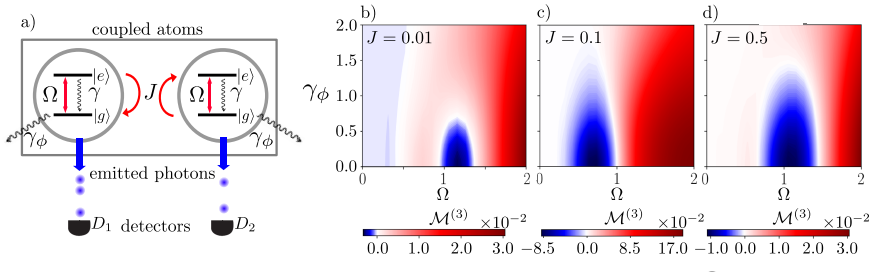


FIGURE 5.2: **Non-classicality witness for emission from coupled atoms**. (a): Third-order Vogel's determinant for a system of two coherently-driven interacting atoms (coupling strength $J$) subject to dephasing, as a function of the dephasing rate $\gamma_\phi$ and Rabi frequency $\Omega$. Plots (b)-(d) are for different coupling strengths: $J = 0.01$ (b), $J = 0.1$ (c), $J = 0.5$ (d). In all cases we observe a sharp separation between classical (positive Vogel's determinant) and quantum states of the emitted radiation (negative regions).

and $\hat{a}_i^\dagger$ of the each mode. A generic operator acting on the two-mode field is defined as $\hat{f} = \sum_{n,m=0}^{\infty} f_{nm} \hat{h}_1^{\dagger n} \hat{h}_2^m$, which is a normally-ordered power series of $\hat{h}_i$ and $\hat{h}_i^\dagger$. The expectation value of $\langle : \hat{f}^\dagger \hat{f} : \rangle$ reads

$$\langle : \hat{f}^\dagger \hat{f} : \rangle = \sum_{n,m,k,l=0}^{\infty} f_{nm} f_{kl}^* \langle \hat{h}_1^{\dagger n+k} \hat{h}_2^{m+l} \rangle = \int_{\mathbb{C}} \mathcal{P}(\alpha_1, \alpha_2) |f(\alpha_1, \alpha_2)|^2 d^2\alpha_1 d^2\alpha_2, \tag{5.7}$$

where the last identity follows from the optical equivalence theorem [130] while

$$f(\alpha_1, \alpha_2) = \sum_{n,m=0}^{\infty} f_{nm} \hat{h}_1^{\dagger n}(\alpha_1, \alpha_1^*) \hat{h}_2^m(\alpha_2, \alpha_2^*) \tag{5.8}$$

and where $\mathcal{P}(\alpha_1, \alpha_2)$ is the Glauber-Sudarshan distribution. Since $\langle : \hat{f}^\dagger \hat{f} : \rangle < 0$ entails $\mathcal{P}(\alpha_1, \alpha_2) < 0$ for some points $(\alpha_1, \alpha_2)$ of the phase space, the negativity of Eq. (5.7) implies non-classicality in radiation fields. Note that Eq. (5.7) is a quadratic form and is non-negative iff all the principal minors of matrix $\mathcal{M}_{nm,kl} = \langle \hat{h}_1^{n+k} \hat{h}_2^{m+l} \rangle$ are positive according to the Sylvester criterion [131]. Referring to the setup in Fig. 5.1 and according to [131, 70], we express the VC in terms of click-counting operators, which, from the open quantum system point of view, take the form $\hat{h}_j = \hat{L}_j^\dagger \hat{L}_j$. Thus the elements of $\mathcal{M}_{nm,kl}$ are the moments of the photon counting stationary distribution $P(K_1, K_2)$, which gives the probability to record $K_1$ clicks at photodetector $D_1$ and $K_2$ at $D_2$. Hence, the criterion is now formulated in terms of time-integrated functions, like the photocurrents defined in Eq. (5.2). The moments in $\mathcal{M}_{nm,kl}$ are easily calculated through iterative derivation of the two-mode moment generating function associated to $P(K_1, K_2)$. Note that the mixed derivatives of the double-biased scaled cumulant generating function $\theta(s_1, s_2)$ give us the mixed scaled cumulants directly linked to the two-mode moments in $\mathcal{M}_{nm,kl}$.

Different setups have been proposed, realized and successfully used [125, 126, 127] in order to measure the click-counting distribution thus uncovering quantum

correlations of radiation fields. The click-counting distribution can approximate $P(K_1, K_2)$ involving photon counting via a long-time measurement through photon-number-resolving detectors. As shown in [131] once the estimated stationary probabilities are known it is clearly possible to recover the moments in $\mathcal{M}_{nm,kl}$. Usually, the higher the order of the calculated moment, the less accurate our estimate will be. In the cases we study next, low-order moments are enough to determine non-classical features of radiation. It was shown [131] that the binomial form for the click-counting probability distribution holds for any positive-operator valued measurement (POVM) either linear or non-linear in the number of emitted photons. Thus the large deviation formalism allows us to inherently access all the cumulants associated to any photon counting process defined by the unraveling of the master equation.

### 5.1.4 Non-classicality in dissipative circuits.

Typical coherent and squeezed radiation sources (pumped cavities, nonlinear active media) can be studied from the point of view of open quantum system theory [6]. Referring to the generic setup in Fig. 5.1, we now consider two different source structures: a pair of coupled two-level atoms, each coherently driven and subject to decay in its own emission channel and two non-interacting atoms whose outputs are correlated via a beam splitter and a phase shifter. In both cases we introduce dephasing on each atom with rate $\gamma_\phi$: such dephasing channel spoils coherence, hence it is expected to affect non-classicality of emitted light.

#### Two coupled atoms

The total Hamiltonian of the system reads

$$\hat{H} = \sum_{i=1}^{2} [\tfrac{\Omega}{2}(\hat{\sigma}_i^+ + \hat{\sigma}_i^-) + \sqrt{\gamma}\left(\hat{\sigma}_i^+ \hat{a}_i + H.c.\right)] + J\left(\hat{\sigma}_1^+ \hat{\sigma}_2^- + H.c.\right), \tag{5.9}$$

where $\gamma$ is the decay rate of the each atom, $\Omega$ the Rabi frequency, $\hat{\sigma}_i^+$ and $\hat{\sigma}_i^-$ are the ladder operators, $\hat{a}_i$ is the annihilation operator of the bosonic mode coupled to the $i$th atom[1] and $J$ is the coupling strength. The jump operators of this elementary network are thus $\hat{J}_1 = \sqrt{\gamma}\hat{\sigma}_1^-$ and $\hat{J}_2 = \sqrt{\gamma}\hat{\sigma}_2^-$. We can straightforwardly compute the large deviation moments matrix and the corresponding Vogel determinants for the joint photon counting probability distribution. It is worth noting that the second-order principal minor ($\mathcal{M}^{(2)}$) does not contain information on the cross-correlations between the emitted field, which is our focus. Thus, it is necessary to consider the

[1] $\hat{a}_i$ operators are intended as time-mode bosonic operator, or input modes i.e. Fourier transform of field normal mode operators $\hat{a}_\omega$ under the assumption of white coupling between system and environment [92].

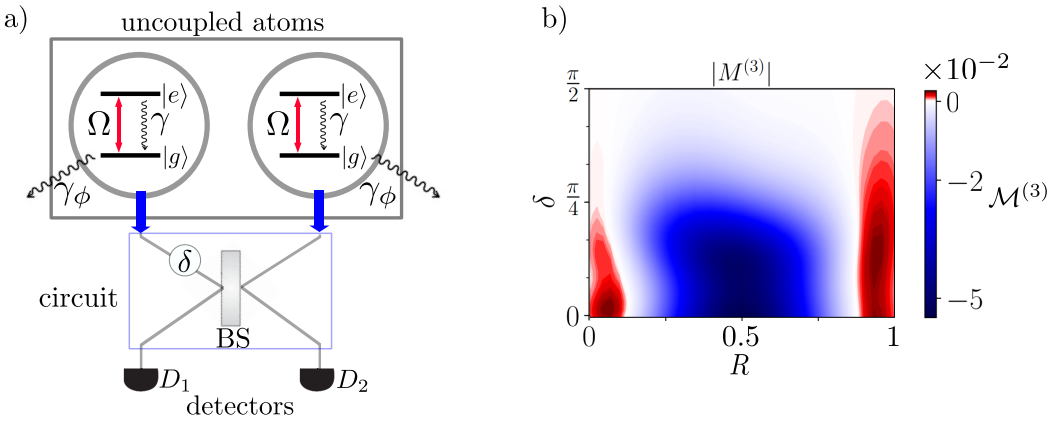


FIGURE 5.3: **Non-classicality witness for emission from optical circuit**. The system (a) is composed of a two coherently-driven non-interacting atoms subject to dephasing $\gamma_\phi$, emitting into the input channel of a generic unitary circuit composed of a phase shifter and a beam splitter. (b) We show the value of the third-order Vogel determinant as a function of reflectivity $R = \sin^2\zeta$ and phase shift $\delta$.

next order minor. A numerical investigation of the third-order principal minor reveals the presence of quantum correlations between detection events in the emission channels. Fig. 5.2 shows $\mathcal{M}^{(3)}$ as a function of the Rabi frequency $\Omega$ and dephasing rate $\gamma_\phi$ for three values of the coupling rate $J$. In each case, non-classicality is reduced as the dephasing rate grows. Negativity grows with $\Omega$, reaching a maximum and then saturating to a positive value. Dephasing destroys quantum coherences making the atoms behave like classical objects, and this results in classical radiation fields, as expected. Higher values of $\Omega$ speed up Rabi oscillations: the effective coarse-graining time-integration is lower bounded by $1/\gamma$. Hence, we expect the time integrated photo-current becomes insensitive to the intensity fluctuations, resulting in a crossover between negative and non-negative values of the determinant. Furthermore we notice that the absolute minimum of the third-order determinant does not grow linearly with the coupling strength, but rather decreases when increasing $J$. It is indeed expected that the strong coupling between the two atoms makes the emission less likely to happen [132]. The strong coupling contribution results in an effective shift of the energy level of the system so that the perfect resonance condition is lost: the dominant component of the output fields becomes vacuum, thus reducing the amount of cross correlations.

**Non-interacting atoms and unitary circuit.**

We consider next the case in which correlations can arise by *processing* the emitted fields of two non-interacting atoms ($J = 0$) through a unitary transformation employing a beam splitter ($\hat{\mathcal{U}}_{BS} = \cos\zeta\ \mathbb{1} + i\sin\zeta\ \hat{\sigma}_x$, with $\sigma_x = \hat{\sigma}^+ + \hat{\sigma}^-$) and a phase shifter (Fig. 5.3). The transformed jump operators read $\hat{J}_1 = \sqrt{\gamma_1}\cos\zeta\ \hat{\sigma}_1^- + i\sqrt{\gamma_2}\sin\zeta\ \hat{\sigma}_2^-$ and $\hat{J}_2 = i\sqrt{\gamma_1}\sin\zeta\ \hat{\sigma}_1^- + \sqrt{\gamma_2}\cos\zeta\ \hat{\sigma}_2^-$. We set $\Omega = 0.5\gamma$ and $\gamma_\phi = 0.1$

and study non-classicality as a function of the reflectivity $R = \sin^2\zeta$ and phase difference $\delta$ between the two channels due to the phase shifter. For total transmission ($\zeta = 0$) and total reflection ($\zeta = \pi/2$), we notice that the determinant is positive. The maximum negativity is reached for a $50/50$ beam splitter and decreases as the phase shift $\delta$ grows. Thus, by adjusting appropriately the parameters of the optical circuit, such as the relative phase shift $\delta$, it is possible to enhance or destroy quantum interference effects of the output state.

## 5.2 Microscopic biasing of discrete-time quantum trajectories

Recalling Sec. 3.4, we address here the problem of tailoring trajectories statistics from a much wider viewpoint in two main respects. On the one hand, we go beyond the master equation approach addressing the question: how should we modify the way system and environment interact at a *microscopic* level in order to turn rare trajectories into typical as desired? On the other hand we go beyond continuous-time processes and address *discrete*-time quantum dynamics corresponding to a sequence of stochastic quantum maps on the open system. To achieve the above, we use a collision model, as described in Sec. 2.2.1: the system of interest unitarily interacts, in a sequential way, with a large collection of ancillary probes, each of which undergoes a projective measurement, whose result is recorded.

Exploiting thermodynamic functionals, we characterize the ensemble of trajectories in collision models and show how the system-probe interaction can be modified so as to bias the statistics of measurement outcomes on the probes. Notably, this unveils the physical mechanism turning rare trajectories into typical. As will be shown, for short collision times, the modified dynamics is obtained by adding extra collisions which enforce the system dynamics far from the average (i.e. unconditional) one so as to sustain a trajectory with desired output.

### 5.2.1 Definition of the collision model

The environmental probes [see Fig. (5.4)] are labeled by $n = 1, 2, ..., N$ and assumed to be non-interacting, each modeled as a qubit with basis states $\{|0\rangle, |1\rangle\}$. Each system-probe collision is described by the pairwise unitary

$$U(H_S, V) = \exp[-i(H_S \otimes \mathbb{1} + V)\Delta t)], \tag{5.10}$$

with $H_S$ the free Hamiltonian of system $S$ (generally including a drive) and $V$ the $S$-probe interaction Hamiltonian. Note that $U$ can be seen as a gate acting on system and probe [37, 7] according to an associated quantum-circuit representation (see Fig. 5.5). Initially, $S$ and the probes are in the uncorrelated state $\varrho_0 = \rho_0 \bigotimes_n \eta_n$ with

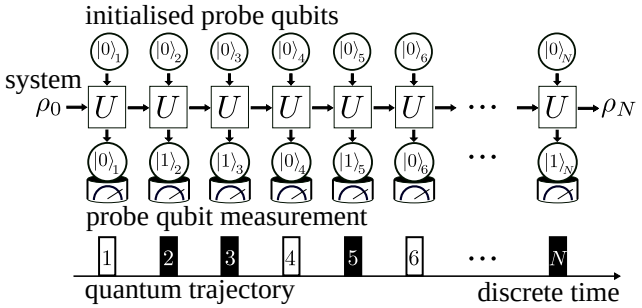


FIGURE 5.4: **Quantum collision model.** The environment consists of a large collection of quantum probes, each modeled as a qubit with computational basis $\{|0\rangle, |1\rangle\}$. This environment is initialized in the state $\otimes_n |0_n\rangle$. The system, whose initial state is described by the density matrix $\rho_0$, collides with the probes one at a time, the $n$th collision being described by a pairwise unitary $U$ on the system and probe $n$. As the collision is complete (and before the system collides with the probe $n+1$), probe $n$ is measured in the basis $\{|k\rangle\}$ with $k = 0, 1$. When the outcome $|1\rangle$ is detected, a quantum jump occurs (black square). The sequence of measurement outcomes uniquely defines a quantum trajectory. Summing over all possible realizations of the measurement provides, instead, the dynamics of the average system state $\rho_n$.

$\rho_0$ ($\eta_n$) the initial state of $S$ (probe $n$). We will set $\eta_n = |0\rangle_n\langle 0|$ (the generalization to mixed states is straightforward).

Right after colliding with $S$ according to unitary $U(H_S, V)$, each probe is measured onto the orthonormal basis $\{|k_n\rangle\}$ with $k = 0, 1$ [see Fig. 5.5(a)]. In an atom-field setup (in which case probes are field time bins, see Chapter 4), outcome $|0\rangle$ means no emission while $|1\rangle$ signals one photon emitted by $S$ and detected. The state of $S$ after $n$ steps, $\rho_n$, is the average over all possible discrete trajectories (unconditional dynamics). Between two next steps, it evolves as $\rho_{n+1} = \mathcal{E}[\rho_n]$, where the map

$$\mathcal{E}[\rho] := \sum_{k=0}^{1} K_k \rho K_k^\dagger \quad \text{with} \quad K_k = \langle k|U(H_S, V)|0\rangle \tag{5.11}$$

is completely positive and trace preserving (CPT) and $K_k$ are the Kraus operators acting on $S$. In particular, trace preservation (equivalent to probability conservation) holds due to $\sum_{k=0,1} K_k^\dagger K_k = \mathbb{1}$.

We take the system-probe coupling in the linear form

$$V = \tfrac{1}{\sqrt{\Delta t}}(J \otimes \sigma_+ + J^\dagger \otimes \sigma_-)\,, \tag{5.12}$$

where $J$ is an operator on $S$ having dimensions of the square root of a frequency, and $\sigma_- = \sigma_+^\dagger = |0\rangle\langle 1|$. In spite of its simplicity, this model of interaction describes a wide variety of representative physical situations [17, 133]. Also, note that (5.11) is independent of the probe label since so are $U$ and $\eta_n$.

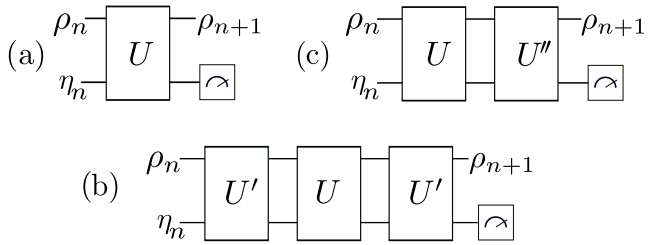


FIGURE 5.5: **Quantum circuits.** (a): Quantum-circuit representation of a system-probe collision followed by a probe measurement. The system, whose state at the discrete time $n$ is given by $\rho_n$, collides with the $n$th probe, initialized in the state $\eta_n$. The collision is unitary and implemented by the operator $U = U(H_S, V)$, which can be represented as a quantum gate. After the collision, measuring the probe returns the updated state of the system $\rho_{n+1}$ (by averaging over all measurement outcomes). (b): Modified collision turning rare trajectories into typical: a pair of extra gates $U' = U(H'_S, V')$ are added to $U$ (before measurement). (c): Same modified collision as in (b) implemented through only one additional collision with unitary $U'' = U(H''_S, V'')$.

### 5.2.2 Biased collisional trajectories

In contrast to the average (deterministic) dynamics generated by (5.11), each specific quantum trajectory is conditioned to the measurement outcomes on the probes and is thus stochastic. At each step, the state of $S$ evolves as [59]

$$|\psi_{n+1}\rangle = K_k |\psi_n\rangle \,/\, \|K_k |\psi_n\rangle\| \tag{5.13}$$

with $p_k = \|K_k |\psi_n\rangle\|^2$ the probability to measure the $n$th probe in state $|k\rangle$ (we have assumed an initial pure state for the system, $\rho_0 = |\psi_0\rangle\langle\psi_0|$, for the sake of argument).

Each $K_k$ is in one-to-one correspondence with a particular measurement outcome. We focus on $K_1$. To study the fluctuations of the probe measurements we need to derive the full counting statistics of the action of $K_1$ in a single trajectory [10, 134]. Let then $P_N(M)$ be the probability of observing $M$ times the action of the $K_1$ in a realization of the collision dynamics up to the discrete time $N$. For large $N$, this is expected to have the form (cf. Eq. (3.29))

$$P_N(M) \sim e^{-N\varphi(m)}\,, \tag{5.14}$$

with $m = M/N$ being the frequency with which the probe has been measured in state $|k = 1\rangle$. The related asymptotic moment generating function of the observable reads

$$Z_N(s) := \sum_{M=0}^{\infty} P_N(M) e^{-sM} \xrightarrow[N\gg 1]{} e^{N\theta(s)}\,, \tag{5.15}$$

where the real variable $s$ is called "counting field", and $\theta(s)$ is the scaled cumulant

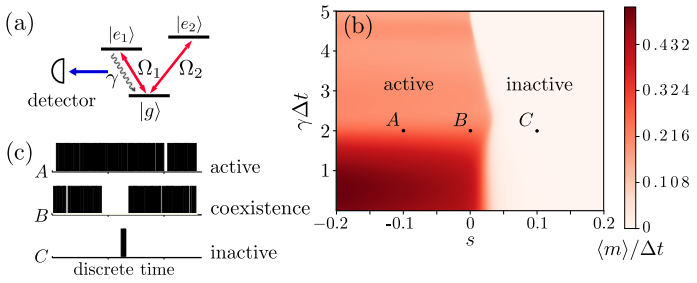


FIGURE 5.6: **Discrete-time quantum trajectories of a three-level system.** (a): Level configuration: each transition $|g\rangle \leftrightarrow |e_k\rangle$ is driven with Rabi frequency $\Omega_k$ with $k = 1, 2$. During each unitary collision, a coherent exchange of excitations occurs between the probe and the system $S$. In particular, only transition $|g\rangle \leftrightarrow |e_1\rangle$ couples to the probe. Thus, measuring the probe in state $|1_n\rangle$ signals that the environment gained an excitation at the expense of the energy of the system $S$ which decays to the ground state $|g\rangle$ (emulating photon emission). (b): Normalized activity (average emission rate divided by $\Delta t$) as a function of $s$ and $\Delta t$. The domain close to the boundary line separating active and inactive phases is a coexistence region. The variation of contrast for growing $\Delta t$ witnesses changes in sharpness of the active-inactive region crossover. (c): Sampled representative trajectories for a collision time $\gamma\Delta t \simeq 2$, with each tick recording a probe measurement in $|1\rangle$. Trajectories in the active phase (see A) show a dense emission of excitations from $S$ into the environment. In the inactive regime (C), instead, probes are rarely detected in $|1\rangle$. Close to the boundary line between these two phases (see B), time intervals in which $S$ emits frequently are intermittent with intervals during which probes are almost never measured in $|1\rangle$.

generating function defined in Eq. (3.28). In line with Section 3.3, the cumulant generating function can be calculated as the logarithm of the largest real eigenvalue of a *tilted* Kraus map [cf. Eq. (5.11)]

$$\mathcal{E}_s[X] = K_0 X K_0 + e^{-s} K_1 X K_1 \,. \tag{5.16}$$

Here, $\mathcal{E}_s$ is the dynamical map corresponding to the the tilted Liouvillian superoperator in Eq. (3.33). As shown before, the probability distribution $P_N(M)$ is determined by the behavior of $\theta(s)$ through derivatives with respect to $s$, taken at the "physical point" $s = 0$, but a set of biased probabilities can be defined as in Eq. (3.37) (we report the expression again for convenience)

$$P_N^s(M) = \frac{e^{-s\,M} P_N(M)}{Z_N(s)} \,. \tag{5.17}$$

So far we have constructed the probabilities Eq. (5.17) by hand and noted that these describe rare dynamical events. Here, we show how it is possible to modify the system-probe collision in a way that $P_N^s(M)$ become *physical* probabilities. In other words we will show how, by tailoring the interaction between system and probes, the rare behavior of the original process can become the typical one of the new dynamics. As mentioned earlier $P_N^s(M)$ is generated by the tilted map $\mathcal{E}_s$ which

is *not* CPT (i.e., it does not represent a legitimate physical process) since probability is not preserved. The task is thus to turn $\mathcal{E}_s$ into a well-defined CPT map. This is achieved by introducing a *Doob* dynamics [135, 10, 73] for *discrete-time* quantum processes, embodied by the auxiliary CPT map

$$\tilde{\mathcal{E}}[X] = \tilde{K}_0 X \tilde{K}_0^\dagger + \tilde{K}_1 X \tilde{K}_1^\dagger \,. \tag{5.18}$$

with

$$\tilde{K}_0 = \frac{1}{\Lambda_s^{1/2}} \ell^{1/2} K_0 \ell^{-1/2} \quad , \quad \tilde{K}_1 = \frac{e^{-s/2}}{\Lambda_s^{1/2}} \ell^{1/2} K_1 \ell^{-1/2} \,. \tag{5.19}$$

where $\ell$ is the left eigen-operator of the tilted map $\mathcal{E}_s$ associated with largest real eigenvalue $\Lambda_s = e^{\theta(s)}$, i.e. $\ell$ is the operator such that

$$\mathcal{E}_s^*[\ell] = \Lambda_s \, \ell \,, \tag{5.20}$$

in analogy with Eq. (3.41) (here we omit the subscript $s$ in $\ell$ operators). The map $\tilde{\mathcal{E}}$ is completely positive and trace preserving since

$$\tilde{\mathcal{E}}^*[\mathbb{1}] = \sum_{k=0,1} \tilde{K}_k^\dagger \tilde{K}_k = \frac{1}{\Lambda_s} \ell^{-1/2} \, \mathcal{E}_s^*[\ell] \ell^{-1/2} = \frac{1}{\Lambda_s} \ell^{-1/2} \, (\Lambda_s \ell) \, \ell^{-1/2} = \mathbb{1} \,. \tag{5.21}$$

Hence the map in Eq. (5.19) is a proper discrete quantum dynamics and, by construction, it reproduces as typical the rare event of the original processes $P_N^s(M)$.

### 5.2.3 Continuous time limit

In the limit of short collision-times $\Delta t \ll 1$, the tilted Kraus map is approximately given by

$$\mathcal{E}_s[\rho] \approx e^{\Delta t \, \mathcal{L}_s}[\rho] \,, \tag{5.22}$$

where $\mathcal{L}_s$ is the tilted Lindblad superoperator (cf. Eq. (3.33))

$$\mathcal{L}_s[\rho] = -i[H_S, \rho] + e^{-s} J \rho J^\dagger - \frac{1}{2} \left\{ \rho, J^\dagger J \right\} \,, \tag{5.23}$$

where $J$ is the same operator appearing in (5.12). As such, the left eigen-operator of $\mathcal{L}_s$ is approximately also the eigen-operator of $\mathcal{E}_s$, $\ell$, at first-order in $\Delta t$. This also implies that the largest real eigenvalue of the tilted map can be written as

$$\Lambda_s \approx e^{\Delta t \, \chi(s)} \,, \tag{5.24}$$

where $\chi(s) = \theta(s)/\Delta t$ here represents the largest real eigenvalue of the tilted Lindbladian map $\mathcal{L}_s$.

Thus the second term on the right hand side of Eq. (5.19) reads

$$\tilde{K}_1 \rho \tilde{K}_1^\dagger \approx \frac{e^{-s}}{e^{\Delta t\, \chi(s)}} \Delta t\, \ell^{1/2} J \ell^{-1/2}\, \rho\, \ell^{-1/2} \tilde{J}^\dagger \ell^{1/2} \approx \Delta t\, \tilde{J} \rho \tilde{J}^\dagger\,; \tag{5.25}$$

with $\tilde{J} = e^{-s/2} \ell^{1/2} J \ell^{-1/2}$ and the last term $e^{\Delta t\, \chi(s)}$ only contributes at the zero-th order in $\Delta t$. Considering the first term on the right hand side of Eq. (5.19), up to first order in $\Delta t$, we obtain

$$\tilde{K}_0 \rho \tilde{K}_0^\dagger \approx 1 + \left[ -i \ell^{1/2} H_{\text{eff}} \ell^{-1/2} \rho + i \rho \ell^{-1/2} H_{\text{eff}}^\dagger \ell^{1/2} - \chi(s) \rho \right] \Delta t\,, \tag{5.26}$$

and this, through a procedure similar to that in Ref. [73], gives

$$\tilde{K}_0 \rho \tilde{K}_0^\dagger \approx 1 - i \left( \tilde{H}_S - \frac{i}{2} \tilde{J}^\dagger \tilde{J} \right) \rho \Delta t + i \rho \left( \tilde{H}_S + \frac{i}{2} \tilde{J}^\dagger \tilde{J} \right) \Delta t\,, \tag{5.27}$$

where $\tilde{H}_S, \tilde{J}$ coincide with the Hamiltonian and the jump operator of the continuous time Doob dynamics. In light of this result, we can write the unitary interaction between system and probe as a new collision model as

$$U(\tilde{H}_S, \tilde{V}) = \exp[-i(\tilde{H}_S \otimes \mathbb{1} + \tilde{V}) \Delta t)]\,, \tag{5.28}$$

with

$$\tilde{V} = \frac{1}{\sqrt{\Delta t}} (\tilde{J} \otimes \sigma_+ + \tilde{J}^\dagger \otimes \sigma_-)\,. \tag{5.29}$$

The replacement $\mathcal{E} \to \tilde{\mathcal{E}}$ [cf. Eq. (5.11)] corresponds to a change of the system-probe collision as

$$U(H_S, V) \to U(\tilde{H}_S, \tilde{V})\,. \tag{5.30}$$

where the new Hamiltonian $\tilde{H}_S$ and jump operator $\tilde{J}$ match those obtained via the Doob transform for continuous-time Lindblad processes (see Eq. (3.40)). Thus the corresponding new Kraus operators read

$$\tilde{K}_k = \langle k | U(\tilde{H}_S, \tilde{V}) | 0 \rangle\,. \tag{5.31}$$

Note that the new system-probe collision unitary (5.30) can be expressed as

$$U(\tilde{H}_S, \tilde{V}) = U(H_S'', V'')\, U(H_S, V) \tag{5.32}$$

with

$$H_S'' = 2H_S'\,, \quad V'' = 2V' + i \tfrac{\Delta t}{2} [\tilde{V}, V]\,. \tag{5.33}$$

This decomposition makes apparent the mechanism by which rare events can be sustained so as to make them typical: an *extra* collision, added to the original one $U(H_S, V)$, drives the system away from typicality, pinning its dynamical behavior to the fluctuations of interest. Note that the second term in $V''$ (cf. Eq. (5.33)) is of

order $\mathcal{O}(1)$ in $\Delta t$, and represents an extra system-probe coupling. It is worth noting that the addition of extra collision is reminiscent of a giant-atom dynamics which can indeed be described as cascaded collisions [8, 111, 136] yet involving the same system $S$ [88] as we showed in detail in Sec. 4.9.

### 5.2.4 Driven three-level system

As an example, let $S$ be a coherently driven three-level system [see Fig. 5.6 (a)]. Each transition $|g\rangle \leftrightarrow |e_k\rangle$, with $k = 1, 2$, is driven with a Rabi frequency $\Omega_k$ according to the Hamiltonian

$$H_S = \sum_k \Omega_k (\hat{\sigma}_+^{(k)} + \hat{\sigma}_-^{(k)}) \,, \tag{5.34}$$

where $\hat{\sigma}_-^{(k)} = |g\rangle_S\langle e_k| = \hat{\sigma}_+^{(k)\,\dagger}$. Additionally, we set $J = \sqrt{\gamma}\,\hat{\sigma}_-^{(1)}$ [cf. Eq. (5.12)], meaning that only state $|e_1\rangle$ can decay with rate $\gamma$ by emitting an excitation into the environment (corresponding to outcome $|1_n\rangle$). For short collision times, intermittent emission is known to occur [79, 137], which can be explained as the coexistence of two deeply different phases of emission much like a first-order phase transition [86]. Notably, the developed framework allows to investigate such transition-like behaviour away from the Lindblad dynamical regime, i.e., for *finite* collision times $\Delta t$. To this end, we plot in Fig. 5.6(b) the time-averaged rate of probe measurements in state $|1\rangle$, $\langle m\rangle/\Delta t = -\partial_s(\theta(s, \Delta t))/\Delta t$, as a function of $s$ and $\Delta t$ for $\Omega_1/\gamma = 1$ and $\Omega_1/\Omega_2 = 1/10$. This dynamical order parameter allows us to distinguish active (bright) and inactive (dark) trajectory regimes [some representative samples of quantum trajectories are shown in Fig. 5.6(c)]. The clearly visible boundary line in Fig. 5.6(b) represents a sharp crossover between the two dynamical regimes. Along this boundary, trajectories feature intermittent emission of excitations from the system. As $\Delta t$ grows up, the crossover occurs at a different value of $s$ and its sharpness changes. Thus, away from the short-$\Delta t$ (Lindblad) regime, both typical and atypical emission rates are modified.

## 5.3 Summary

In Sec. 5.1, we have shown how to detect signatures of non-classicality through the statistics of time-integrated quantities such as the photon counts. This allows to benchmark approaches for producing quantum resources for information and computation via general optical circuits and open quantum systems. Our findings can be extended both to imperfect detection and to recently proposed high-performing photon-number-resolving detection schemes [138].

In Sec. 5.2 we presented a microscopic framework for the statistical characterization of quantum trajectories in discrete-time processes. We provided a quantitative tool for studying dynamical fluctuations beyond the standard continuous-time regime corresponding to the Lindblad master equation. A recipe was given allowing to turn a preselected set of rare quantum trajectories into typical upon addition

of extra collisions between the system and each probe. The method we introduced shows how to engineer open quantum dynamics in order to produce desired emission patterns without the need for changing the detection/ post-selection scheme [82].

# Conclusion

In the Introduction we raised many questions about unconditioned and conditioned dynamics of open quantum optical systems. Here, we will address them in light of what we have shown so far.

The basic theory of open quantum systems has been formulated in a very simple and intuitive way in Chapter 1. We preferred to show this fundamental topic in terms of a "physics-oriented" description by neglecting deliberately, as much as possible, any explicit reference to the formalism of stochastic processes so as to achieve a self-consistent and friendly viewpoint. In the same spirit we formulated the abstract collision model of Chapter 2.

The above theory largely underpins our study of one-dimensional quantum optical systems in Chapter 4. We applied the collisional picture to derive a general Lindblad master equation of a set of giant emitters coupled to a generally chiral waveguide for an arbitrary white-noise Gaussian state of the field (environment). We obtained a general master equation describing a wide variety of systems of interest in quantum optics and waveguide QED.

Although collision models are, of course, just one of the many possible tools one can use, the collision unitary concept makes this picture particularly advantageous to carry out tasks such as deriving in a natural way CPT master equations, jump operators or effective decoherence-free Hamiltonians, even in presence of generally complex systems with many emitters. In particular we have seen that it becomes crucial for the description and the understanding, so far incomplete, of the microscopic mechanisms underlying the emergence of decoherence-free subspaces in one-dimensional quantum optical systems.

By modelling the interaction between field and coupling points of giant atoms placed along the waveguide as a cascaded collision model, we have shown how the topology of coupling points configurations affects the order in which the system undergoes generally non-commuting collisions and how, under particular conditions, this leads very intuitively to the occurrence of trivial/non-trivial decoherence-free Hamiltonians. Providing evidence to the reader that collision models have a predictive power beyond derivation of master equations, is the another main result of this thesis.

Finally if, having reached the conclusion, the reader is of the opinion that the subject of large deviation theory (Sec. 2.2) is a mostly obvious generalization of the well-known Central Limit theorem, we have achieved our last goal.

Large deviation theory is the the proper framework in which problems of statistical mechanics and classical thermodynamics can be formulated rigorously [63], and very recently it has been successfully employed for studying quantum jump trajectories [86, 10, 61, 122].

Even though these studies received wide attention from the statistical mechanics community, this was not the case for the quantum optics community. The main problem is the asymptotic meaning of the large deviation estimates since many experiments in quantum optics are mostly focused on short-time scale phenomena.

Our idea of exploiting large deviations to set up a protocol for witnessing nonclassicality takes advantages of this asymptotic nature: the Vogel criterion needs very high emission statistics also in its original formulation. Remarkably, by exploiting large deviation formalism it is possible to directly link the signatures of nonclassicality to the physical parameters governing the open dynamics, accessing the information about many body interactions or other physical processes taking place inside the source and generating radiation exhibiting manifestly non-classical features.

In the last part of Chapter 3 we have shown how the knowledge of asymptotic emission full-counting statistics provides a recipe for biasing quantum trajectories. This is a rather new subject and, despite the complexity of the formalism as summarized in Sec. 3.4, is receiving growing interest in its growing [139]. Nevertheless there are lots of open questions that concern the practical implementation as well as the physical interpretation. We made significant steps forward in both respects. By linking quantum Doob transform to collision models we provided a solution to the interpretational issues and a very simple description of the biasing process. We showed that it can be seen as a simple modular change of the collision model describing the original dynamics. Furthermore we extended the existing formalism to generic discrete quantum maps, which in principle applies even beyond the weak coupling regime.

The formalism here developed can be implemented to tackle a wide variety of problems ranging from pure quantum optics to many-body quantum physics.

While in the presented collision models we did not consider lossy photonic environments [140, 141, 91], the framework could be naturally extended to accommodate these. Likewise, a generalization to giant atoms in gapped structured reservoirs [142] appears viable. Moreover, the joint decoherence-free emitters-field dynamics is in fact mapped into an effective quantum circuit, which can help quantum simulations and allows to potentially take advantage of already developed quantum information/computing techniques. The circuital description of collision models and our biasing protocol could find interesting experimental applications in quantum simulators for instance based on trapped ions [143] or Rydberg atoms [144, 145].

# Bibliography


[1] Vittorio Gorini, Andrzej Kossakowski, and Ennackal Chandy George Sudarshan. "Completely positive dynamical semigroups of N-level systems". In: *Journal of Mathematical Physics* 17.5 (1976), pp. 821–825.

[2] Goran Lindblad. "On the generators of quantum dynamical semigroups". In: *Communications in Mathematical Physics* 48.2 (1976), pp. 119–130.

[3] Heinz-Peter Breuer and Francesco Petruccione. *The Theory of Open Quantum Systems*. Oxford University Press, 2007. ISBN: 978-0-19-170634-9.

[4] Serge Haroche and Jean Michel Raimond. *Exploring the Quantum: Atoms, Cavities, and Photons*. Oxford: Oxford Univ. Press, 2006. DOI: 10.1093/acprof:oso/9780198509141.001.0001. URL: https://cds.cern.ch/record/993568.

[5] John Preskill. "Lecture notes for physics 229: Quantum information and computation". In: *California Institute of Technology* 16 (1998).

[6] Howard Carmichael. *An open systems approach to quantum optics: lectures presented at the Université Libre de Bruxelles, October 28 to November 4, 1991*. Vol. 18. Springer Science & Business Media, 2009.

[7] Francesco Ciccarello. "Collision models in quantum optics". In: *Quantum Measurements and Quantum Metrology* 4.1 (2018). ISSN: 2299-114X. DOI: 10.1515/qmetro-2017-0007.

[8] V. Giovannetti and G. M. Palma. "Master equations for correlated quantum channels". In: *Physical Review Letters* 108.4 (2012), p. 40401. ISSN: 00319007. DOI: 10.1103/PhysRevLett.108.040401. eprint: 1105.4506. URL: https://link.aps.org/doi/10.1103/PhysRevLett.108.040401.

[9] Ludwig Boltzmann. "Über die beziehung dem zweiten Hauptsatz der mechanischen Wärmetheorie und der Wahrscheinlichkeitsrechnung respektive den Sätzen über das Wärmegleichgewicht". In: *Wiener Berichte, 76, 373-435, in WA II, Paper 42.* (1877).

[10] Juan P Garrahan and Igor Lesanovsky. "Thermodynamics of quantum jump trajectories". In: *Phys. Rev. Lett.* 104.16 (2010), p. 160601.

[11] Hannes Pichler and Peter Zoller. "Photonic Circuits with Time Delays and Quantum Feedback". In: *Physical Review Letters* 116.9 (2016), p. 93601. ISSN: 10797114. DOI: 10.1103/PhysRevLett.116.093601.

[12] Arne L. Grimsmo. "Time-Delayed Quantum Feedback Control". In: *Physical Review Letters* 115.6 (2015), p. 60402. ISSN: 10797114. DOI: 10.1103/PhysRevLett.115.060402.

[13] S. J. Whalen, A. L. Grimsmo, and H. J. Carmichael. "Open quantum systems with delayed coherent feedback". In: *Quantum Science and Technology* 2.4 (2017), p. 44008. ISSN: 20589565. DOI: 10.1088/2058-9565/aa8331.

[14] Dario Cilluffo and Francesco Ciccarello. "Quantum non-Markovian collision models from colored-noise baths". In: *Advances in Open Systems and Fundamental Tests of Quantum Mechanics*. Springer, 2019, pp. 29–40.

[15] Kevin A. Fischer et al. "Scattering into one-dimensional waveguides from a coherently-driven quantum-optical system". In: *Quantum* 2 (2018), p. 69. ISSN: 2521-327X. DOI: 10.22331/q-2018-05-28-69.

[16] Kevin Fischer. "Derivation of the quantum-optical master equation based on coarse-graining of time". In: *Journal of Physics Communications* 2.9 (2018), p. 91001. ISSN: 23996528. DOI: 10.1088/2399-6528/aadaf8.

[17] Jonathan A Gross et al. "Qubit models of weak continuous measurements: markovian conditional and open-system dynamics". In: *Quantum Science and Technology* 3.2 (2018), p. 024005. ISSN: 2058-9565. DOI: 10.1088/2058-9565/aaa39f. URL: http://dx.doi.org/10.1088/2058-9565/aaa39f.

[18] S. J. Whalen. "Collision model for non-Markovian quantum trajectories". In: *Phys. Rev. A* 100 (5 2019), p. 052113.

[19] Anita Dkabrowska, Gniewomir Sarbicki, and Dariusz Chruscinski. "Quantum trajectories for a system interacting with environment in a single-photon state: Counting and diffusive processes". In: *Phys. Rev. A* 96 (5 2017), p. 053819. DOI: 10.1103/PhysRevA.96.053819.

[20] Gé Vissers and Luc Bouten. "Implementing quantum stochastic differential equations on a quantum computer". In: *Quantum Information Processing* 18.5 (2019), p. 152.

[21] Anita Dkabrowska, Gniewomir Sarbicki, and Dariusz Chruscinski. "Quantum trajectories for a system interacting with environment in N-photon state". In: *Journal of Physics A: Mathematical and Theoretical* 52.10 (2019), p. 105303.

[22] Anita Magdalena Dkabrowska. "From a posteriori to a priori solutions for a two-level system interacting with a single-photon wavepacket". In: *JOSA B* 37.4 (2020), pp. 1240–1248.

[23] Mikkel Heuck, Kurt Jacobs, and Dirk R. Englund. "Photon-photon interactions in dynamically coupled cavities". In: *Phys. Rev. A* 101 (4 2020), p. 042322. DOI: 10.1103/PhysRevA.101.042322. URL: https://link.aps.org/doi/10.1103/PhysRevA.101.042322.

[24] Mikkel Heuck, Kurt Jacobs, and Dirk R. Englund. "Controlled-Phase Gate Using Dynamically Coupled Cavities and Optical Nonlinearities". In: *Phys. Rev. Lett.* 124 (16 2020), p. 160501. DOI: 10.1103/PhysRevLett.124.160501. URL: https://link.aps.org/doi/10.1103/PhysRevLett.124.160501.

[25] Carlton M. Caves and G. J. Milburn. "Quantum-mechanical model for continuous position measurements". In: *Physical Review A* 36.12 (1987), pp. 5543–5555. ISSN: 10502947. DOI: 10.1103/PhysRevA.36.5543.

[26] Todd A. Brun. "A simple model of quantum trajectories". In: *American Journal of Physics* 70.7 (2002), 719–737. ISSN: 1943-2909. DOI: 10.1119/1.1475328. URL: http://dx.doi.org/10.1119/1.1475328.

[27] Tomáš Rybár et al. "Simulation of indivisible qubit channels in collision models". In: *Journal of Physics B: Atomic, Molecular and Optical Physics* 45.15 (2012), p. 154006. ISSN: 09534075. DOI: 10.1088/0953-4075/45/15/154006. eprint: 1202.6315. URL: http://stacks.iop.org/0953-4075/45/i=15/a=154006.

[28] F. Ciccarello, G. M. Palma, and V. Giovannetti. "Collision-model-based approach to non-Markovian quantum dynamics". In: *Physical Review A - Atomic, Molecular, and Optical Physics* 87.4 (2013), 040103(R). ISSN: 10502947. DOI: 10.1103/PhysRevA.87.040103. eprint: 1207.6554. URL: https://link.aps.org/doi/10.1103/PhysRevA.87.040103.

[29] N. K. Bernardes et al. "Environmental correlations and Markovian to non-Markovian transitions in collisional models". In: *Physical Review A - Atomic, Molecular, and Optical Physics* 90.3 (2014), p. 32111. ISSN: 10941622. DOI: 10.1103/PhysRevA.90.032111. eprint: 1404.0019. URL: https://link.aps.org/doi/10.1103/PhysRevA.90.032111.

[30] Ruari McCloskey and Mauro Paternostro. "Non-Markovianity and system-environment correlations in a microscopic collision model". In: *Physical Review A - Atomic, Molecular, and Optical Physics* 89.5 (2014), p. 52120. ISSN: 10941622. DOI: 10.1103/PhysRevA.89.052120. eprint: 1402.4639. URL: https://link.aps.org/doi/10.1103/PhysRevA.89.052120.

[31] Jiasen Jin et al. "All-optical non-Markovian stroboscopic quantum simulator". In: *Phys. Rev. A* 91 (1 2015), p. 012122. DOI: 10.1103/PhysRevA.91.012122. URL: https://link.aps.org/doi/10.1103/PhysRevA.91.012122.

[32] Silvan Kretschmer, Kimmo Luoma, and Walter T. Strunz. "Collision model for non-Markovian quantum dynamics". In: *Physical Review A* 94.1 (2016), p. 12106. ISSN: 24699934. DOI: 10.1103/PhysRevA.94.012106. URL: https://link.aps.org/doi/10.1103/PhysRevA.94.012106.

[33] Salvatore Lorenzo, Francesco Ciccarello, and G. M. Palma. "Class of exact memory-kernel master equations". In: *Physical Review A* 93.5 (2016), p. 52111. ISSN: 24699934. DOI: 10.1103/PhysRevA.93.052111. URL: https://link.aps.org/doi/10.1103/PhysRevA.93.052111.

[34] Salvatore Lorenzo, Francesco Ciccarello, and G. M. Palma. "Composite quantum collision models". In: *Physical Review A* 96.3 (2017), p. 32107. ISSN: 24699934. DOI: 10.1103/PhysRevA.96.032107. eprint: 1705.03215. URL: https://link.aps.org/doi/10.1103/PhysRevA.96.032107.

[35] S. N. Filippov et al. "Divisibility of quantum dynamical maps and collision models". In: *Physical Review A* 96.3 (2017), p. 32111. ISSN: 24699934. DOI: 10.1103/PhysRevA.96.032111.

[36] Steve Campbell et al. "System-environment correlations and Markovian embedding of quantum non-Markovian dynamics". In: *Phys. Rev. A* 98 (1 2018), p. 012142. DOI: 10.1103/PhysRevA.98.012142. URL: https://link.aps.org/doi/10.1103/PhysRevA.98.012142.

[37] Valerio Scarani et al. "Thermalizing Quantum Machines: Dissipation and Entanglement". In: *Phys. Rev. Lett.* 88.9 (Feb. 2002), p. 097905. DOI: 10.1103/PhysRevLett.88.097905. URL: https://link.aps.org/doi/10.1103/PhysRevLett.88.097905 (visited on 07/14/2018).

[38] Dragi Karevski and Thierry Platini. "Quantum nonequilibrium steady states induced by repeated interactions". In: *Physical Review Letters* 102.20 (2009), p. 207207. ISSN: 00319007. DOI: 10.1103/PhysRevLett.102.207207. eprint: 0904.3527. URL: https://link.aps.org/doi/10.1103/PhysRevLett.102.207207.

[39] Raam Uzdin and Ronnie Kosloff. "The multilevel four-stroke swap engine and its environment". In: *New Journal of Physics* 16.9 (2014), p. 95003. ISSN: 13672630. DOI: 10.1088/1367-2630/16/9/095003. eprint: 1404.6182. URL: http://stacks.iop.org/1367-2630/16/i=9/a=095003.

[40] S. Lorenzo et al. "Landauer's Principle in Multipartite Open Quantum System Dynamics". In: *Physical Review Letters* 115.12 (2015), p. 120403. ISSN: 10797114. DOI: 10.1103/PhysRevLett.115.120403. eprint: 1503.07837. URL: https://link.aps.org/doi/10.1103/PhysRevLett.115.120403.

[41] Philipp Strasberg et al. "Quantum and Information Thermodynamics: A Unifying Framework Based on Repeated Interactions". In: *Phys. Rev. X* 7 (2 2017), p. 021003. DOI: 10.1103/PhysRevX.7.021003. URL: https://link.aps.org/doi/10.1103/PhysRevX.7.021003.

[42] Gabriele De Chiara et al. "Reconciliation of quantum local master equations with thermodynamics". In: *New Journal of Physics* 20.11 (2018), p. 113024. ISSN: 13672630. DOI: 10.1088/1367-2630/aaecee. eprint: 1808.10450. URL: https://doi.org/10.1088{\%}2F1367-2630{\%}2Faaecee.

[43] Dvir Kafri and J. M. Taylor. "A noise inequality for classical forces". In: *arXiv:1311.4558 [quant-ph]* (2013). eprint: 1311.4558. URL: http://arxiv.org/abs/1311.4558.

[44] Natacha Altamirano et al. "Unitarity, feedback, interactions - Dynamics emergent from repeated measurements". In: *New Journal of Physics* 19.1 (2017), p. 13035. ISSN: 13672630. DOI: 10.1088/1367-2630/aa551b.

[45] Kevin Lalumière et al. "Input-output theory for waveguide QED with an ensemble of inhomogeneous atoms". In: *Physical Review A - Atomic, Molecular, and Optical Physics* 88.4 (2013), p. 43806. ISSN: 10502947. DOI: 10.1103/PhysRevA.88.043806.

[46] Bharath Kannan et al. "Waveguide Quantum Electrodynamics with Giant Superconducting Artificial Atoms". In: *arXiv preprint arXiv:1912.12233* (2019).

[47] Zeyang Liao et al. "Photon transport in a one-dimensional nanophotonic waveguide QED system". In: *Physica Scripta* 91.6 (2016), p. 63004. ISSN: 14024896. DOI: 10.1088/0031-8949/91/6/063004.

[48] Dibyendu Roy, C. M. Wilson, and Ofer Firstenberg. "Colloquium: Strongly interacting photons in one-dimensional continuum". In: *Reviews of Modern Physics* 89.2 (2017), p. 21001. ISSN: 15390756. DOI: 10.1103/RevModPhys.89.021001.

[49] Xiu Gu et al. "Microwave photonics with superconducting quantum circuits". In: *Physics Reports* 718-719 (2017), pp. 1–102. ISSN: 03701573. DOI: 10.1016/j.physrep.2017.10.002.

[50] Jung Tsung Shen and Shanhui Fan. "Theory of single-photon transport in a single-mode waveguide. I. Coupling to a cavity containing a two-level atom". In: *Physical Review A - Atomic, Molecular, and Optical Physics* 79.2 (2009), p. 23837. ISSN: 10502947. DOI: 10.1103/PhysRevA.79.023837.

[51] Sofia Arranz Regidor et al. *Modelling quantum light-matter interactions in waveguide-QED with retardation and a time-delayed feedback: matrix product states versus a space-discretized waveguide model*. 2020. arXiv: 2011.12205 [quant-ph].

[52] Lingzhen Guo et al. "Giant acoustic atom: A single quantum system with a deterministic time delay". In: *Phys. Rev. A* 95 (5 2017), p. 053821.

[53] Anton Frisk Kockum, Göran Johansson, and Franco Nori. "Decoherence-Free Interaction between Giant Atoms in Waveguide Quantum Electrodynamics". In: *Phys. Rev. Lett.* 120 (14 2018), p. 140404.

[54] Anton Frisk Kockum. "Quantum optics with giant atoms–the first five years". In: *arXiv preprint arXiv:1912.13012* (2019).

[55] Anton Frisk Kockum, Per Delsing, and Göran Johansson. "Designing frequency-dependent relaxation rates and Lamb shifts for a giant artificial atom". In: *Physical Review A - Atomic, Molecular, and Optical Physics* 90.1 (2014), p. 13837. ISSN: 10941622. DOI: 10.1103/PhysRevA.90.013837. arXiv: 1406.0350.

[56] Martin V. Gustafsson et al. "Propagating phonons coupled to an artificial atom". In: *Science* 346.6206 (2014), pp. 207–211. ISSN: 10959203. DOI: 10.1126/science.1257219. arXiv: 1404.0401.

[57] G Massimo Palma, Kalle-Antti Suominen, and Artur Ekert. "Quantum computers and dissipation". In: *Proceedings of the Royal Society of London. Series A: Mathematical, Physical and Engineering Sciences* 452.1946 (1996), pp. 567–584.

[58] Howard Mark Wiseman. "Quantum trajectories and feedback". PhD thesis. University of Queensland, 1994.

[59] Todd A. Brun. "Continuous measurements, quantum trajectories, and decoherent histories". In: *Physical Review A* 61.4 (2000). ISSN: 1094-1622. DOI: 10.1103/physreva.61.042107. URL: http://dx.doi.org/10.1103/PhysRevA.61.042107.

[60] P Zoller, M_ Marte, and D F Walls. "Quantum jumps in atomic systems". In: *Phys. Rev. A* 35.1 (1987), p. 198.

[61] Juan P Garrahan, Andrew D Armour, and Igor Lesanovsky. "Quantum trajectory phase transitions in the micromaser". In: *Phys. Rev. E* 84.2 (2011), p. 021115.

[62] RS Ellis. "An overview of the theory of large deviations and applications to statistical mechanics." In: *Insurance Mathematics and Economics* 3.17 (1996), pp. 232–233.

[63] Hugo Touchette. "The large deviation approach to statistical mechanics". In: *Physics Reports* 478.1-3 (2009), pp. 1–69.

[64] Angelo Vulpiani et al. "Large deviations in physics". In: *The Legacy of the Law of Large Numbers (Berlin: Springer)* (2014).

[65] Daniel Manzano and Pablo I Hurtado. "Symmetry and the thermodynamics of currents in open quantum systems". In: *Phys. Rev. B* 90.12 (2014), p. 125138.

[66] H. J. Carmichael et al. "Photoelectron waiting times and atomic state reduction in resonance fluorescence". In: *Physical Review A* 39.3 (1989), pp. 1200–1218. ISSN: 10502947. DOI: 10.1103/PhysRevA.39.1200. URL: https://link.aps.org/doi/10.1103/PhysRevA.39.1200.

[67] Richard J. Cook. "Photon number statistics in resonance fluorescence". In: *Phys. Rev. A* 23 (3 1981), pp. 1243–1250. DOI: 10.1103/PhysRevA.23.1243. URL: https://link.aps.org/doi/10.1103/PhysRevA.23.1243.

[68] L. Mandel. "Sub-Poissonian photon statistics in resonance fluorescence". In: *Opt. Lett.* 4.7 (1979), pp. 205–207. DOI: 10.1364/OL.4.000205. URL: http://ol.osa.org/abstract.cfm?URI=ol-4-7-205.

[69] Mikhail Pletyukhov and Vladimir Gritsev. "Quantum theory of light scattering in a one-dimensional channel: Interaction effect on photon statistics and entanglement entropy". In: *Physical Review A - Atomic, Molecular, and Optical Physics* 91.6 (2015), p. 63841. ISSN: 10941622. DOI: 10.1103/PhysRevA.91.063841. arXiv: 1504.03350. URL: https://link.aps.org/doi/10.1103/PhysRevA.91.063841.

[70] Evgeny V Shchukin and Werner Vogel. "Nonclassical moments and their measurement". In: *Phys. Rev. A* 72.4 (2005), p. 043808.

[71] Evgeny Shchukin, Th Richter, and Werner Vogel. "Nonclassicality criteria in terms of moments". In: *Phys. Rev. A* 71.1 (2005), 011802(R).

[72] J. Sperling et al. "Quantum Correlations from the Conditional Statistics of Incomplete Data". In: *Phys. Rev. Lett.* 117 (8 2016), p. 083601.

[73] Federico Carollo et al. "Making rare events typical in Markovian open quantum systems". In: *Phys. Rev. A* 98.1 (2018), p. 010103.

[74] Angel Rivas and Susana F Huelga. *Open quantum systems*. Vol. 13. Springer, 2012.

[75] Michael A. Nielsen and Isaac L. Chuang. *Quantum Computation and Quantum Information: 10th Anniversary Edition*. Cambridge University Press, 2010. DOI: 10.1017/CBO9780511976667.

[76] John Preskill. *Lecture notes for ph219/cs219: Quantum information and computation*. 2001.

[77] Jayaseetha Rau. "Relaxation Phenomena in Spin and Harmonic Oscillator Systems". In: *Phys. Rev.* 129 (4 1963), pp. 1880–1888. DOI: 10.1103/PhysRev.129.1880. URL: https://link.aps.org/doi/10.1103/PhysRev.129.1880.

[78] F. Ciccarello, G. M. Palma, and V. Giovannetti. "Collision-model-based approach to non-Markovian quantum dynamics". In: *Phys. Rev. A* 87 (4 2013), p. 040103. DOI: 10.1103/PhysRevA.87.040103. URL: https://link.aps.org/doi/10.1103/PhysRevA.87.040103.

[79] M. B. Plenio and P. L. Knight. "The quantum-jump approach to dissipative dynamics in quantum optics". In: *Rev. Mod. Phys.* 70 (1 1998), pp. 101–144. DOI: 10.1103/RevModPhys.70.101. URL: https://link.aps.org/doi/10.1103/RevModPhys.70.101.

[80] Howard M. Wiseman and Gerard J. Milburn. *Quantum measurement and control*. Vol. 9780521804424. Cambridge university press, 2009, pp. 1–460. ISBN: 9780511813948. DOI: 10.1017/CBO9780511813948.

[81] Walter Greiner, Ludwig Neise, and Horst Stöcker. *Thermodynamics and statistical mechanics*. Springer Science & Business Media, 2012.

[82] Adrián A. Budini. "Large deviations of ergodic counting processes: A statistical mechanics approach". In: *Phys. Rev. E* 84 (1 2011), p. 011141.

[83] Federico Carollo et al. "Making rare events typical in Markovian open quantum systems". In: *Phys. Rev. A* 98.1 (2018), p. 010103.

[84] Oskar Perron. "Zur theorie der matrices". In: *Mathematische Annalen* 64.2 (1907), pp. 248–263.

[85] Charles Jordan and Károly Jordán. *Calculus of finite differences*. Vol. 33. American Mathematical Soc., 1965.

[86] Juan P Garrahan. "Aspects of non-equilibrium in classical and quantum systems: Slow relaxation and glasses, dynamical large deviations, quantum non-ergodicity, and open quantum dynamics". In: *Physica A: Statistical Mechanics and its Applications* 504 (2018), pp. 130–154.

[87] Dario Cilluffo et al. "Collisional picture of quantum optics with giant emitters". In: *Phys. Rev. Research* 2 (4 2020), p. 043070. DOI: 10.1103/PhysRevResearch.2.043070. URL: https://link.aps.org/doi/10.1103/PhysRevResearch.2.043070.

[88] Angelo Carollo, Dario Cilluffo, and Francesco Ciccarello. "Mechanism of decoherence-free coupling between giant atoms". In: *Phys. Rev. Research* 2 (4 2020), p. 043184. DOI: 10.1103/PhysRevResearch.2.043184. URL: https://link.aps.org/doi/10.1103/PhysRevResearch.2.043184.

[89] Markus Aspelmeyer, Tobias J. Kippenberg, and Florian Marquardt. "Cavity optomechanics". In: *Reviews of Modern Physics* 86.4 (2014), pp. 1391–1452. ISSN: 15390756. DOI: 10.1103/RevModPhys.86.1391. eprint: 1303.0733. URL: https://link.aps.org/doi/10.1103/RevModPhys.86.1391.

[90] Klemens Hammerer, Anders S. Sørensen, and Eugene S. Polzik. "Quantum interface between light and atomic ensembles". In: *Rev. Mod. Phys.* 82 (2 2010), pp. 1041–1093. DOI: 10.1103/RevModPhys.82.1041. URL: https://link.aps.org/doi/10.1103/RevModPhys.82.1041.

[91] Thomas M Karg et al. "Remote Hamiltonian interactions mediated by light". In: *Physical Review A* 99.6 (2019), p. 063829.

[92] Crispin Gardiner, Peter Zoller, and Peter Zoller. *Quantum noise: a handbook of Markovian and non-Markovian quantum stochastic methods with applications to quantum optics*. Springer Science & Business Media, 2004.

[93] Bharath Kannan et al. "Waveguide quantum electrodynamics with superconducting artificial giant atoms". In: *Nature* 583.7818 (2020), 775–779. ISSN: 1476-4687. DOI: 10.1038/s41586-020-2529-9. URL: http://dx.doi.org/10.1038/s41586-020-2529-9.

[94] M. Arcari et al. "Near-Unity Coupling Efficiency of a Quantum Emitter to a Photonic Crystal Waveguide". In: *Physical Review Letters* 113.9 (2014), p. 93603. ISSN: 10797114. DOI: 10.1103/PhysRevLett.113.093603. eprint: 1402.2081.

[95] Tao Shi, Darrick E. Chang, and J. Ignacio Cirac. "Multiphoton-scattering theory and generalized master equations". In: *Physical Review A - Atomic, Molecular, and Optical Physics* 92.5 (2015), p. 53834. ISSN: 10941622. DOI: 10.1103/PhysRevA.92.053834. eprint: 1507.08699.

[96] Joshua Combes, Joseph Kerckhoff, and Mohan Sarovar. "The SLH framework for modeling quantum input-output networks". In: *Advances in Physics: X* 2.3 (2017), pp. 784–888. ISSN: 23746149. DOI: 10.1080/23746149.2017.1343097.

[97] Peter Lodahl et al. "Chiral quantum optics". In: *Nature* 541.7638 (2017), pp. 473–480. ISSN: 14764687. DOI: 10.1038/nature21037.

[98] In Eq. (4.22), we neglected the contribution coming from interval between $[t/\Delta t]\Delta t$ and $t$ since this vanishes in the limit $\Delta t \to 0$.

[99] Wilhelm Magnus. "On the exponential solution of differential equations for a linear operator". In: *Communications on pure and applied mathematics* 7.4 (1954), pp. 649–673.

[100] Subscripts "vac","th" and "sq" come from "vacuum", "thermal" and "squeezed". The corresponding Hamiltonian terms are indeed proportional to $[b_t, b_t^{\dagger'}]$, $b_t^{\dagger'} b_t$ and $b_t^\dagger b_t^{\dagger'}$, respectively, reflecting the fact that $\hat{\mathcal{H}}^{(1)}_{\text{vac}}$ arises for any field state, while typical field states for which $\hat{\mathcal{H}}^{(1)}_{\text{th}}$ ($\hat{\mathcal{H}}^{(1)}_{\text{sq}}$) occurs are thermal (squeezed) states.

[101] C. W. Gardiner. "Driving a quantum system with the output field from another driven quantum system". In: *Phys. Rev. Lett.* 70 (15 1993), pp. 2269–2272. DOI: 10.1103/PhysRevLett.70.2269.

[102] Yao Lung L. Fang, Francesco Ciccarello, and Harold U. Baranger. "Non-Markovian dynamics of a qubit due to single-photon scattering in a waveguide". In: *New Journal of Physics* 20.4 (2018), p. 43035. ISSN: 13672630. DOI: 10.1088/1367-2630/aaba5d.

[103] See e.g. Section 2.1.1 in Ref. [7].

[104] Hannes Pichler et al. "Quantum optics of chiral spin networks". In: *Physical Review A - Atomic, Molecular, and Optical Physics* 91.4 (2015), p. 042116. ISSN: 10941622. DOI: 10.1103/PhysRevA.91.042116.

[105] P. O. Guimond et al. "Delayed coherent quantum feedback from a scattering theory and a matrix product state perspective". In: *Quantum Science and Technology* 2.4 (2017), p. 44012. ISSN: 20589565. DOI: 10.1088/2058-9565/aa7f03.

[106] H. J. Carmichael. "Quantum trajectory theory for cascaded open systems". In: *Phys. Rev. Lett.* 70 (15 1993), pp. 2273–2276. DOI: 10.1103/PhysRevLett.70.2273.

[107] Jieyu You et al. "Waveguide quantum electrodynamics in squeezed vacuum". In: *Phys. Rev. A* 97 (2 2018), p. 023810. DOI: 10.1103/PhysRevA.97.023810.

[108] A. Gonzalez-Tudela et al. "Entanglement of two qubits mediated by one-dimensional plasmonic waveguides". In: *Physical Review Letters* 106.2 (2011), p. 20501. ISSN: 00319007. DOI: 10.1103/PhysRevLett.106.020501. eprint: 1010.5048.

[109] D. E. Chang et al. "Cavity QED with atomic mirrors". In: *New Journal of Physics* 14.6 (2012), p. 63003. ISSN: 13672630. DOI: 10.1088/1367-2630/14/6/063003. eprint: 1201.0643.

[110] Tommaso Tufarelli, Francesco Ciccarello, and M. S. Kim. "Dynamics of spontaneous emission in a single-end photonic waveguide". In: *Phys. Rev. A* 87 (1 2013), p. 013820. DOI: 10.1103/PhysRevA.87.013820. URL: https://link.aps.org/doi/10.1103/PhysRevA.87.013820.

[111] V. Giovannetti and G. M. Palma. "Master equation for cascade quantum channels: A collisional approach". In: *Journal of Physics B: Atomic, Molecular and Optical Physics* 45.15 (2012), p. 154003. ISSN: 09534075. DOI: 10.1088/0953-4075/45/15/154003. URL: http://stacks.iop.org/0953-4075/45/i=15/a=154003.

[112] Salvatore Lorenzo et al. "Heat flux and quantum correlations in dissipative cascaded systems". In: *Phys. Rev. A* 91 (2 2015), p. 022121. DOI: 10.1103/PhysRevA.91.022121. URL: https://link.aps.org/doi/10.1103/PhysRevA.91.022121.

[113] Dario Cilluffo et al. "Witnessing nonclassicality through large deviations in quantum optics". In: *Phys. Rev. Research* 2 (2 2020), p. 023078. DOI: 10.1103/PhysRevResearch.2.023078. URL: https://link.aps.org/doi/10.1103/PhysRevResearch.2.023078.

[114] Dario Cilluffo et al. *Microscopic biasing of discrete-time quantum trajectories*. 2020. arXiv: 2007.15659 [quant-ph].

[115] Richard P Feynman. "Simulating physics with computers". In: *International journal of theoretical physics* 21.6 (1982), pp. 467–488.

[116] Daniel Loss and David P. DiVincenzo. "Quantum computation with quantum dots". In: *Phys. Rev. A* 57 (1 1998), pp. 120–126.

[117] Alexandre Blais et al. "Cavity quantum electrodynamics for superconducting electrical circuits: An architecture for quantum computation". In: *Phys. Rev. A* 69 (6 2004), p. 062320.

[118] Andrea Mari and Jens Eisert. "Positive Wigner functions render classical simulation of quantum computation efficient". In: *Phys. Rev. Lett.* 109.23 (2012), p. 230503.

[119] Gonzalo Manzano Paule. "Dissipative Complex Quantum Networks". In: *Thermodynamics and Synchronization in Open Quantum Systems*. Springer, 2018, pp. 233–254.

[120] Pieter Kok et al. "Linear optical quantum computing with photonic qubits". In: *Rev. Mod. Phys.* 79 (1 2007), pp. 135–174.

[121] Giuseppe Buonaiuto et al. "Dynamical creation and detection of entangled many-body states in a chiral atom chain". In: *New Journal of Physics* 21.11 (2019), p. 113021.

[122] Dario Cilluffo et al. "Quantum jump statistics with a shifted jump operator in a chiral waveguide". In: *Journal of Statistical Mechanics: Theory and Experiment* 2019.10 (2019), p. 104004.

[123] J Sperling et al. "Uncovering quantum correlations with time-multiplexed click detection". In: *Phys. Rev. Lett.* 115.2 (2015), p. 023601.

[124] Georg Harder et al. "Single-Mode Parametric-Down-Conversion States with 50 Photons as a Source for Mesoscopic Quantum Optics". In: *Phys. Rev. Lett.* 116 (14 2016), p. 143601.

[125] G Harder et al. "Time-multiplexed measurements of nonclassical light at telecom wavelengths". In: *Phys. Rev. A* 90.4 (2014), p. 042105.

[126] M Avenhaus et al. "Accessing higher order correlations in quantum optical states by time multiplexing". In: *Phys. Rev. Lett.* 104.6 (2010), p. 063602.

[127] Jan Peřina Jr et al. "Nonclassicality and entanglement criteria for bipartite optical fields characterized by quadratic detectors". In: *Phys. Rev. A* 96.4 (2017), p. 043845.

[128] Roy J. Glauber. "The Quantum Theory of Optical Coherence". In: *Phys. Rev.* 130 (6 1963), pp. 2529–2539.

[129] Kevin E Cahill and Roy J Glauber. "Ordered expansions in boson amplitude operators". In: *Phy. Rev.* 177.5 (1969), p. 1857.

[130] Wolfgang P Schleich. *Quantum optics in phase space*. John Wiley & Sons, 2011.

[131] J Sperling, W Vogel, and G S Agarwal. "Correlation measurements with on-off detectors". In: *Phys. Rev. A* 88.4 (2013), p. 043821.

[132] Motoaki Bamba et al. "Origin of strong photon antibunching in weakly nonlinear photonic molecules". In: *Phys. Rev. A* 83 (2 2011), 021802(R).

[133] A. C. Doherty and K. Jacobs. "Feedback control of quantum systems using continuous state estimation". In: *Physical Review A* 60.4 (1999), 2700–2711. ISSN: 1094-1622. DOI: 10.1103/physreva.60.2700. URL: http://dx.doi.org/10.1103/PhysRevA.60.2700.

[134] Philipp Stegmann, Jürgen König, and Stephan Weiss. "Coherent dynamics in stochastic systems revealed by full counting statistics". In: *Phys. Rev. B* 98 (3 2018), p. 035409. DOI: 10.1103/PhysRevB.98.035409. URL: https://link.aps.org/doi/10.1103/PhysRevB.98.035409.

[135] Robert L. Jack and Peter Sollich. "Large Deviations and Ensembles of Trajectories in Stochastic Models". In: *Progress of Theoretical Physics Supplement* 184 (Mar. 2010), pp. 304–317. ISSN: 0375-9687. DOI: 10.1143/PTPS.184.304. eprint: https://academic.oup.com/ptps/article-pdf/doi/10.1143/PTPS.184.304/5250023/184-304.pdf. URL: https://doi.org/10.1143/PTPS.184.304.

[136] Salvatore Lorenzo et al. "Heat flux and quantum correlations in dissipative cascaded systems". In: *Phys. Rev. A* 91 (2 2015), p. 022121. DOI: 10.1103/PhysRevA.91.022121. URL: https://link.aps.org/doi/10.1103/PhysRevA.91.022121.

[137] H. J. Kimble, Richard J. Cook, and Ann L. Wells. "Intermittent atomic fluorescence". In: *Phys. Rev. A* 34 (4 1986), pp. 3190–3195. DOI: 10.1103/PhysRevA.34.3190. URL: https://link.aps.org/doi/10.1103/PhysRevA.34.3190.

[138] Daniel Malz and J Ignacio Cirac. "Number-resolving photon detectors with atoms coupled to waveguides". In: *arXiv preprint arXiv:1906.12296* (2019).

[139] Dominic Charles Rose, Juan P Garrahan, and Jamie F Mair. "A reinforcement learning approach to rare trajectory sampling". In: *New Journal of Physics* (2020). URL: http://iopscience.iop.org/article/10.1088/1367-2630/abd7bd.

[140] Anders Søndberg Sørensen and Klaus Mølmer. "Entangling atoms in bad cavities". In: *Phys. Rev. A* 66 (2 2002), p. 022314. DOI: 10.1103/PhysRevA.66.022314. URL: https://link.aps.org/doi/10.1103/PhysRevA.66.022314.

[141] Florentin Reiter and Anders S. Sørensen. "Effective operator formalism for open quantum systems". In: *Phys. Rev. A* 85 (3 2012), p. 032111. DOI: 10.1103/PhysRevA.85.032111. URL: https://link.aps.org/doi/10.1103/PhysRevA.85.032111.

[142] A. González-Tudela, C. Sánchez Muñoz, and J. I. Cirac. "Engineering and Harnessing Giant Atoms in High-Dimensional Baths: A Proposal for Implementation with Cold Atoms". In: *Phys. Rev. Lett.* 122 (20 2019), p. 203603. DOI: 10.1103/PhysRevLett.122.203603. URL: https://link.aps.org/doi/10.1103/PhysRevLett.122.203603.

[143] P. Schindler et al. "Quantum simulation of dynamical maps with trapped ions". In: *Nature Physics* 9.6 (2013), 361–367. ISSN: 1745-2481. DOI: 10.1038/nphys2630. URL: http://dx.doi.org/10.1038/nphys2630.

[144] Antoine Browaeys and Thierry Lahaye. "Many-body physics with individually controlled Rydberg atoms". In: *Nature Physics* 16.2 (2020), 132–142. ISSN: 1745-2481. DOI: 10.1038/s41567-019-0733-z. URL: http://dx.doi.org/10.1038/s41567-019-0733-z.

[145] Hendrik Weimer et al. "A Rydberg quantum simulator". In: *Nature Physics* 6.5 (2010), 382–388. ISSN: 1745-2481. DOI: 10.1038/nphys1614. URL: http://dx.doi.org/10.1038/nphys1614.

# *Acknowledgements*

Desidero ringraziare per primo il mio supervisor, il Prof. Francesco Ciccarello. Senza di lui questo percorso non sarebbe mai giunto a compimento. Grazie per la sua serietà, la sua perseveranza e ai suoi suggerimenti, giunti molto spesso senza che io li richiedessi ma esattamente nel momento in cui erano indispensabili. Entrare almeno un po' nel suo modo di ragionare e di vedere la fisica resterà per me il successo più grande di questi anni.
Ringrazio il Prof. Massimo Palma per le infinite discussioni sui problemi che di volta in volta ho incontrato nei miei studi e per i momenti di rottura ad alto contenuto culturale, i film di Tarkovsky, i podcast, la cancelleria, i tantissimi té, la ricerca della stilografica migliore. Grazie per le lezioni di temperanza e umanità.
Grazie al gruppo di ottica quantistica di Palermo. Ringrazio il Dr. Salvatore Lorenzo, sempre aperto al dialogo, sempre con la soluzione giusta per ogni problema. Grazie al Dr. Angelo Carollo per aver condiviso con me tante delle sue grandi conoscenze.
Outside the department, I must thank Prof. Igor Lesanovsky for welcoming me to his group in Nottingham and in Tübingen. Thanks to Bea, Jemma, Ed, Paolo, Ben, Filippo and all the people who made unique my periods in the United Kingdom and in Germany.
Grazie in particolare al Dr. Giuseppe Buonaiuto, fisico brillante e persona speciale che ha saputo farmi sentire a casa e tra amici fin dal primo incontro. Grazie al Dr. Federico Carollo per la collaborazione, la sua pazienza e i molti insegnamenti.
A special thank to Dr. Jonathan Gross for the comments and the fruitful collaboration. I should like to thank Dr. Andrea Smirne and Dr. Kimmo Luoma for having carefully read my work, the valuable advice and their helpful and encouraging comments.
Ringrazio tutti gli amici e le persone che ho incontrato in questi anni e che hanno condiviso con me questo periodo. Grazie a Federico Roccati per le discussioni esilaranti, a Luca Leonforte per i tanti consigli da smanettone. Ringrazio Dario Alexander Chisholm e Claudio Pellitteri preziosi colleghi e compagni di stanza.
In particolare ringrazio Alessia Castellini per essere stata ed essere sempre un confronto e un'amica preziosa. La Natura ha ricompensato le nostre innumerevoli trasferte insieme con tanti eventi catastrofici di cui probabilmente rideremo per sempre.

Ringrazio la mia famiglia.
Grazie per essere stati sempre con me durante le mie peregrinazioni e i miei infiniti ripensamenti. Grazie per essere rimasti "casa". Grazie a mamma, per avermi insegnato a trasformare in casa mia ogni bugigattolo, a papà per esserci sempre stato e avermi insegnato come tenere duro salendo i gradini uno alla volta, anche quando sono scivolosi. A mio fratello Danilo per essere sempre un confronto positivo e un punto di riferimento insostituibile.
Desidero ringraziare Simona Michela Mazzola, Simona. Grazie per aver creduto in

me quando non ci credevo nemmeno io. Grazie per aver provato ad ascoltarmi anche quando era impossibile e aver sopportato più di chiunque altro la mia infelicità. Per non essersi mai arresa. Sei una delle principali ragioni che mi hanno spinto sin qui.